The Pennsylvania State University
The Graduate School
Department of Energy and Mineral Engineering

NETWORK MODELING AND TRACKING OF LIQUID PREFERENTIAL ROUTES IN NATURAL GAS PIPELINE SYSTEMS

A Thesis in
Petroleum and Mineral Engineering
by

David Essenfeld

Submitted in Partial Fulfillment
of the Requirements
for the Degree of

Master of Science

May 2010

The thesis of David Essenfeld was reviewed and approved* by the following:

Luis F. Ayala H.
Assistant Professor of Petroleum and Natural Gas Engineering
Thesis Advisor

Larry Grayson
Professor of Energy and Mineral Engineering

John Yilin Wang
Assistant Professor of Petroleum and Natural Gas Engineering

Yaw D. Yeboah
Department Head of Energy and Mineral Engineering

*Signatures are on file in the Graduate School

ABSTRACT

Liquids, water in particular, are responsible for additional pressure losses in natural gas surface production systems. For the case of natural gas stripper well facilities, the optimization of these surface fluid transportation operations is vital for a successful business. This research work is aimed at developing and testing an analytical tool able to track and map the preferential route of water in natural gas network systems so that the operator can make better decisions regarding system optimization, resulting in a more economically viable operation. The accurate mapping of the pressure, velocities of the phases and fluid re-distribution inside the network is critical, since it can reduce additional compression costs caused by the liquid phase, help to make decisions regarding water removal from the network, and also affect the design and location of surface production and separation equipment.

This study was undertaken in stages, starting with the development of a one-dimensional, steady state tool for modeling the flow of a single phase fluid (gas) in pipes. This model was then expanded to account for the additional pressure drop due to the appearance of multiphase flow conditions in the system by employing the Beggs and Brill model (1999). In the final stage, tee junction sequences were incorporated to create network-wide prediction capabilities. The products of each of the stages were validated and crosschecked independently and as a group with commercial simulators and field data. The present work shows that the proposed model is capable of handling two-phase splits at tee junctions, especially for the common case of uneven splits—which commercially available network simulators do not model and cannot capture. As a result, the proposed multiphase network model is able to tackle realistic field scenarios where flowing phases do take their own preferential paths-resulting in sections of the network having dry and wet flow regions. The proposed model thus allows the user to effectively trace the liquid's path and plan to undertake the adequate corrective operational measures to maintain system capacity and minimize compression requirements, thereby improving the performance of the entire network.

TABLE OF CONTENTS

LIST OF FIGURES v

LIST OF TABLES ix

LIST OF SYMBOLS x

ACKNOWLEDGEMENTS xii

CHAPTER 1 INTRODUCTION 1

CHAPTER 2 LITERATURE SURVEY 3

CHAPTER 3 PROBLEM STATEMENT 10

CHAPTER 4 MODEL DESCRIPTION 11

4.1 Single-phase flow equations 11

Flowrate (Q) formulation 15

Pressure (P) formulation 16

4.2 Single-phase network solver 17

4.3 Pressure drop in multiphase system 20

4.3.1 Segregated flow 20

4.3.2 Intermittent flow 21

4.3.3 Distributed or bubbly flow 21

4.3.4 Transition flow 22

4.4 Tee junction treatment 23

4.5 Inflow Performance Relationship (IPR) 30

4.6 Model integration 31

CHAPTER 5 RESULTS AND DISCUSSIONS 33

CHAPTER 6 CONCLUSIONS AND RECOMMENDATIONS 62

BIBLIOGRAPHY 64

APPENDIX A INPUT FILE STRUCTURE 68

APPENDIX B BEGGS AND BRILL ALGORITHM 76

APPENDIX C SAMPLE INPUT DATA FILES 80

LIST OF FIGURES

Figure 1 Flow-pattern map for horizontal pipes (reproduced from Mandhane 1974) 5
Figure 2 Tee-junction classification, A) Splitting tee B) Splitting impacting tee, C) Converging tee D) Converging impacting tee 7
Figure 3 Single pipe at an angle to describe energy changes 11
Figure 4 Two loop network (S) indicates supply (D) indicates demand (B) indicates pipe and the dashed arrows indicate assumed flow direction 15
Figure 5 Segregated flow regimes 21
Figure 6 Intermittent flow regimes 21
Figure 7 Distributed flow regimes 22
Figure 8 Tee junction to describe the split factor 24
Figure 9 Flow highly perturbed at the T block and steady state afterwards. Also explain the Dual Stream Model (four stream lines) (A) inlet to run gas, (B) inlet to run liquid (C) inlet to branch gas and (D) inlet to branch liquid 27
Figure 10 Route selectivity map using Hart's Model, experimental data from the University of Amsterdam (reproduced from Hart *et al. 1991*) 29
Figure 11 Types of flows entering or leaving a tee junction that will be used in the code for tee classification 29
Figure 12 Impossible tee junctions 30
Figure 13 Equivalent system representation to handle multiple junctions 30
Figure 14 Flow diagram of GASNET two phase 32
Figure 15 Model of the Network 1 solved for two phases (10 nodes 11 pipes 2 loops) 33
Figure 16 Equivalent model for Network 1 solved for two phases (12 nodes 13 pipes 2 loops) 34
Figure 17 Results for single phase simple gas network system. Run with GASNET (single phase) and PIPESIM (12 nodes 13 pipes 2 loops) 35
Figure 18 Results for two phases of simple gas network system. Run with GASNET (Even Split) and PIPESIM (12 nodes 13 pipes 2 loops) 35
Figure 19 Fluid distribution (gas, liquid) and pressure distribution (psia) for each node obtained from two phases GASNET (Even Split and Kinetic Energy Model) 36

Figure 20 Model of the Network 2. Solved for single phase, two phases Even Split and two phase with Kinetic Energy Model (22 nodes 25 pipes 4 loops)..... 38
Figure 21 Results for single phase simple gas Network 2. Run with GASNET (single phase) and PIPESIM (22 nodes 25 pipes 4 loops)..... 39
Figure 22 Results for two phases in a gas Network 2. Run with GASNET (Even Split) and PIPESIM..... 39
Figure 23 Results for two phases in gas Network 2. Run with GASNET..... 40
Figure 24 Liquid and gas distribution in a gas Network 2. Solved with two phases GASNET 40
Figure 25 Results for two phases in a gas Network 2. Run with GASNET (Kinetic Energy Split) (22 nodes 25 pipes 4 loops) for low flowrates of water and water and changing the demands on several nodes..... 41
Figure 26 Liquid and gas distribution in a gas Network 2. Solved with two phase GASNET (22 nodes 25 pipes 4 loops). By reducing all the supplies and demand, it was found that there is one dry pipe that initially had liquid (Pipe B-9)..... 41
Figure 27 Liquid and gas distribution in gas Network 2. Solved with two phase GASNET (22 nodes 25 pipes 4 loops). By reducing all the supplies and demand by 10 %..... 42
Figure 28 Results for two phases in a gas Network 2. Run with GASNET (Kinetic Energy Split and Dual Stream Model) (22 nodes 25 pipes 4 loops)..... 43
Figure 29 Structure for a NCL Pennsylvania gathering center distribution network 44
Figure 30 Results for a single phase of the NCL Pennsylvania gas distribution system. Run with GASNET (single phase) and PIPESIM (38 nodes 38 pipes 1 loops) 46
Figure 31 Results for two phases of the NCL Pennsylvania gas distribution system. Run with GASNET (Even Split) and PIPESIM (38 nodes 38 pipes 1 loops) 46
Figure 32 Results for two phases in the NCL Pennsylvania gas distribution system. Run with GASNET (Even Split and Kinetic Energy Split) (38 nodes 38 pipes 1 loops)..... 47
Figure 33 Results for two phases in the NCL Pennsylvania gas distribution system. Run with GASNET Kinetic Energy Split, while increasing the water content from the well on node 20 48
Figure 34 Results for two phases in the NCL Pennsylvania gas distribution system. Run with GASNET Kinetic Energy Split, while increasing the water content from the well in node 20 48
Figure 35 Model of the Korea gas distribution network (A) and the equivalent system (B) (To avoid more than three pipes on a node) Network solved for two phase (34 nodes 40 pipes 7 loops). 50

Figure 36 Results for single phase of the Korea gas distribution system. Run with GASNET (single phase) and PIPESIM (34 nodes 40 pipes 7 loops) 51
Figure 37 Results for two phases of the Korea gas distribution system. Run with GASNET (Even Split) and PIPESIM (34 nodes 40 pipes 7 loops)..... 52
Figure 38 Results for two phases in the Korea gas distribution system. Run with GASNET (Even Split and Kinetic Energy Split) (34 nodes 40 pipes 7 loops) 52
Figure 39 Liquid distribution profile for initial parameter of the Korea gas distribution system GASNET (Kinetic Energy Split) (34 nodes 40 pipes 7 loops) 53
Figure 40 Results for two phases in the Korea gas distribution system. Run with GASNET (Kinetic Energy Split and dual stream model) (34 nodes 40 pipes 7 loops)..... 54
Figure 41 Model of complex gas distribution network solved for two phase (26 nodes 31 pipes 6 loops) 55
Figure 42 Results for single phase of the complex gas distribution network. Run with GASNET (single phase) and PIPESIM (26 nodes 31 pipes 6 loops) 56
Figure 43 Results for two phases in a complex gas distribution network. Run with GASNET (Even Split) and PIPESIM (26 nodes 31 pipes 6 loops) 57
Figure 44 Results for two phases in a complex gas distribution network. Run with GASNET (Even Split and Kinetic Energy Split) (26 nodes 31 pipes 6 loops)..... 57
Figure 45 Model of liquid and gas preference route for a complex gas distribution network 58
Figure 46 Model of liquid and gas preference route for a complex gas distribution network, changing the position of the demand 58
Figure 47 Results for two phases in a complex gas distribution network. Run with GASNET (Kinetic Energy Split and the Dual Stream Model) (26 nodes 31 pipes 6 loops) 59
Figure 48 Results for two phases in a complex gas distribution network. Run with GASNET (Kinetic Energy Split) changing the P specified from node 14 to node 26 (26 nodes 31 pipes 6 loops) 60
Figure 49 Results for two phases in a complex gas distribution network. Run with GASNET (Kinetic Energy Split) changing the P specified from 60 psia to 100 psia on node 21 (26 nodes 31 pipes 6 loops) 60
Figure 50 Results for two phases in a complex gas distribution network. Run with GASNET (Kinetic Energy Split) changing the water-gas ratio from 0.01 to 0.1 for the two inlets (26 Nodes 31 Pipes 6 Loops) 61
Figure 51 Equivalent system to avoid more than three pipes in a single node 68

Figure 52 90 degrees pipe definition 71
Figure 53 Final view of input file for the problem shown in the APPENDIX 74
Figure 54 Initial message when the program starts to run 75
Figure 55 Display after convergence is achieved 75
Figure 56 Input file for Network 1 80
Figure 57 Input file for Network 2 81
Figure 58 Input file for Network 3 82
Figure 59 Input file for Network 4 83
Figure 60 Input file for Network 5 84

LIST OF TABLES

Table 1 Number of equations and unknowns for the Q formulation 16
Table 2 Number of equations and unknowns in the P Formulation 17
Table 3 Parameters used in popular gas equations 17
Table 4 Operating conditions for Network 1 34
Table 5 Operating conditions for Network 2 38
Table 6 Operating conditions for Network 3 45
Table 7 Supply for Network 3 45
Table 8 Operating conditions for Network 4 51
Table 9 Operating conditions for Network 5 55

LIST OF SYMBOLS

Roman

A	Area of the cross flow	[ft^2]
B_n	Pipe/Branch number (1,2….n)	[-]
C	Pipe conductivity	[ft^3/psi]
C_{well}	Well performance constant	[mcfd/psi^{2nwell}]
d	Pipe internal diameter	[in]
D_n	Demand on node number (1,2….n)	[STBD, MMscfd]
dp/dz	Pressure drop	[psia/ft]
$E_{k,}$	Beggs and Brill acceleration ratio	[-]
e_{max}	Max. difference between Even Split, Kinetic Energy Ratio and DSM [%]	
f	Friction (Moody Fanning) factor	[-]
g	Gravity acceleration	[ft/Sec^2]
g_c	Gravity correction factor	[32.2 lbm ft/(lbf s^2)]
Hl	Height of the pipe	[ft]
I	Current	[A]
KE_r	Kinetic energy ratio	[-]
L	Length of the pipe	[ft]
L_{on}	Loop number (I,II….n)	[-]
m	Diameter power	[-]
m	Fluid mass	[lb]
M_w	Molecular weight	[lb/lbmol]
M_{wair}	Air molecular weight	[29 lb/lbmol]
n	Flow power	[-]
N_{an}	Node number (1,2….n)	[-]
n_{well}	Value to characterize flow	[-]
P_{DS}	Pressure downstream	[psia]
P_{SC}	Pressure at standard conditions	[14.7 psia]
P_{SHUT}	Well head shut in pressure	[psia]
P_{WH}	Flowing well head pressure	[psia]
P_{US}	Pressure upstream	[psia]
q_g	Gas flowrate	[scf/d]

q_L	Liquid flowrate	[STBD]
q_{SC}	Flowrate at standard conditions	[scf/d]
R	Resistance	[ohms]
R	Universal gas constant	[10.731 psi ft^3/ (lbmol R)]
R_{es}	Pipe resistivity	[psi/scf]
S	Supply flowrate	[STBD, MMscfd]
T_{AV}	Average temperature	[R]
T_{SC}	Temperature at standard conditions	[520 R]
U_{SG}	Superficial velocity of gas	[lb/sec]
U_{SL}	Superficial velocity of liquid	[lb/sec]
v	Fluid velocity	[ft/Sec]
V	Voltage	[volt]
WGR	Water gas ratio	[STB/scf]
W_{zy}	Root square of the axial velocity	[lb/s]
Z, Z_{av}	Compressibility factor	[-]

Greek

θ	Inclination angle	[deg]
ρ	Density	[lb/ft^3]
ρ_g, ρ_l	Gas/Liquid density	[lb/ft^3]
γ_g	Gas specific gravity	[-]

ACKNOWLEDGEMENTS

First, I thank God, who allows me to succeed in all my life endeavors, especially the challenges of graduate work. This research is a part of my learning experience in Petroleum and Natural Gas Engineering

This research was possible with the sponsorship of the Department of Energy of the United States (DOE) and was successfully completed with the guidance, counsel and support of Dr. Luis F. Ayala H. to whom I am especially grateful. I would also like to thank Dr. Turgay Ertekin and Dr. Zuleima Karpyn for their invaluable impact on my professional development.

I would not be where I am today without the love , support, advice and guidance of my parents; Raquel Abbo, Martin and Betty Essenfeld who gave me my education, my moral and ethical principles that allowed me to continue especially during the hard times. My sister and my brother in law Debbie and Daniel, my nephew and niece Yoel and Orly, both of whom gave me the hope and strength to continue, and also thanks to the rest of my extended family Essenfeld Abbo.

I wish to take the opportunity also to thank Dennis Alexis Arun, Bander Al Ghamdi, Juan Emilio Fernandez Luengo and Doruk Alp, Gabriela Caraballo, Yesica Alvarez, Alisha Fernandez, Enette Louw, Sarah Luchner, Roy Borkhoche, the Heim, the Avillion, the Glasner, the Tabares, the Meretsky and the Halpern families for their patience, guidance and friendship during my stay at Penn State.

I also appreciate my friends and loved ones, I have you all in my heart and I am thankful for your love, help and support.

Thank you all.

CHAPTER 1

INTRODUCTION

One of the most frequent problems that the hydrocarbon industry and more specifically the gas industry faces is the presence of liquids in the pipelines. This liquid will reduce the transportation (transmission) capacity of the pipelines as well as create some other problems such as corrosion of the pipelines and the equipment at the discharge point, hydrates plugging the pipes and other problems. Therefore, the presence of liquids in the pipelines will have an economic impact on the operators, as well as on the final customers.

Any gas that enters the gathering system is generally water saturated even after the produced free water has been successfully removed at the wellheads. Therefore, it is inevitable that some production water will enter the pipeline system, and with pressure and temperature changes in the lines, this water turned to liquid phase will eventually reach the gathering center and compression stations, causing a great deal of operational problems. Any kind of fluid that enters the system either as liquid or product of condensation will generally increase the friction losses in the system, distributing the flowing phases unevenly, and perturbing their forward movement towards the final destination (either gathering center or final consumer), decreasing the pipeline capacity and increasing compression expenses.

Most of the pipeline networks incorporate compressor stations to compensate the pressure losses due to friction allowing the movements of the fluids towards their final destination. Any compressor system must be water free to operate under optimal conditions. This study will focus on the development of a model that allows tracing the points or locations where the second phase distributes along the pipeline network, based on the application of mass and energy balances under isothermal conditions. The development of the second phase will act as a bottleneck, since the appearance of an additional liquid-phase for any reason (either because of direct injection, retrograde condensation or precipitation of moisture content) certainly increases the frictional losses, thereby increasing the compression costs. If the second phase is properly traced, this will allow the operators to take corrective actions and improve productivity by improving the system transmissibility and/or lowering compression costs.

Currently available models and commercial simulators for natural gas networks heavily rely on simplifying assumptions in order to solve complex pipeline network systems. One of the potentially most troublesome assumptions is that of the imposition of wholly single-phase flow

throughout the network system, or, when incorporating multiphase flow conditions, the simplified treatment of tee-junction splits as a uniform and even phenomenon for all incoming phases. As a result, reliable prediction of actual pressure drops and fluid misdistribution in these systems can become severely compromised. Exacerbated network pressure losses in stripper-well gathering systems can easily force production to go below economic limits for an operation, even for the cases where the liquid dropout inside the system is low. Even small improvements in the accuracy of the pressure drops, liquid hold-up, and actual fluid distribution calculations may result in a significant reduction in the cost of operations and increased revenue from additionally realizable gas volumes. The effect of this inaccuracy will be discussed and confirmed in Chapters 4 and 5.

A summary of the most significant results of the comprehensive research study are presented in this report. The work has led to the development of a tool which is capable of improving the predictions for pressure drops in network systems, addressing properly the multiphase flow in pipelines as well as the uneven split at tee junctions. Model testing has been completed using different networks (Wonmo Sung, 1998) which include field measurements and a Centre County network case for a variety of water-loading scenarios.

CHAPTER 2

LITERATURE SURVEY

For several years authors had tried to analyze and model multiphase flow in pipeline networks. Oranje (1973) reports the impact of the condensation of liquids while evaluating a pipeline system he had data for; the network that he studied was exposed to very low temperatures in the environment which are more favorable for liquid condensation. He considered this phenomenon to be a seasonal effect. However, he tried to determine what would happen to the system when pressure and temperature changed i.e. under which conditions of the system (pressure or temperature) would the liquid phase form, by condensation and create the aforementioned problems. Oranje also wanted to investigate which route the liquid would follow as a preferential path to the exit point.

Most of the simulation programs currently used for multiphase flow in pipeline networks heavily rely on simplifications or approximations, such as considering the entire system as a single-phase problem, and assume an Even Split of the fluids at tee junctions. These approximations can lead to incorrect estimates for the pressure drop values in different pipeline segments, because these models do not account for any liquids along the pipeline system, or if they account for liquid presence they assume it to be evenly distributed across the entire system. The result of these assumptions has caused that the pressure drops predicted for the systems in some cases to be significantly different from the ones experienced in the real two-phase systems.

Multiphase flow analysis is a widely researched area since this is a phenomenon that occurs in several industrial fields. In chemical engineering two-phase flow can be found in reactors, boilers, as well as in evaporation and distillation towers. In the nuclear reactor industry multiphase flow is present during Loss of Coolant Accidents (LOCA) and is used for designing safety programs. In the space industry two-phase flow has been studied under zero-gravity effects, for the purpose of power generation. More closer to us, in the oil industry, two-phase and multiphase flow can occur during several phases such as during production, or transportation of the hydrocarbons, downhole or at the surface in horizontal, vertical and inclined planes (pipelines or porous media). Regardless of the specific industry or field location where multiphase flow occurs, this phenomenon is generally relevant and important because of its effects on the entire system being considered (Shoham, 2005).

The multiphase development era can be classified according to the following criteria: the empirical period, the awakening years and the modeling period as indicated by Ayala *et al.* (2007). The empirical period is the beginning of the revolutionary concepts in multiphase flow and incorporates some of the following correlations: Lockhart Martinelli (1949), Eaton *et al*. (1967), Beggs and Brill (1963), and Olimans (1976). As part of this early period there were relevant research efforts for multiphase flow in the wellbore tubulars as undertaken by Hagedorn and Brown (1965), Duns and Ross (1963) and Orkiszewski (1967). With the continued progress in the available technology it was possible to digitize the empirical equations and convert them into functional models, this period is known as the awakening years. With the development of robust equipment and faster computers, the modeling period took over. In this period, some of the better known programs were formulated (RELAP5, MEKIN, COBRA, CATHARE and TRAC) which are currently used in the nuclear industry. A comprehensive mechanistic model for two-phase flow in vertical wells, horizontal pipes and deviated wells was developed by Ansari, Xiao, Kaya and co-workers in the 1990s. Several years of progress in the multiphase-flow field allowed the development of powerful and innovative tools such as OLGA, PIPESIM, and PIPEFLOW used nowadays. It is expected that future models can incorporate some of the ideas presented in this work.

As soon as the second phase has developed in a pipeline, the liquid content, which can be as small as 5%, can cause a significant increase in the pressure drop of the system (Ottens, 2001). Hope *et al*. (1977) compared three of the single-phase equations (AGA, Colebrook and Panhandle) with three of the equations for the two-phase case (Baker *et al*. 1954, Duckler 1964 and Beggs and Brill 1973). The comparison used a gas flowrate of 900 MMSCFD and 5 bbls of liquid per MMSCFD of gas, reaching the conclusion that single-phase models gave better predictions than the available two-phase models. Later, Ullah (1987) performed a similar study for 1 bbl of liquid per MMSCF of gas, reaching the same conclusions. However, older studies (Gould *et al.,* 1975) and some other authors published similar studies for 10-20 bbls/MMSCF and reported opposite results, concluding that the two-phase-flow correlations are better to predict pressure drops and fluid properties in two-phase systems. One clear point derived from this discussion of results is that the correlations are very sensitive to the flowrates, flow profile and fluid properties (Asante, 2000).

In a study performed by Waly *et al.* (1996) the authors evaluate a model that uses a revised Beggs and Brill correlation, and the Aziz and Govier correlation, as the best fit for an

eight wells field. The authors conclude that high gas/liquid ratio wells (greater than 1500 SCF/STB) were best modeled using the Aziz and Govier multiphase correlation, while the low gas/liquid ratio wells (less than 1500 SCF/STB) were best modeled using the revised Beggs and Brill multiphase pressure-drop correlations. Finally, they conclude that for high pressure drops the best modeling fit was obtained using the Olieman's multiphase pressure drop correlation, whereas for the low pressure-drop wells the best modeling correlation was that of Mukherjee and Brill (1985).

Depending on the pressures, fluid properties and fluid velocity, the flow pattern might vary. According to this variation, flow pattern maps can be developed. Baker (1954) was a pioneer in developing fluid-flow maps for horizontal systems. Recent work on flow-pattern maps has been published by Ahmed Fazeli (2006). This author developed a computer code (FLOPAT) that allows the generation of such flow-pattern maps.

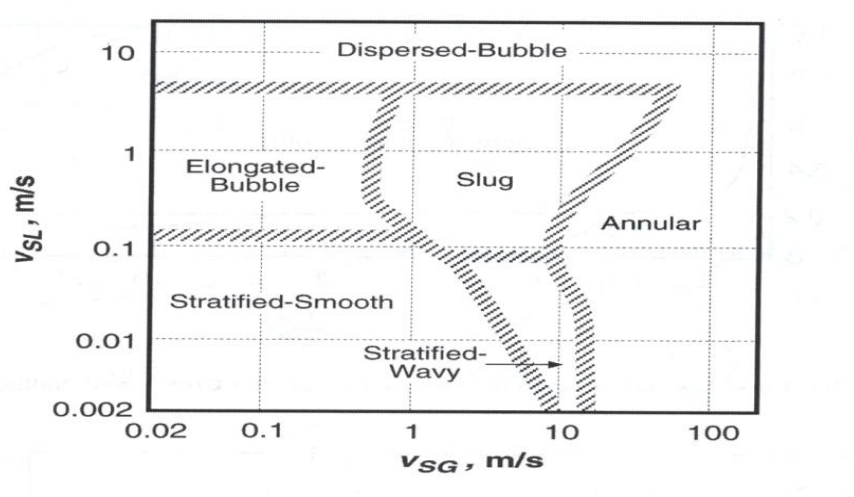

Figure 1 Flow-pattern map for horizontal pipes (reproduced from Mandhane 1974)

Current models are based on the physical mechanisms which determine the transition between the different flow regimes. Figure 1 shows a sample flow map for horizontal pipes. If the pipe position is changed from horizontal to an inclined or vertical position, then the flow pattern and map will change as well. Once the flow pattern is defined and the transition zones identified, it is possible to estimate the physical properties for the fluids and in addition their behavior inside the pipe can be predicted. Although the idea of using flow maps to describe the flow regimes prevailing for different phase-velocity conditions is useful, the fact remains that such maps are not universal, but rather apply to specific existing conditions, geometric or otherwise.

An important fact which has been sufficiently reported is that each equation developed to study and analyze multiphase flow across pipelines or annulus, uses several assumptions and some of them work for horizontal flow, some others for vertical flow and finally some others work for inclined flow (always considering the three main energy components: acceleration, elevation and friction, as will be discussed in later sections. Further, formulations work for certain types of flow according to the region of the flow map that they fall on, as can be seen in Figure 1. A remarkable finding is that the approach that generally works best is the Beggs and Brill correlation. Since the objective of this research is to develop a model with the most general application and accepted principles, Beggs and Brill was the correlation selected to be used.

Hein (1985) established that one of the energy methods used to evaluate pressure drop is the Beggs and Brill correlation. The author changed one of the lower limits for the liquid holdup value to 10^{-6} (for convenience purposes) which differs from the one previously established by Beggs and Brill (10^{-5}). This is brought out here to confirm that even though Beggs and Brill is the most general procedure that can be used to model two-phase pressure drop in a single pipeline, it has some limitations, and therefore different researchers have tried to improve on it.

Since there are several and different flow patterns, when a system contains more than one phase it is understandable that phases can move at a different speed. However, a common simplification used when working with pipeline network systems is to assume that both phases move at the same speed. But the truth is that different phases do not move at the same speed and therefore it is important that Beggs and Brill accounts for slippage between the phases. Chapter 4 includes a formal classification for the flow profile phenomenon.

As the fluids continue their movement through the network, there are constraint points such as the branching conduits, generally known as T junctions, where the fluid either can split into two different flowstreams or merge with another, until the exit point is reached. At the Tee junction the fluid will experience a volume expansion and therefore a pressure drop that can lead to condensation of the liquids present in the gas phase. Since the fluid is moving along the pipe it has certain inertia, and when the second phase (liquid) appears, or the injected liquid approaches the junction, some liquid will continue with the inertia of the original flow path but some other will follow a different path. This phenomenon is well known, and has been named fluid flow route selectivity.

Regarding the fluid stream splits when reaching tee-junctions in pipeline network systems, development has proceeded from even-split concepts, to Kinetic-Energy concepts, and finally to Dual-Stream approaches. Thus, Shoham *et al.* (1987) developed a geometrical model that is hard to apply and not always consistent with experimental findings. Also Azzopardi *et al.* (1989) developed a phenomenological model to predict the split in horizontal and vertical pipes. However this model is not always accurate. Hart *et al.* (1991) established that the only time when a fluid can split evenly in a tee or junction is when the kinetic energy ratio value is close to unity, which is very unusual since the split at the tee depends on several factors such as: mass flowrates and fluid properties (gas and liquids), interaction between phases (surface tension) and gas liquid contact angle as well as pipe diameters (inlet, run and branch), roughness of the pipe and angle at the junctions. Hart (1991) proved that the effect of an uneven split is more remarkable in systems with a very small amount of liquids, meaning holdups less than 0.06 (λ_L<0.06). A T-junction is characterized by joining a set of three flow lines shown as equal-diameter inlet, run and branch arms. According to the position of the arms, a Tee can be classified as shown in Figure 2.

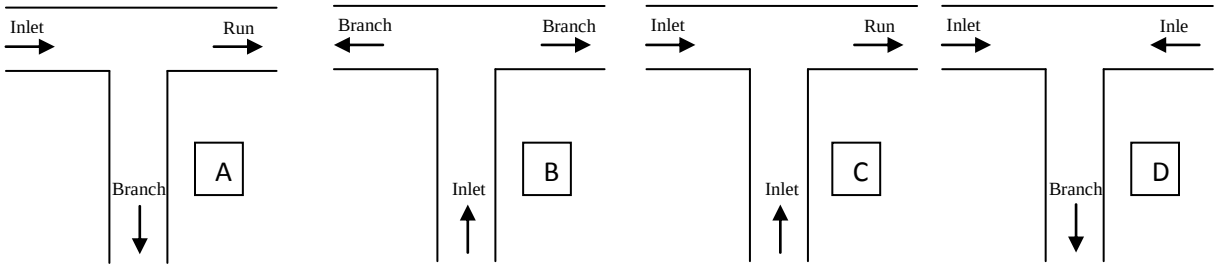

Figure 2 Tee-junction classification, A) Splitting tee B) Splitting impacting tee, C) Converging tee D) Converging impacting tee

According to Hart *et al.* (1991) to fully understand the flowstream splitting phenomenon it is important to consider the following parameters as the flow enters the Tee: mass flow rates of gas and liquid in the inlet, which will help to formulate the material balance for the entire system; densities and viscosities of gas and liquid; as well as surface tension and gas-liquid-solid contact angle, which will be used to handle the fluid superficial velocities and mixture velocity. Diameters at inlet, run and branch, will have an impact on the pressure drop when the fluid reaches the T. Other parameters of interest are the inclination angles of the main pipe and the side-arm, angle of the junction, radius at the connection between the main pipe and the branch (sharp edged or radiused). All these parameters will have an impact on the estimated value for the split factors.

For this research project, the split calculations are handled in three different ways, allowing the user of the newly developed model to select the most convenient procedure according to the system specifications and the desired approach, and also allowing comparison with commercial simulators. The three methods are:

Even Split: This method is used by commercial simulators such as PIPESIM and other previously developed codes (Adewumi, 1994).

Split factor based on Kinetic Energy ratios: In reality, the fluid split which occurs at the junction depends on several factors including fluid flow and geometrical properties, and it is rarely even. This simplified model calculates the kinetic energy ratio as the primary term governing the split and neglects the effect of other parameters such as irreversibilities and geometrical factors.

The Dual Stream Model (DSM): One of the models used for handling the split factors in branches or junctions was proposed by Hart *et al.* (1990) and is known as the "double stream model (DSM)". DSM is based on energy-balance equations for the gas and liquid phases. This model uses Gardel correlations (1957) for the calculation of irreversibilities originally proposed for the single-phase system. This model was later improved by Ottens *et al.* (2001), and renamed Advanced Double Stream Model (ADSM).

Later Shoham (2005) published a text that summarizes the variables involved in two-phase flow as follows: mass and volumetric flowrates for liquid, gas and mixture; liquid holdup (H_L) and gas void fraction (α); superficial velocities (V_{sl} and V_{sg} in ft/s), mixture velocity, mass flux (G), actual velocities, slip velocity, drift velocity, drift flux, diffusion velocities, quality, mass concentration, slip holdup, slip density, and average fluid properties. These parameters where incorporated to the Tee junction analysis by Singh (2008), Alp (2009) and Fernandez Luengo (2010).

In several papers, texts and commercial software documentation, it is clear that the single-phase problem has been solved with adequate precision and that accurate pressure drops and flow distributions can be determined with well established routines. However, the same is not true for two-phase and multiphase flow. In fact, the two-phase flow phenomenon is much more complicated than the single-phase is.

As part of the past developments for handling the problem of two-phase flow in complex gas transport networks, Adewumi *et al.*(1991) worked on single-phase and multiphase systems

applying the linear theory method which converts the nonlinear flow equations of the multiphase problem into a linear system. In two published papers Adewumi (1991 and 1994) uses the most common equations Weymouth, Panhandle A and Panhandle B for the single-phase gas problem and the Beggs and Brill correlation for the multiphase case. Further, they were combined with the electric circuit analogy using the first and second Kirchhoff's law for electrical circuits. Then, the energy and mass-balance equation can be solved for different flow profiles. This is a common ground between Adewumi's work and the present research. However, the main difference between Adewumi's approach and the current research is that Adewumi does not address the split factor for the multiphase flow at the tee junctions. The handling of T-junctions and uneven split factors (dual stream) used in the current research will be discussed in following sections.

On the other hand, commercial simulators such as PIPESIM (2007) assume Even Split at the Tee junctions. This is an unrealistic assumption which leads to allocating water in the entire system, and predicts higher pressure drops in pipes where there is no water and lower pressure drops in pipelines with a high content of water, which again is an unrealistic situation. Until 2007 marching algorithms were the rule rather than the exception in the determination of pressure distribution in long multiphase-flow pipes, and they are the basis of most two-fluid models. However Kehlner *et al.* (2007) opened the possibility to explore if there are cases where marching algorithms are not adequate. In Chapter 4 we will confirm that the governing equations for the multiphase flow are nonlinear. Therefore, it is not desirable to use a marching algorithm which will divide a single pipe into multiple small pipes or blocks. Instead it is recommended to solve the entire system simultaneously, at one time, which is now possible with iterative algorithms such as Newton Raphson. This is one of the contributions of the current work.

It is well known that improvements of the gas pipeline distribution network can significantly decrease the operational cost of systems already installed, as was demonstrated by Sung *et al.* (1998), Krishnamurthy (2008), Alexis (2009). The final stage of the present work will be to test the new model approach on several networks and validate the results.

CHAPTER 3

PROBLEM STATEMENT

Natural gas gathering and production systems often cover significant areas, using a large number of pieces of equipment and pipeline segments, which require a water-liquid free system to perform adequately. This makes it difficult for the operators to effectively evaluate the performance of the network, due to the lack of critical information and the strong interdependence of all elements in the system.

Here a tool that helps map and track the liquid in the system was to be developed, allowing operators to: evaluate single-phase and multiphase systems to detect bottleneck points in the pipeline network, thereby establishing the route selection which optimizes the liquid removal system for the pipeline network, thus maximizing the fraction of pipeline capacity available for gas transportation. This should lead to lowering the expenses and other operational costs required for gas compression.

The objective was to develop and test a model capable of properly distributing liquid paths in a gas pipeline network system. The integrated research product, i.e. the GASNET Two-Phase Model, was tested as independent modules and as a combined product, before final deployment using different networks: Wonmo(1998), the NCL from Center County Pennsylvania, and three additional networks. This allowed the research team to test and evaluate several scenarios.

CHAPTER 4

MODEL DESCRIPTION

4.1 Single-phase flow equations

The governing equations for single-phase flow can be derived by analyzing the energy changes in a fluid that travels inside a pipeline. Equation (1) represents an energy balance in a single pipe that is inclined at a given angle, considering that a change in energy will lead to a change in pressure, which could lead in turn to condensation and phase changes. Let us consider the system of a single pipe as shown in Figure 3.

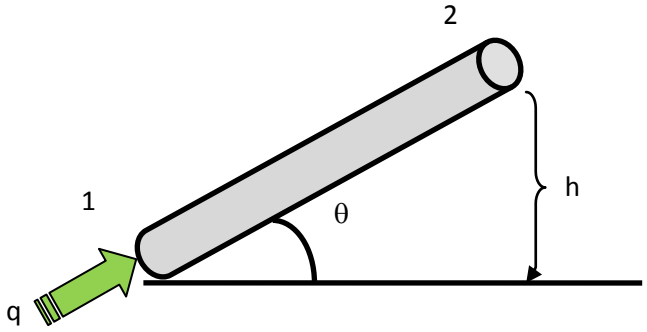

Figure 3 Single pipe at an angle to describe energy changes

The change in energy in the system shown above can be discretized as follows:

$$\Delta E = \Delta E_{Potential} + \Delta E_{Kinetic} + \Delta E_{Friction} \tag{1}$$

Considering that the change in energy is nothing more than a change in pressure in the system. Equation (1) can be rewritten in a differential form as shown in Equation (2):

$$\left(\frac{dP}{dX}\right)_{Total} = \left(\frac{dP}{dX}\right)_{Elevation} + \left(\frac{dP}{dX}\right)_{Velocity} + \left(\frac{dP}{dX}\right)_{Friction} \tag{2}$$

where:

$$\left(\frac{dP}{dX}\right)_{Elevation} = -\rho\left(\frac{g}{g_c}\right) Sin(\theta) \tag{3}$$

$$\left(\frac{dP}{dX}\right)_{Velocity} = -\left(\frac{\rho v}{g_c}\right)\left(\frac{dv}{dX}\right)$$

(4)

$$\left(\frac{dP}{dX}\right)_{Friction} = -\left(\frac{2f\rho v^2}{g_c d}\right)$$

(5)

The pressure drops due to elevation and velocity changes can be considered as reversible pressure drops, since they can be recovered by a change in elevation of the system and change of the velocity; however, pressure drops due to friction are considered irreversible since they cannot be recovered by any natural method.

For the horizontal case the angle will be equal to zero. Therefore, the energy loss due to elevation (Equation (3)) will be equal to zero as well, and the velocity factor will be neglected because it will generally be less than 1% of the friction loss. Hence, the final expression for pressure drop will be:

$$\left(\frac{\partial P}{\partial X}\right)_{Total} = \left(\frac{\partial P}{\partial X}\right)_{Friction} = -\left(\frac{2f\rho v^2}{g_c d}\right)$$

(6)

$$\left(\frac{\partial P}{\partial X}\right)_{Total} = -\left(\frac{2f\rho}{g_c d}\right)\left(\frac{\dot{m}}{\rho A}\right)^2$$

(7)

Here, the density can be replaced using the general gas equation, and can be rearranged to prepare for integrations as shown in Equation (8).

$$\frac{Mw}{\bar{Z}\overline{RT}}\int_{P_1}^{P_2} PdP = -\frac{2f\dot{m}^2}{g_c dA^2}\int_0^L dX$$

(8)

$$\frac{Mw}{\bar{Z}\overline{RT}}\frac{1}{2}(P_1^2 - P_2^2) = -\frac{2f\dot{m}^2}{g_c dA^2}L$$

(9)

Then clearing for $\dot{m}$:

$$\dot{m} = \sqrt{\frac{\pi^2 g_c M w_{Air}}{64R}} \sqrt{\frac{1}{f}} \sqrt{\frac{(P_1^2 - P_2^2)}{\gamma_g L T_{av} Z_{av} L}}\, d^{2.5} \tag{10}$$

Finally replacing

$$\dot{m} = \rho_{sc} q_{sc} \tag{11}$$

$$q_{sc} = K \left(\frac{T_{sc}}{P_{sc}}\right) \sqrt{\frac{1}{f}} \sqrt{\frac{(P_1^2 - P_2^2)}{\gamma_g L T_{av} Z_{av}}}\, d^{2.5} \tag{12}$$

From a thermodynamic energy balance, a fundamental Generalized Gas Flow Equation which corresponds to the general one-dimensional, steady-state isothermal gas-flow equation in pipes is developed and presented as Equation (12). It is based on the following assumptions:

1. Flow is steady state along the pipe length.
2. The flow is assumed to be isothermal.
3. The compressibility of the gas is assumed to have a constant average value.
4. The kinetic energy change in the line is assumed to be negligible (the Kinetic Energy term is neglected).
5. The flowing velocity is assumed to be accurately characterized by the apparent bulk average velocity.
6. The friction factor is assumed to be constant along the pipe segment.
7. The change of pressure with elevation is assumed to be a function of some constant mean density at the mean section pressure.

To better understand the fluid behavior in pipeline networks, a commonly accepted analogy uses electrical systems. If an analogy is made of the movement of flow in one direction to the movement of electrons in a circuit, and the pipelines are analogous to the electric lines connected in such a circuit, it is clear that one might represent flow and pressure drop with an expression analogous to the voltage drop and Ohm's law as shown in Equation (13).

$$V = IR \tag{13}$$

The equivalent expression for pressure drop in hydraulic systems is as follows:

$$(P_1^2 - P_2^2) = R_{es} q_{sc}^n \tag{14}$$

$$q_{sc} = C(P_1^2 - P_2^2)^{1/n}$$

$$q_{sc} = C(P_{US}^2 - P_{DS}^2)^{1/n} \tag{15}$$

where R_{es} is the pipeline resistivity [psi/scf], C is the pipeline conductivity [scf/psi], and P_{US} represents the pressure in the upstream end of the pipe segment whereas P_{DS} represents the pressure in the downstream end of the pipe segment.

Several operational equations are derived from the general gas flow equation, such as the Colebrook-White Equation, Modified Colebrook, AGA (Menon, 2005) and others. However, the most common ones used in the gas industry are the Weymouth, Panhandle A and Panhandle B equations. Therefore, they are the ones that will be addressed and discussed from here onwards.

For every system, several elements will be handled such as nodes, pipes and T-junctions (node-connecting elements) and loops. The equations can be written for every pipe of the system and will then allow formulating a system of equations for an entire network as shown in Figure 4. Since the system shown will be analyzed under steady-state conditions, the following rule applies:

$$B = L + N - 1 \tag{16}$$

where:

B Pipes or branches (Node-connecting elements, also known as bridges)

N Nodes (Junctions that connect two or a maximum of three pipes)

L Loops (Closed-circuit network of pipes and nodes)

Further, after establishing the analogy with the electric circuit, and since every element of the system will have resistance and conductance, it is possible to propose that the use of an expression such as Kirchhoff ‘s Law (for voltage drop) to estimate the pressure drop for the system is a valid approach.

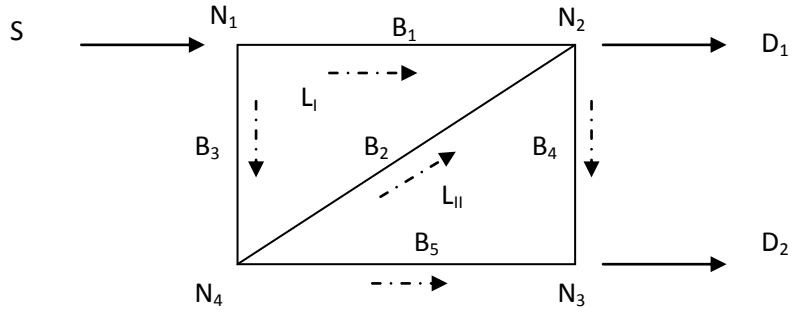

Figure 4 Two-loop network (S) indicates supply (D) indicates demand (B) indicates pipe and the dashed arrows indicate assumed flow direction

For the above mentioned case, there are two ways to solve the entire network:

Flowrate (Q) formulation: It means that the system will be solved using material balance for the flowrate and then calculate the pressure drop through every pipe, and assuming flow in the direction of the dashed arrows direction, the following system of equations applies:

Node equations:

N_1: $S - q_1 - q_3 = 0$

N_2: $q_1 + q_2 - q_4 - D_1 = 0$

N_3: $q_4 + q_5 - D_2 = 0$

N_4: $q_3 - q_2 - q_5 = 0$

(17)

A review of these equations leads one to conclude that the balance on node 4 is a linear combination of the expressions for nodes 1, 2 and 3 ($N_4=N_1+N_2+N_3$) and that it is not an independent equation. Therefore, it is not possible to use that expression to solve the system. Hence, it will be necessary to develop two more independent equations to solve the system for a unique solution. Those required equations are loop equations, and correspond to Kirchhoff’s Law applied to hydraulic flow (for estimating the pressure drop) as indicated above, and they are as follows:

L_I: $R_1 * q_1^n - R_2 * q_2^n - R_3 * q_3^n = 0$

L_{II}: $R_2 * q_2^n + R_4 * q_4^n - R_5 * q_5^n = 0$

Loop equations are nonlinear expressions that complete the system of equations that needs to be solved using a numerical protocol such as the Newton Raphson method. Table 1 shows the inventory of equations and unknowns for Figure 4, assuming that Supply (S), Demand (D_1 and D_2) are specified.

Table 1 Number of equations and unknowns for the Q formulation

Unknowns	Equations
q_1, q_2, q_3, q_4, q_5	3 Node Continuity equations 2 Loops Continuity equations
Total: 5 unknowns	Total: 5 Equations
Specifications: 1 Node Pressure, Qg, Qw at inlet and outlet Closure relationships: q_{sc} as P explicit	

Pressure (P) formulation: In this case, the nodal continuity equations are written for each participating node. The resulting system of equations can then be solved in terms of pressures as primary unknowns. Once the system is solved and the pressure in each node is found, the flowrate in each pipe is then calculated using Equation (15). For the sample system shown in Figure 4 the system of equations is as follows:

Node equations:

N_1: $S - C_1(P_1^2 - P_2^2)^{1/n} - C_3(P_1^2 - P_4^2)^{1/n} = 0$

N_3: $C_4(P_2^2 - P_3^2)^{1/n} + C_5(P_4^2 - P_3^2)^{1/n} - D_2 = 0$

N_4: $C_3(P_1^2 - P_4^2)^{1/n} - C_2(P_4^2 - P_2^2)^{1/n} - C_5(P_4^2 - P_3^2)^{1/n} = 0$

(15)

An inventory of the equations needed and unknowns of the system is presented in Table 2 (for the example of Figure 4 with P_2 specified).

Table 2 Number of equations and unknowns in the P Formulation

Unknowns	Equations
P_1, P_3, P_4	3 Node continuity equations
Total: 3 unknowns	Total: 3 Equations (N-1) N: Number of nodes in the system
Specifications: 1 Node Pressure	

It is clear that this P-formulation requires less information from the user than the Q-formulation. On the other hand, it is important to indicate that, in order to solve any of these two systems, an initial direction of flow has to be assumed. Then, the final solution will tell the user if the assumed direction was correct or if flow is in the opposite direction. For simplicity in the logic and coding, the P formulation is used in this study for the entire development of the model. The following sections are devoted to discuss the principles of this implementation.

4.2 Single-phase network solver

As indicated above, and to be able to use the P formulation in combination with Kirchhoff's Law, the next step in the formulation process is to describe the equations that will help to determine the pipe conductivity (Weymouth, Panhandle A and Panhandle B). The corresponding expressions are summarized in Table 3.

Table 3 Parameters used in popular gas equations

Equation	F *	Kf **	C	m	n
Weymouth	$f = \frac{0.008}{d^{1/3}}$	$K_f = \frac{\gamma_g Z_{av} T_{av}}{C^2}\left(\frac{P_{sc}}{T_{sc}}\right)^2$	433.39	5.3333	2.000
Panhandle A	$f = \frac{0.019231}{\left(\frac{q_{sc}\gamma_g}{d}\right)^{0.14}}$	$K_f = \frac{\gamma_g^{0.85} Z_{av} T_{av}}{C^{1.854}}\left(\frac{P_{sc}}{T_{sc}}\right)^2$	435.87	4.8540	1.854
Panhandle B	$f = \frac{0.003586}{\left(\frac{q_{sc}\gamma_g}{d}\right)^{0.03922}}$	$K_f = \frac{\gamma_g^{0.961} Z_{av} T_{av}}{C^{1.96}}\left(\frac{P_{sc}}{T_{sc}}\right)^2$	737.0	4.9600	1.960

*** Equations 18, 19, 20**

**** Equations 21, 22, 23**

$$R_{es} = \frac{K_f L}{d^m} \tag{24}$$

$$q_{sc} = C(P_{us}^2 - P_{ds}^2)^{1/n} \tag{15}$$

$$C = \left(\frac{1}{R_{es}}\right)^{1/m} \tag{25}$$

where:

C	Pipe conductivity	[scfd/psi]
d	Internal diameter	[in]
m	Diameter power	[dimensionless]
M_{wair}	Air molecular weight	[29 lb/lbmol]
n	Flow power	[dimensionless]
P_{SC}	Pressure at standard conditions	[14.7 psia]
P_{DS}	Pressure downstream	[psia]
P_{US}	Pressure upstream	[psia]
q_{sc}	Flowrate	[scfd]
R	Universal gas constant	[10.731 psia R/(ft^3lbmol)]
R_{es}	Resistivity of the pipe	[psi/scfd]
T_{AV}	Average temperature	[R]
T_{SC}	Temperature at standard conditions	[520 R]
Z_{AV}	Average compressibility factor	[dimensionless]
γ_g	Specific gravity of the gas	[dimensionless]

For application in the single-phase mode, the new model works as follows:

The program starts initializing the constant values; reads and extracts all the required information from an input file (the sample input file format is included as APPENDIX A). As the next step, the program will check for input data consistency (i.e. establishing communication between nodes of the system by checking for interconnectivity, fluid and pipes properties are in tolerance, etc.) Once the input consistency checks are completed in a sequential manner, the main part of the model starts to execute.

The execution will continue determining the initial pipe conductivity, according to the user selection and the equations presented in Table 3. After all pipe conductivities are determined, and before proceeding with further calculations, one last test is run: an interconnectivity test to assure that all the elements in the system are connected. At this point the model is ready to solve all the node equations simultaneously. Since the resulting node continuity equations are highly nonlinear in nature, a Newton-Raphson iterative protocol is necessary and is implemented to solve the system of equations.

The Newton Raphson protocol is built to solve a nonlinear system of equations, by determining the derivative of each function of the system (either in an analytical or a numerical way) and will try to find the roots that will satisfy all the equations representing the system under study. The Newton Raphson protocol can be summarized as follows:

1) Assign an initial value of P for each node
2) Enter the Newton Raphson Method
    a. Calculate the residual:

$$q_{sc} = C(P_{us}^2 - P_{ds}^2)^{1/n} \tag{15}$$

the coefficients for n will depend on the single phase user selection according to the Table 3

    b. Introduce perturbation, node by node: $P_{pert}=P+\Delta P^n$
    c. Calculate the residual:

$$q_{Pert} = C(P_{usPert}^2 - P_{ds}^2)^{1/n} \tag{15}$$

    d. Determine the entry to the Jacobian:

$$Jac = \frac{(q_{pert} - q_{sc})}{Pert} \tag{26}$$

a Jacobian matrix is a square matrix whose main entries are composed by all the derivatives with respect to pressure of the equations that conform the system. In that sense, the Jacobian matrix appears as indicated in equation (27) :

$$\begin{bmatrix} \frac{\partial f_1}{\partial p_1} \frac{\partial f_1}{\partial p_2} \frac{\partial f_1}{\partial p_3} \dots & \frac{\partial f_1}{\partial p_n} \\ \frac{\partial f_2}{\partial p_1} \frac{\partial f_2}{\partial p_2} \frac{\partial f_2}{\partial p_3} \dots & \frac{\partial f_2}{\partial p_n} \\ \frac{\partial f_3}{\partial p_1} \frac{\partial f_3}{\partial p_2} \frac{\partial f_3}{\partial p_3} \dots & \frac{\partial f_3}{\partial p_n} \\ \dots & \\ \frac{\partial f_n}{\partial p_1} \frac{\partial f_n}{\partial p_2} \frac{\partial f_n}{\partial p_3} \dots & \frac{\partial f_n}{\partial p_n} \end{bmatrix}^k \begin{bmatrix} \Delta p_1 \\ \Delta p_2 \\ \Delta p_3 \\ \dots \\ \Delta p_n \end{bmatrix}^{k+1} = - \begin{bmatrix} f_1 \\ f_2 \\ f_3 \\ \dots \\ f_n \end{bmatrix}^k \tag{27}$$

where the first matrix in the left-hand side is the Jacobian matrix, the second matrix is the differential matrix and the matrix in the right-hand side is the residual matrix. After every iteration, improvements are applied to the residual matrix, and the iteration process will continue until convergence. Then the process continues with the following steps:

e. Remove the perturbation for the node and move on to the next node.
f. Check that the main diagonal of the Jacobian is not zero, and Jacobian normalization.
g. Solve the Jacobian.
h. Update the value of P in each node.

3) If convergence is achieved, meaning that the node`s pressure was found and the residual value is close to zero, the model will display a message indicating the pressure at each node, flow for each pipe and pipe conductivity. Then the model proceeds to calculate the pressure drops due to the presence of the second phase. If convergence has not been achieved, step 2 is repeated with the updated pressure values.

4.3 Pressure drop in multiphase system

Several authors have worked on pressure drops due to multiphase flow in pipelines, developing specific procedures such as: Poettmann and Carpenter (1952) who were attempting to solve the multiphase flow issue, then Orkiszewski, Duns and Ros (1963) used mostly for mist flow, Hagedorn and Brown (1965) used mostly for bubbly and slug flow, and Beggs and Brill Correlation (1976) which has become the most widely used correlation for the multiphase flow case and therefore is the one that this thesis will focus on. APPENDIX B presents a detailed procedure for the implementation of the Beggs and Brill model.

As discussed in APPENDIX B as preliminary step in the pressure-drop calculations due to two-phase flow, the flow pattern in each pipe is determined based on the non-slip liquid holdup and Froude number. The flow pattern can be classified as Segregated, Distributed, Intermittent and Transition as shown in Figure 5, Figure 6 and Figure 7.

4.3.1 Segregated flow: This is the flow process of two phases of liquid and vapor that have been separated due to the gravity effect. As soon as the fluid velocity increases, the profile will change from stratified to wavy; then if the flow rate is higher the flow profile becomes annular.

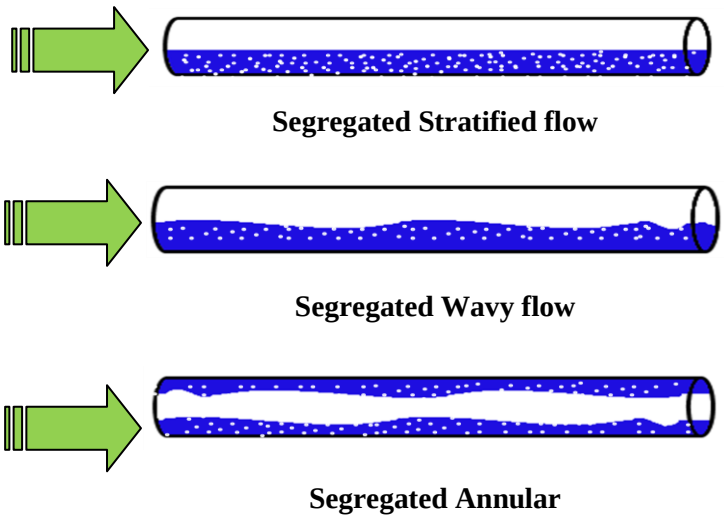

Figure 5 Segregated flow regimes
(The blue color represents the liquid portion of the flow, and the rest is vapor)

If the fluid velocity keeps increasing, the flow pattern evolves from segregated flow to intermittent flow.

4.3.2 Intermittent flow: In this case, the fluids will not be as separated as in the segregated pattern, but rather there will be some batches of one fluid or another as shown:

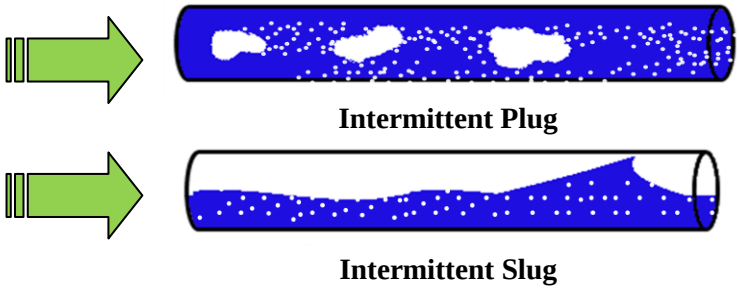

Figure 6 Intermittent flow regimes
(The blue color represents the liquid portion of the flow, and the rest is vapor)

At maximum fluid velocity, the flow regime can be identified as distributed bubbly or distributed mist.

4.3.3 Distributed or bubbly flow: In this case the high fluid velocity forces the gas to be transported by the liquid in the form of bubbles, drops or mist as shown below:

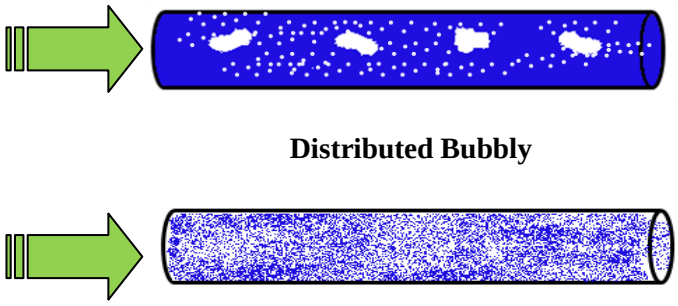

Figure 7 Distributed flow regimes
(The blue color represents the liquid portion of the flowstream, and the rest is vapor)

Since the change in the flow profile due to the velocity increase does not occur immediately, it is reasonable to think of one more possible flow regime: Transition flow.

4.3.4 Transition flow: This condition occurs when the flow pattern, due to the velocity profile, can be placed between segregated-intermittent or intermittent–distributed flow.

Regardless of the fact that one can describe the flow profile according to the Reynolds number as laminar, turbulent or transitional, the Beggs and Brill procedure will use the classification indicated above (Figure 5, Figure 6 and Figure 7) but only with the general classification (segregated, distributed, intermittent or transitional).

Once the flow pattern has been recognized, fluid properties are recalculated (liquid, gas and mixture densities ρ_l, ρ_g, ρ_m [lb/ft^3], volumetric flowrates and mixture velocities, gas and liquid fractions and gas and liquid slippage holdup for horizontal and inclined pipes). Then the friction gradient, elevation gradient and kinetic gradient are determined to calculate the two phase pressure drop with Equation (28).

$$\frac{dp}{dz} = \frac{\left(\frac{dp}{dz}\right)_{el} + \left(\frac{dp}{dz}\right)_{fric}}{1 - Ek} \tag{28}$$

This equation takes into consideration the angle of elevation which will be determined from the length of the pipe, and an elevation parameter. However, not only are the pipe elevations and angles important, but also important are the angles for the different branches. This will become apparent in the next section of this Chapter 4.

Based on the pressure drop calculation (dp/dz) above, and the known values of upstream pressure (P_{US}), the downstream pressure (P_{DS}) is calculated. The two-phase gas pipe conductivity can be determined using Equation (29):

$$C_g = \frac{q_{gas\ pipe}}{(P_{us}^2 - P_{ds}^2)^{1/n}} \tag{29}$$

Since the flow of gas becomes hindered due to the presence of the second phase, the newly updated pipe capacities (i.e., two-phase pipe gas capacities) are expected to be lower compared to their single-phase counterparts. Once the pipe capacities are updated, the flow rates of the gas in all the pipes in the system are recalculated based on the new nodal pressures obtained from the Beggs and Brill subroutine.`

The Beggs and Brill correlation was developed from experimental results in a system of 90 ft long transparent acrylic pipes with diameters between 1 and 1.5 in, gas flowrates between 0.0 to 0.3 MMscfd, and liquid flow rates between 0 and 30 Gal/min. Average pressure between 35 to 95 psia, pressure gradients from 0.0 to 0.8 psi/ft, liquid holdup fractions from 0 to 0.870 and inclination angles between -90° to 90°. Its application has been extended to the whole spectrum of flow situations that may be encountered in oil and gas operations, namely uphill, downhill, horizontal, inclined and vertical flow, mostly for small diameters up to 7 in, low and high pressure drops. The Beggs and Brill model is frequently used and cited by researchers as the best known and reasonably accurate multiphase flow correlation in two-phase gas/liquid hydrocarbon systems. It is important to consider that, as with any other empirical correlation, Beggs and Brill is sensitive to properties changes. The farther the properties are from the original values used in their experimental work, the least the expected accuracy of the predictions from the correlation.

4.4 Tee junction treatment

Tee junctions provide the means of connecting three pipes in a network and thus become the basic building block of complex networks. What happens at the T-junction in terms of even or uneven split of phases during multiphase flow regimes largely determines route selectivity of each of the phases in the multiphase network environment. As discussed in Chapter 2 Oranje (1973) was the first to identify this uneven split phenomenon or route selectivity (or preference). As such, properly accounting for this phenomenon is very important since it will affect the design and operation conditions for the surface equipment, installation of separators or dehydrators, and

compressor stations. In a typical T-junction, the different pipe sections making up the tee-junction can be identified as inlet pipe, run pipe and the branch pipe as shown in Figure 8 which also illustrates the concept of split factors, that are used to quantify the uneven split phenomenon at T-junctions.

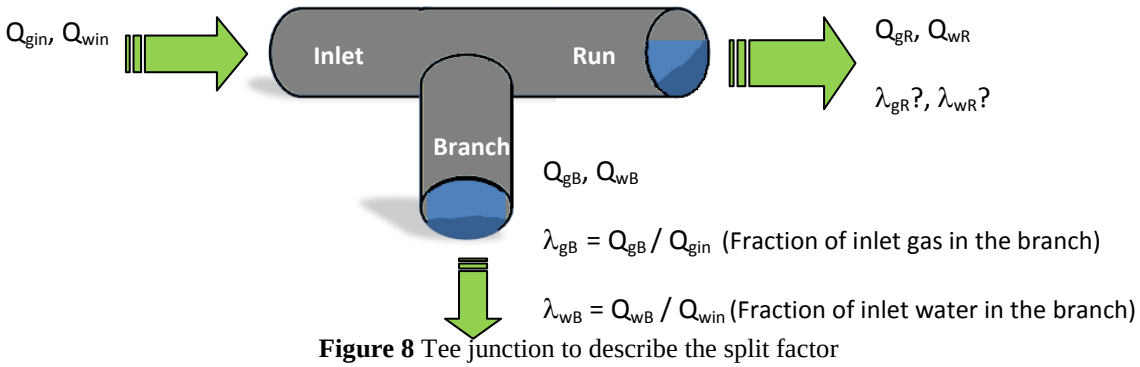

Figure 8 Tee junction to describe the split factor

A convenient way to evaluate and account for the split phenomenon at tees is through the definition of split factors. Split factors are simply defined as the ratio of the amount of phase leaving one of the outlets (either branch or run) to the amount of phase that originally entered the T-junction. Obviously, the split factor can range from 0 to 1 and can be defined for both the liquid (water) and gas phases, as illustrated in Figure 8 and Equation 30. In Figure 8, λ_{gR} and λ_{wR} represent the mass fraction of gas and water flowing through the run of the T-junction with respect to the original volume injected at the inlet. In other words,

$$\lambda_{GB} = \frac{\dot{M}_{gB}}{\dot{M}_{gIn}} \; ; \; \lambda_{WR} = \frac{\dot{M}_{wB}}{\dot{M}_{wIn}} \tag{30}$$

Where

λ_{GR} Run pipe gas mass intake fraction [dimensionless]

M_{gR} Mass flow rate of gas in the run pipe [lb/sec]

M_{gIn} Mass flow rate of gas in the inlet pipe [lb/sec]

λ_{WR} Run pipe water mass intake fraction [dimensionless]

M_{wR} Mass flow rate of water in the run pipe [lb/sec]

M_{wIn} Mass flow rate of water in the inlet pipe [lb/sec]

λ_{GB} and λ_{WB} represent the mass fractions of gas and water running through the branch of the T-junction with respect to the original masses injected at the inlet. That is:

$$\lambda_{GB} = \frac{\dot{M}_{gB}}{\dot{M}_{gIn}} \; ; \; \lambda_{WB} = \frac{\dot{M}_{wB}}{\dot{M}_{wIn}} \tag{31}$$

Note that:

$$\lambda_{GR} + \lambda_{GB} = 1 \text{ and } \lambda_{WR} + \lambda_{WB} = 1$$

but

$$\lambda_{GR} + \lambda_{WR} \neq 1 \text{ and } \lambda_{GB} + \lambda_{WB} \neq 1 \tag{32}$$

It should also be noted that for nearly incompressible fluids such as water, defining the split ratio either as a ratio of mass flow rates or volumetric flow rates does not make a difference. In the case of natural gas split, the split ratio can be defined in terms of a ratio of mass rates or volumetric flow rates as long as the latter is always calculated at standard conditions. For the purpose of this research project, the split calculations are handled in three different ways allowing the user of the program to select the most convenient procedure according to the system specifications and the desired approach.

Case 1: Even Split

As it has been indicated previously, the Even Split approach is the most common way to handle the split in multiphase network models; however, this approach is far from realistic. This method is included here for comparison purposes. The method is used by commercial simulators such as PIPESIM and other previously developed models (Adewumi, 1994), and can be expressed to mean that the liquid mass intake fraction in the branch arm will be equal to the gas mass intake fraction in the branch arm, as implied by the following expression:

$$\lambda_{GB} = \lambda_{WB} \text{ and } \lambda_{GR} = \lambda_{WR} \tag{33}$$

This scenario implies that the T-splits are uniform and that they always occur at equal proportions, i.e., neglecting phase inertia and well-established uneven distribution phenomena at T-junction. Results comparing Even Split with other options are discussed in the next section.

Case 2: Split factor based on Kinetic Energy ratios

The fluid split that occurs at the junction depends on several factors, including fluid properties and the geometrical factors, and it is rarely even. Experimental observations have firmly established that one of the controlling factors in the split is the relative inertia of the phases. When the inertia of the heavy (liquid) phase increases and dominates, its tendency is generally seen to prefer to follow the path of the run (see Figure 8) and miss most of the T-branch. The Kinetic Energy ratio quantifies this relative inertial effect, as shown below:

$$KE_r = \frac{\frac{1}{2}\rho_g v_g^2}{\frac{1}{2}\rho_l v_l^2} \tag{34}$$

This approach calculates the Kinetic Energy ratio as the primary, first-order contributor to the uneven split at junctions, and neglects the effect of other parameters. Based on this approach, the liquid split factor at the branch can be readily related to the gas split factor at the branch through the expression:

$$\lambda_{\mathrm{LB}} = \lambda_{\mathrm{GB}} * KE_r \tag{35}$$

In Equation (35) λ_{LB} cannot become larger than unity, and thus its maximum value is capped at 1. The split factor calculation based on Kinetic Energy ratios can be considered as an intermediate step between the Even Split assumption and the Dual Stream Model, to be discussed next.

Case 3: The Dual Stream Model (DSM)

The Dual Stream Model (DSM) treats the flow of each phase at the T-junction as that of independent streams, allowing the phases to move at different velocities and for the Bernoulli equation to be applied to each phase independently. The model was first proposed by Hart *et al*. (1991) who established that the only time when a fluid can split evenly in a tee or junction is when the Kinetic Energy ratio nears unity, and that for all other cases the split at the tee would

depend on several factors such as mass flowrates and fluid properties, geometric considerations such as pipe diameters (inlet, run and branch), roughness of the pipe and angle at the junctions. Hart *et al.* proved that the effect of an uneven split is more remarkable in systems with very small amounts of liquids, meaning holdups less than 0.06 and proposed a model applicable for such systems. In their model, the characteristic equation that governs the uneven split phenomenon is the extended Bernoulli equation as shown in its general form as Equation (36)

$$\left(P_x - P_y\right)_{LG} + \frac{1}{2}\rho_{LG}\left(W_{LGX}^2 - W_{LGy}^2\right) + \rho_{LG}g\left(Z_{LGx} - Z_{LGy}\right) = K_{xy}\frac{1}{2}\rho_{LG}W_{LG\,X}^2 \tag{36}$$

where the sub-indices have the following meaning:

X Refers to inlet arm,

Y Refers to run or branch arm,

LG Refers to liquid or gas phase.

Using this nomenclature:

P_x Pressure at the upstream end of the inlet arm [psia]

ρ_{LG} Density of the liquid (gas) phase [lb/ft^3]

W_{zy} Root square of the axial velocity of the liquid (gas) phase at the run (branch) arm and [lb/s] depends on the velocity profile and hold up,

K_{xy} Kinetic Energy ratio for inlet-run or inlet branch.

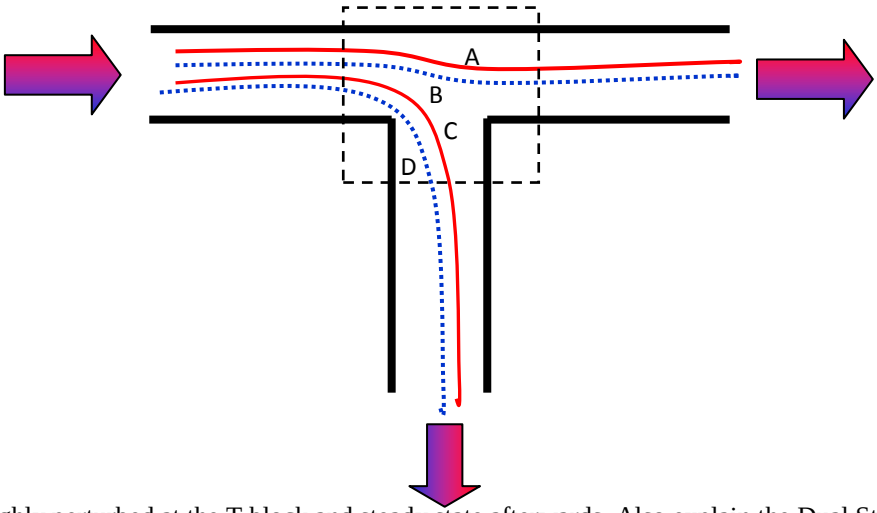

Figure 9 Flow highly perturbed at the T block and steady state afterwards. Also explain the Dual Stream Model (four stream lines) (A) inlet to run gas, (B) inlet to run liquid (C) inlet to branch gas and (D) inlet to branch liquid

By assuming that the phases can be treated independently in terms of the application of Bernoulli's equation (as shown in Figure 9), Equation (36) can be written four times for the four different streamlines (A, B, C, D) shown in that figure. By manipulating these four equations, the authors showed that it is then possible to obtain the equation describing route selectivity, as follows:

$$\frac{\rho_G W_{Gin}^2}{\rho_L W_{Lin}^2}\left[\frac{W_{GR}^2}{W_{Gin}^2}-\frac{W_{GB}^2}{W_{Gin}^2}\right]-\left[\frac{W_{LR}^2}{W_{Lin}^2}-\frac{W_{LB}^2}{W_{Lin}^2}\right]+\frac{2g}{W_{Lin}^2}\left\{\frac{\rho_G}{\rho_L}(Z_{GR}-Z_{GB})-(Z_{LR}-Z_{LB})\right\} = \frac{\rho_G W_{Gin}^2}{\rho_L W_{Lin}^2}(K_{13}-K_{12})-(K'_{13}-K'_{12})$$

(37)

where:

in = Inlet

R = Run

B = Branch

The expression above can also be simplified for splits in horizontal T-junction systems as shown in equation (38). As indicated before and as it is clear from Equation (37), for the DSM it is crucial to know which pipe is on the branch (90 Deg.) and which one is the run. In the proposed model, it is thus required that the user specify the 90 Deg. pipe in the context of each T-junction defined in the network.

$$\lambda_{LB} = \lambda_O + KE_r(\lambda_{GB}-\lambda_O)$$

(38)

where λ_O is a factor that accounts for irreversibilities.

Hart *et al.* (1990) implemented Equations (37) and (38) to relate the liquid branch fraction (λ_{LB}) to the gas branch fraction (λ_{GB}) or gas take-off, through the so-called Route Selectivity Plot presented in Figure 10. The straight lines represent the results using the Double Stream Model (DSM) while the dots represent the experimental results obtained by the University of Amsterdam as quoted in their paper. It can be seen that a very close match is achieved between the experimental and the calculated values. For this project, an improved version of the DSM developed by Fernandez *et al.* (2010) was used. It is important to indicate that in most cases the route selectivity does not follow the Even Split approach incorporated by most commercially available simulators for gas network systems.

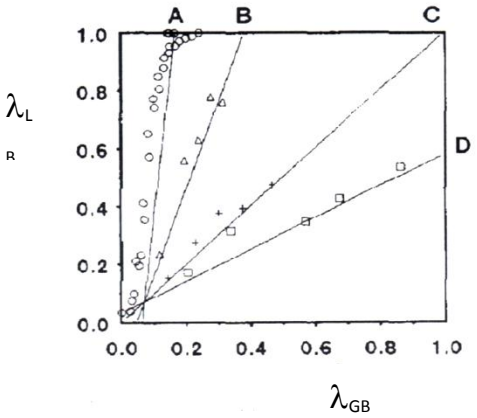

Figure 10 Route selectivity map using Hart's Model, experimental data from the University of Amsterdam (reproduced from Hart *et al. 1991*)

Once the flow paths have been established, flow reversal might occur during the iteration process. The new model is able to identify the flow reversal by evaluating the pressure in each node. If the pressure in the downstream node is higher than the pressure in the upstream node, the flow will move from down-node to up-node and the developed code will put a negative sign in front of the flow. As in the pipes, flow reversal also occurs in the tee junctions, converting a splitting tee or splitting junction into a merging junction. The system can also identify the type of junction by checking the number of neighbor pipes to a Tee node and nodes present in a tee block. If the total number of neighbor pipes connected to a single node is equal to three (3) the node will be marked as a tee junction; then if the total number of downstream flows in a tee junction (DNN) is two and the number of upstream flows is equal to one (UPN) the tee will be classified as a merging tee. On the other hand, if the total upstream flows (UPN) are equal to 2 and the downstream (DNN) flows are equal to one, the tee will be classified as a splitting tee. The possible scenarios can be summarized in Figure 11 as follows:

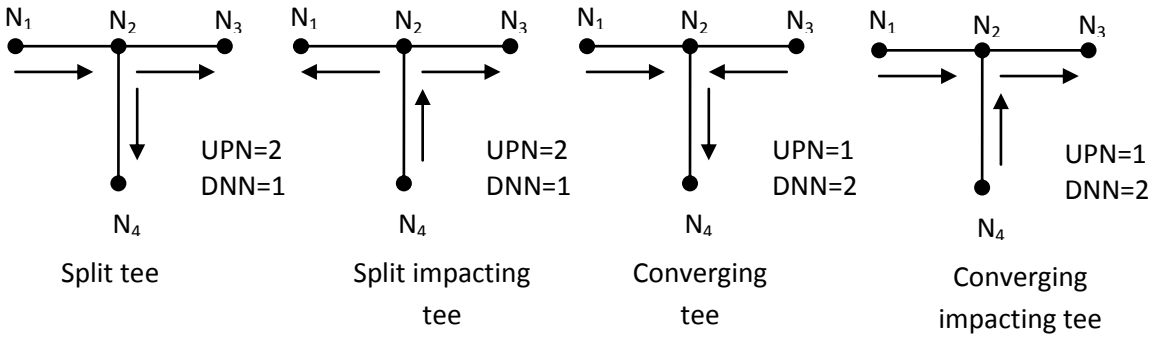

Figure 11 Types of flows entering or leaving a tee junction that will be used in the code for tee classification

There are two more possibilities that can be defined by the user in the input file that will lead to an impossible determination of the system; and they are indicated in Figure 12.

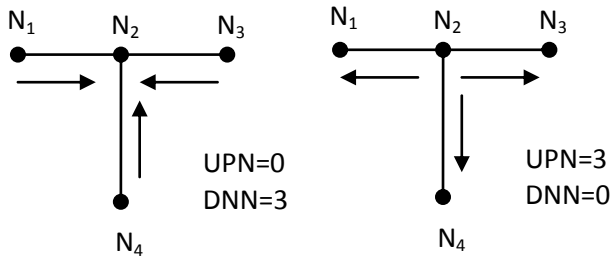

Figure 12 Impossible tee junctions

It is important to note that for the multiphase final program, a multi-junctions system such as the one indicated on node 5 of Figure 13-A represents a computational difficulty as well as an unrealistic situation that can be circumvented as follows. It will be required that the user applies a procedure of conversion into an equivalent system, such as the one shown in Figure 13-B:

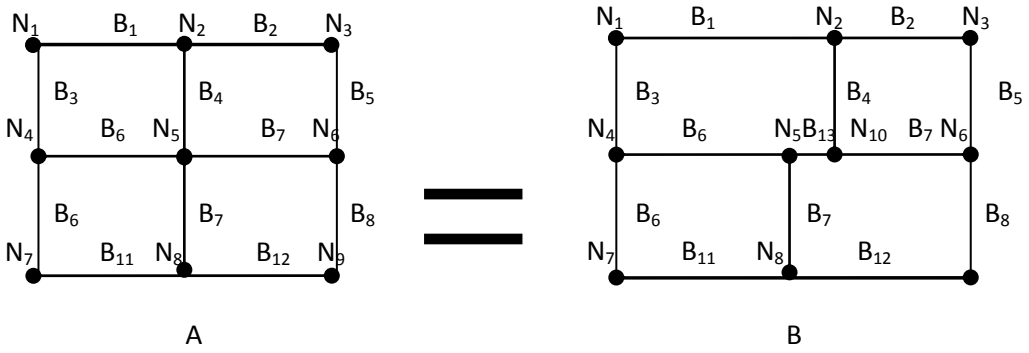

Figure 13 Equivalent system representation to handle multiple junctions

Since the pipes merging at node number 5 can have different diameters, if the diameter of the extra pipe is not known, the smallest diameter on the merging node must be selected.

4.5 Inflow Performance Relationship (IPR)

In any network, the supply nodes can be replaced by producing wells. Changes in pressure losses in surface pipeline networks would affect directly the well performance and its ability to deliver fluids. A common correlation used in the field of gas-well testing to characterize the deliverability from a producing well (Kelkar, 2008) is indicated below:

$$q_{sc} = C_{Well}\left(P_{SHUT}^2 - P_{WH}^2\right)^{nwell}$$

(39)

where,

$q_{SC:}$ Gas production flowrate [mscfd]

C_{well} Well performance constant, a function of rock and fluid properties, formation thickness, external boundary radius and wellbore radius [mcfd/psi^{2nwell}]

P_{SHUT} Well head shut in pressure at the average reservoir pressure [psia]

P_{WH} Flowing well head pressure [psia]

n_{well} Value to characterize turbulent or laminar flow of fluid and varies between 0.5 and 1.0 with 0.5 representing completely turbulent flow and 1 representing completely laminar flow.

In the GASNET Two-Phase Model, an IPR option can be activated as per the user request, in the nodes section of the input file. APPENDIX A shows clearly how the information should be included in the input file in order for the IPR option to work. The user should provide IPR parameters (C_{well}, P_{SHUT}, P_{WH} and n_{well}) if the IPR option is selected. If the pressure requirements are equal to the shut-in pressure, the well located in such a node will cease to flow.

4.6 Model integration

The main goal for the present work is to combine the widely used Beggs and Brill simulation to the single phase model, converting the single-phase simulation into a two-phase model. Then, by incorporating proper water-splitting conditions proposed by Hart *et al.* (1991) and already tested by Martinez (1994), Alp (2009) and Fernandez Luengo (2010), the model would be capable to help the operators to effectively track the water in the entire network.

As previously discussed, the starting point for the proposed model development is the definition of the network connectivity information (as required by the input file and shown in APPENDIX A) and the development of consistency checks of the input data. Then, a single-phase network model is solved (Section 4.2) using the universal gas flow equation with the corresponding flow equation options (Weymouth, Panhandle A, Panhandle B) and the iterative protocol of Newton Raphson. Then a two-phase split factor is calculated according to the user's selection. Once two-phase-flow conditions are invoked, the Beggs and Brill module is used to determine the two-phase pressure drop and the new two-phase pipe capacity (Section 4.3). Three options are made available to handle the split at the Tee junctions: Even Split, Kinetic Energy Model and the Dual Stream Model (DSM) that will run according to the user input (Section 4.4)

for the determination of fluid distribution. The resulting system of equations is solved using a multivariate Newton Raphson subroutine and an iterative process. Each time new pressures are found, the system will recalculate fluid properties and two-phase pipe conductivities. The cycle continues until pressure convergence is achieved, according to the flow diagram presented in Figure 14.

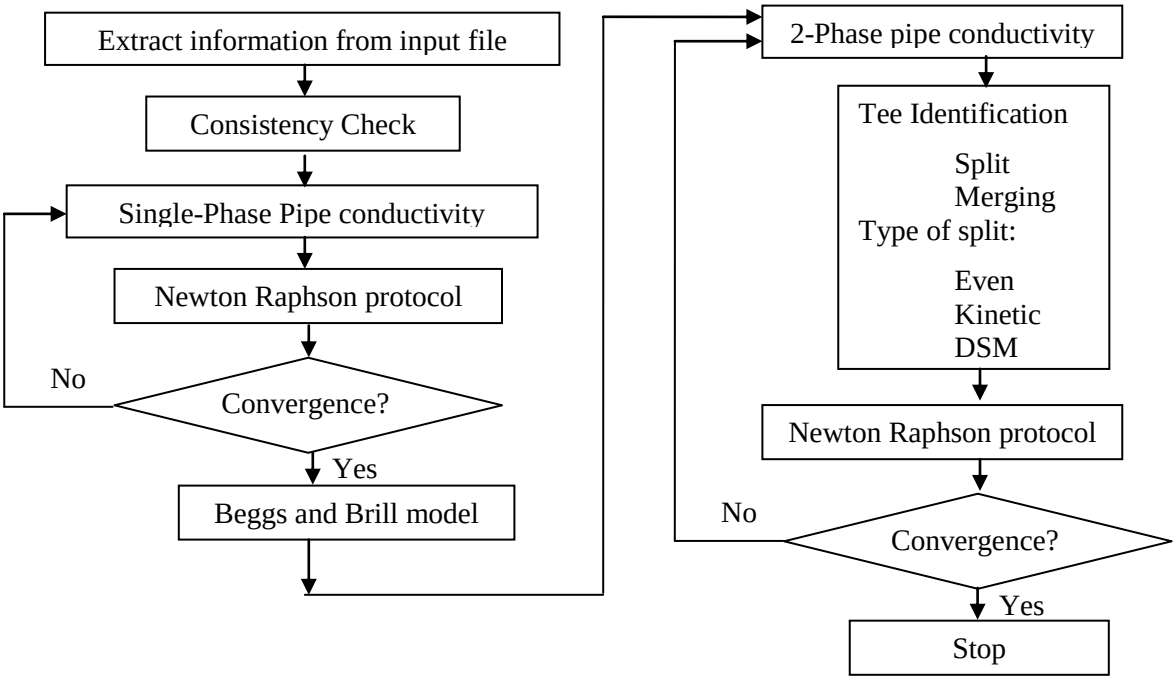

Figure 14 Flow diagram of GASNET two phase

With the entire model integrated and each of its individual sections validated independently, the capabilities of the proposed tool were tested using the scenarios discussed in Chapter 5. APPENDIX A discusses the typical structure of the input file required by the proposed model.

CHAPTER 5

RESULTS AND DISCUSSIONS

Several networks were deployed for study as part of the testing and validation process. Model predictions were compared with PIPESIM predictions for the cases of single phase and Even Split, and the results are shown and discussed below.

Network 1

The first model tested is depicted in Figure 15. It is important to note that the presence of nodes with more than three connected pipes is an unrealistic situation since most pipe connections in actual networks are accomplished through T-junctions—that is, 3-pipe connections. Hence, a more realistic representation of the network in Figure 15 is shown in Figure 16. Some of the operating conditions for this network are presented in Table 4, and detailed input files are found in APPENDIX A and APPENDIX C. It is important to note that liquid demands cannot be specified, since their determination represents the primary objective of the water distribution prediction model. Given the desired gas demand information, the model would be able to pinpoint resulting liquid preferential routes within the network.

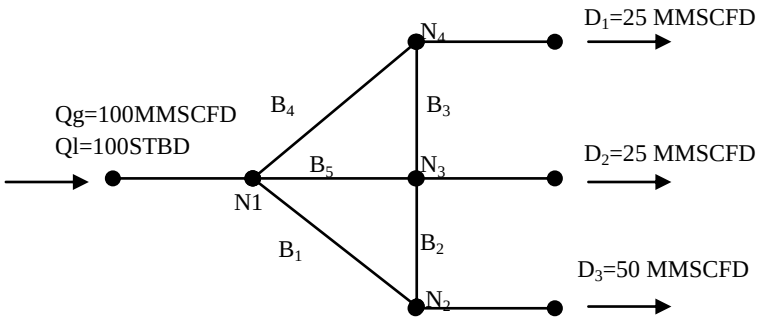

Figure 15 Model of the Network 1 solved for two phases (10 nodes 11 pipes 2 loops)

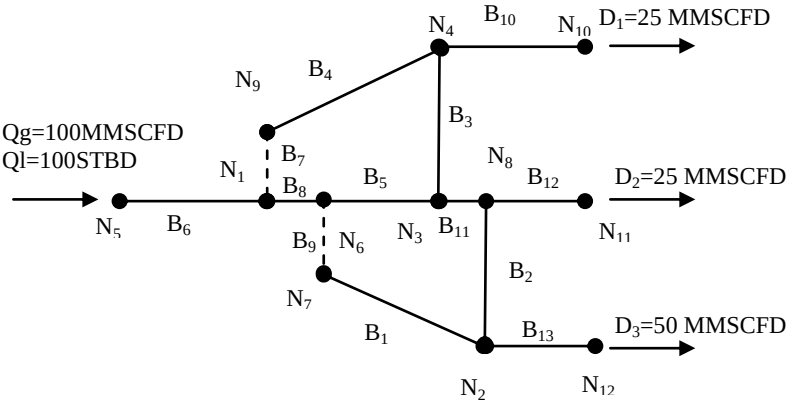

Figure 16 Equivalent model for Network 1 solved for two phases (12 nodes 13 pipes 2 loops)

Table 4 Operating conditions for Network 1

Number of Pipes			13	**T average of the system**			82 [F]
Number of Nodes			12	**Flow efficiency**			1 [-]
Number of Loops			2	**Pipe Roughness**			0.0006 [in]
Supply and Demand Information				**Gas Comp. Factor (Z)**			0.8900 [-]
Node	5	**Supply q_g**	100 [MMscfd]	**Gas Specific Gravity**			0.6200 [-]
Node	5	**Supply q_L**	100 [STBD]	**Gas Viscosity**			0. 0127 [cp]
Node	10	**Dem. q_g**	50 [MMscfd]	**T_{SC}**	60 [F]	**P_{SC}**	14.7 [psia]
Node	11	**Dem. q_g**	25 [MMscfd]	**Liquid Density**			62.4 [lb/ft^3]
Node	12	**Dem. y q_g**	25 [MMscfd]	**Liquid Viscosity**			0.8566 [cp]
Node	10	**P Specif.**	400 [psia]	**Surface Tension**			59.6667 [dynes/cm]

Pipe	**Diameter [in]**	**Length [ft]**	**Pipe**	**Diameter [in]**	**Length [ft]**
1	10.0	198000	7	2.0	1
2	8.0	99000	8	2.0	1
3	6.0	99000	9	2.0	1
4	8.0	198000	10	4.0	10
5	10.0	171600	11	2.0	1
6	4.0	10	12	2.0	10

Network performance results using the proposed model (GASNET) and a commercial simulator (PIPESIM) are presented in Figure 17, Figure 18 and Figure 19. Figure 17 shows the performance comparison when single-phase conditions are assumed throughout the network and incoming liquid rates are ignored. In this figure, the left-hand-side plot shows pressure predictions (Y axis representing pressure and X axis representing node numbers). The right-hand-side plot in Figure 17 displays the predicted gas distribution in each pipe as forecasted by PIPESIM (in black) and GASNET (in red). For the single phase case, the range of differences between GASNET and a commercial simulator is found between 0.0 to 4.5% for the pressure

drop with an average of 3.6%. For the gas flow distribution calculations, the differences range is found between 0.0 to 25.4% with an average of 4.6%.

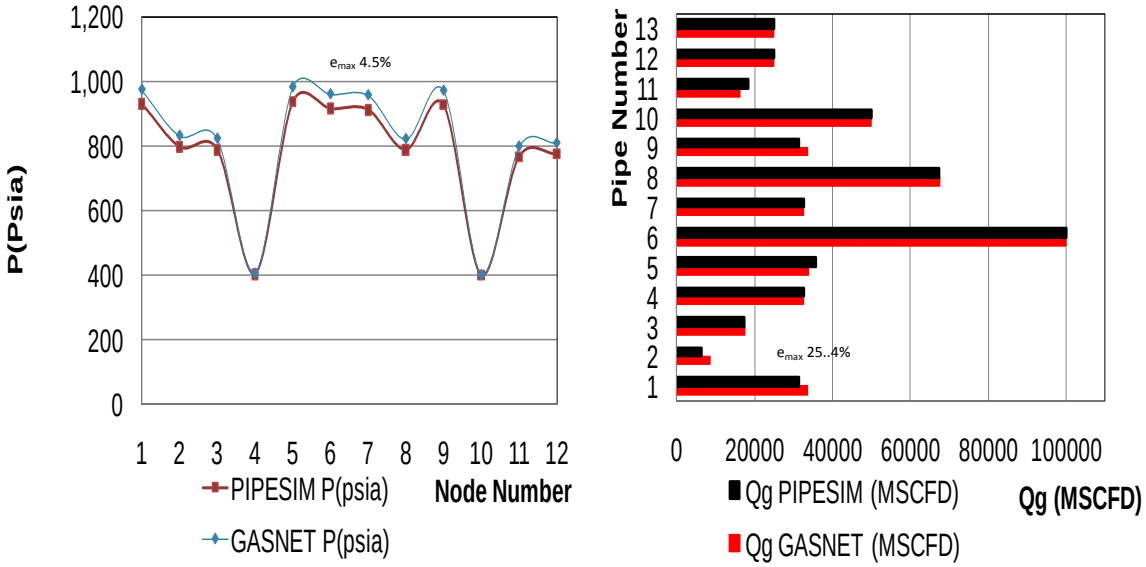

Figure 17 Results for single phase simple gas network system. Run with GASNET (single phase) and PIPESIM (12 nodes 13 pipes 2 loops)

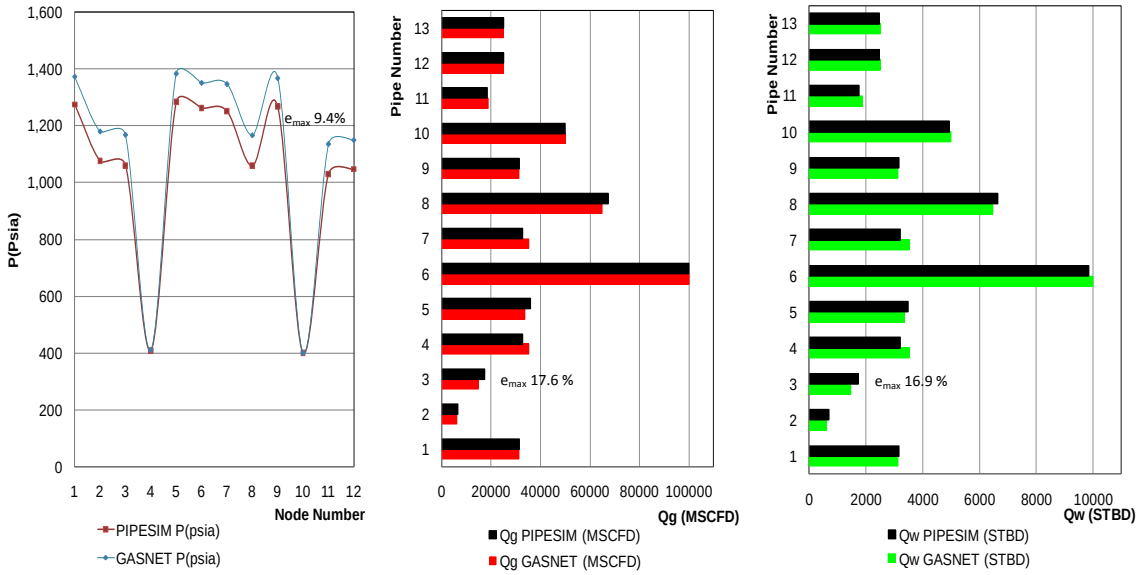

Figure 18 Results for two phases of simple gas network system. Run with GASNET (Even Split) and PIPESIM (12 nodes 13 pipes 2 loops)

Figure 18 and Figure 19 present performance results for Network 1 when two-phase flow is considered. In both cases, the simulation results from the commercial simulator are the same; while the proposed model (GASNET) is shown in different modes. In Figure 18, GASNET

assumes Even Split at all junctions (Case 1 discussed above) and in Figure 19, a more realistic case of Kinetic Energy ratio split (Case 2) is considered. It is clear that a good match between the models is achieved only in Figure 18. For this case, the pressure drop differences range is found between 0.0 to 9.4% with an average difference of 6.8%. The gas distribution values differences range is found between 0.0 to 17.6% with an average difference of 3.9%, and for the water distribution calculations the differences range is found between 1.4 and 16.9% with an average difference of 5.4%. These results demonstrate that the even-split assumption is the basic building block of commercial simulators. Figure 19 shows, however, what happens when more realistic cases are considered (Kinetic Energy ratio split). While pressure predictions are not significantly different, in this case the differences range is found between 0.0 to 14.8 % with an average difference of 7.3%. There is a clear difference in the gas and water distribution, the differences range can be found between 0.0 to 102.5% with an average of 19.3 % for the gas and, between 0.0 to 177.9% with an average of 73 % for the liquid. This difference in the water distribution in the system is attributed to the phenomenon of route selectivity, as indicated in this study. This case demonstrates that realistic water-tracking capabilities are only possible when even-split assumptions are not embraced.

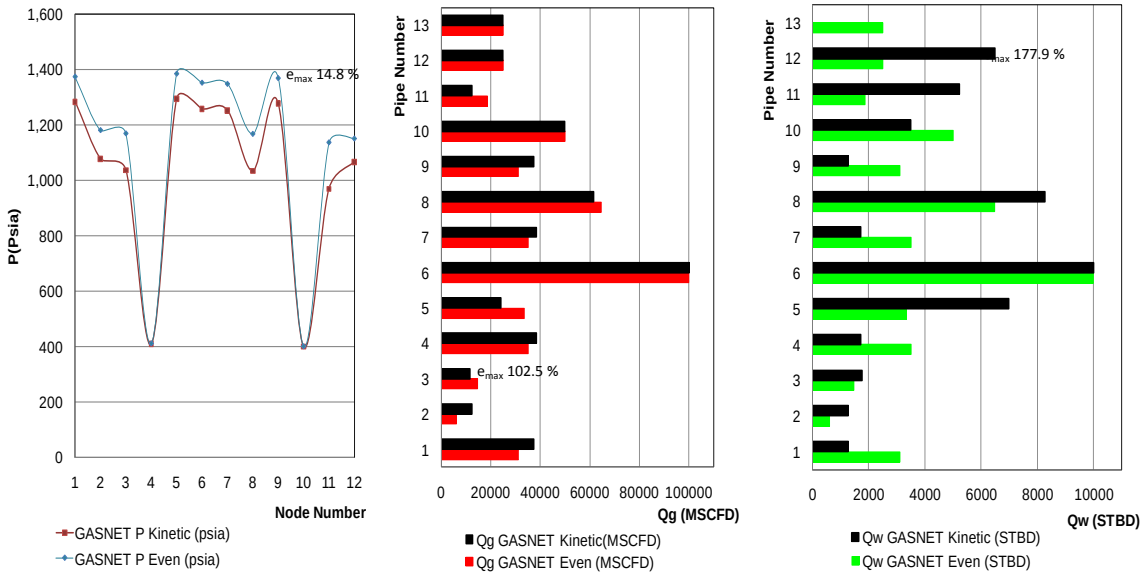

Figure 19 Fluid distribution (gas, liquid) and pressure distribution (psia) for each node obtained from two phases GASNET (Even Split and Kinetic Energy Model)

From here on, the format for every plot will be maintained: the red bars for the gas flowrate using GASNET Even Split and the black lines for either the results of PIPESIM or the

results of GASNET for the Kinetic Energy Model. Similarly for the water distribution: the green bars represent the water flowrates obtained with GASNET Even Split and the black bars represent the water flowrates from PIPESIM or GASNET using the Kinetic Energy Ratio to handle the fluid split at the junctions.

Network 2

The second network tested with the GASNET model consists of 1 supply, 7 demands, 25 pipes, 22 nodes and 4 loops as is shown in Figure 20. Some of the conditions of operation for this network are presented in Table 5 and Figure 57 of the APPENDIX C. This scenario increases the complexity of the proposed network. Again, it can be demonstrated that excellent matches between predictions from commercial simulators and the proposed model are possible for single-phase and two phase conditions as shown in Figure 21and Figure 22. For the single phase case, the differences range for the pressure drop is found between 0.0 to 8.2% with an average of 2.9%. For the gas distribution profile a differences range is found between 0.0 to 11.2% with an average of 1.8%. For the two-phase flow conditions every time the even-split assumption is embraced (Figure 22), the differences range in the pressure distribution profile is found between 0.0 and 3.2% with an average of 1.4%. The gas distribution differences range is found between 0.0 to 3.1% with an average of 0.8% and for the liquid distribution differences range is found between 0.0 to 3.6% with an average of 1.1%. Figure 23 show that significantly different results in terms of water distribution are indeed obtained when the Kinetic Energy option is activated, which stresses the need for such capability to be present in two-phase network models. The differences range for the pressure distribution profile is found between 0.0 to 93.9% with an average of 31.1%. The gas distribution differences range is found between 0.0 to 288.8% with an average of 38.9% and for the liquid distribution profile the differences range is found between 0.0 to 386.0% with an average of 74.0%. Figure 24 shows the resulting water distribution when the Kinetic Energy Model is used.

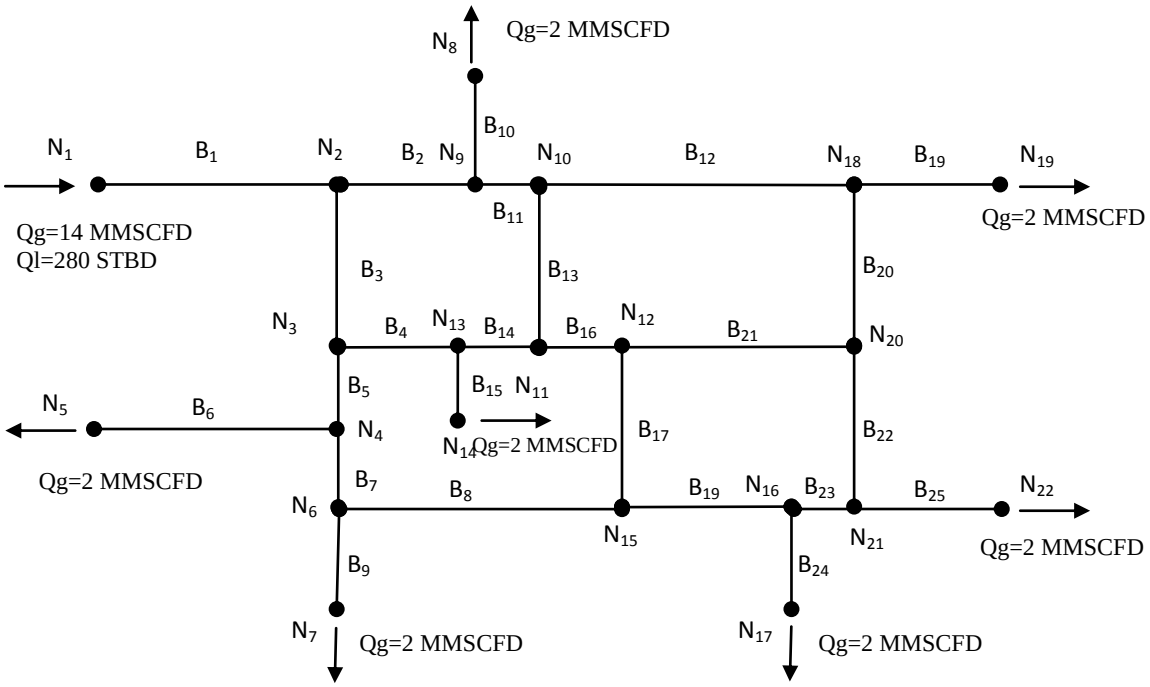

Figure 20 Model of the Network 2. Solved for single phase, two phases Even Split and two phase with Kinetic Energy Model (22 nodes 25 pipes 4 loops)

Table 5 Operating conditions for Network 2

Network		2		**T average of the system**		70 [F]	
Number of Pipes		25		**Flow efficiency**		1 [-]	
Number of Nodes		22		**Pipe Roughness**		0.0006 [in]	
Number of Loops		4		**Gas Comp. Factor (Z)**		0.9000 [-]	
Supply and Demand Information				**Gas Specific Gravity**		0.7000 [-]	
Node	1	**Supply q_g**	14 [MMscfd]	**Gas Viscosity**		0. 0180 [cp]	
Node	1	**Supply q_L**	280 [STBD]	**T_{SC}**	60 [F]	**P_{SC}**	14.7 [psia]
Node	5	**Dem. q_g**	2 [MMscfd]	**Liquid Density**		62.4 [lb/ft^3]	
Node	7	**Dem. q_g**	2 [MMscfd]	**Liquid Viscosity**		1.0000 [cp]	
Node	8	**Dem. q_g**	2 [MMscfd]	**Surface Tension**		8.41 [dynes/cm]	
Node	14	**Dem. q_g**	2 [MMscfd]				
Node	17	**Dem. q_g**	2 [MMscfd]				
Node	19	**Dem. q_g**	2 [MMscfd]				
Node	19	**P Specif.**	100 [psia]				

Pipe	**Diameter (in)**	**Length (ft)**	**Pipe**	**Diameter (in)**	**Length (ft)**	**Pipe**	**Diameter (in)**	**Length (ft)**
1	4.0	500	10	4.0	500	19	4.0	500
2	4.0	7900	11	4.0	500	20	4.0	7900
3	4.0	7900	12	4.0	7900	21	4.0	7800
4	4.0	7800	13	4.0	7900	22	4.0	7900
5	4.0	500	14	4.0	500	23	4.0	7800
6	4.0	500	15	4.0	500	24	4.0	500
7	4.0	7200	16	4.0	500	25	4.0	500
8	4.0	8100	17	4.0	7900			
9	4.0	500	18	4.0	500			

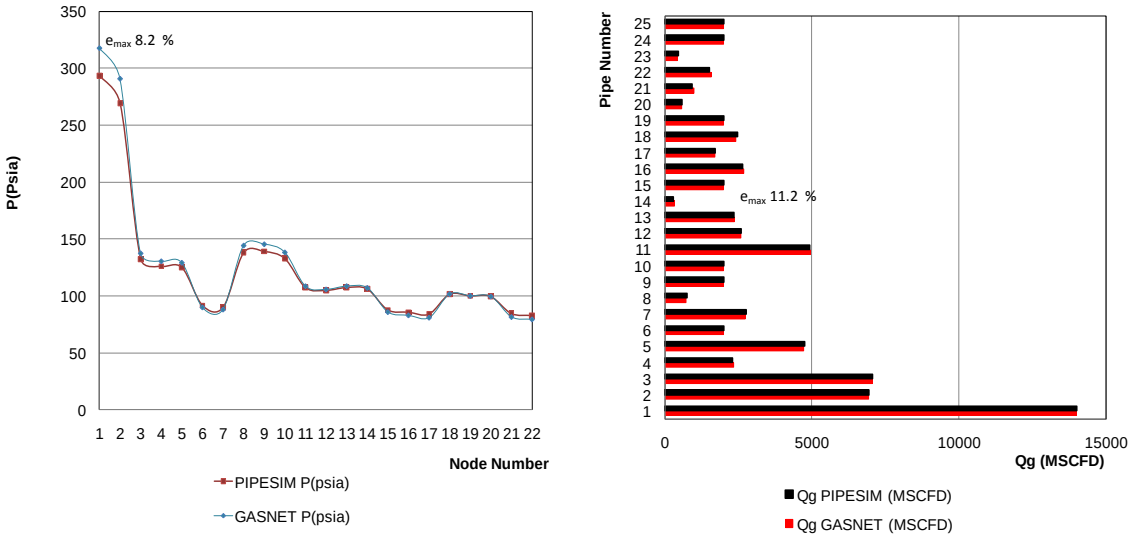

Figure 21 Results for single phase simple gas Network 2. Run with GASNET (single phase) and PIPESIM (22 nodes 25 pipes 4 loops)

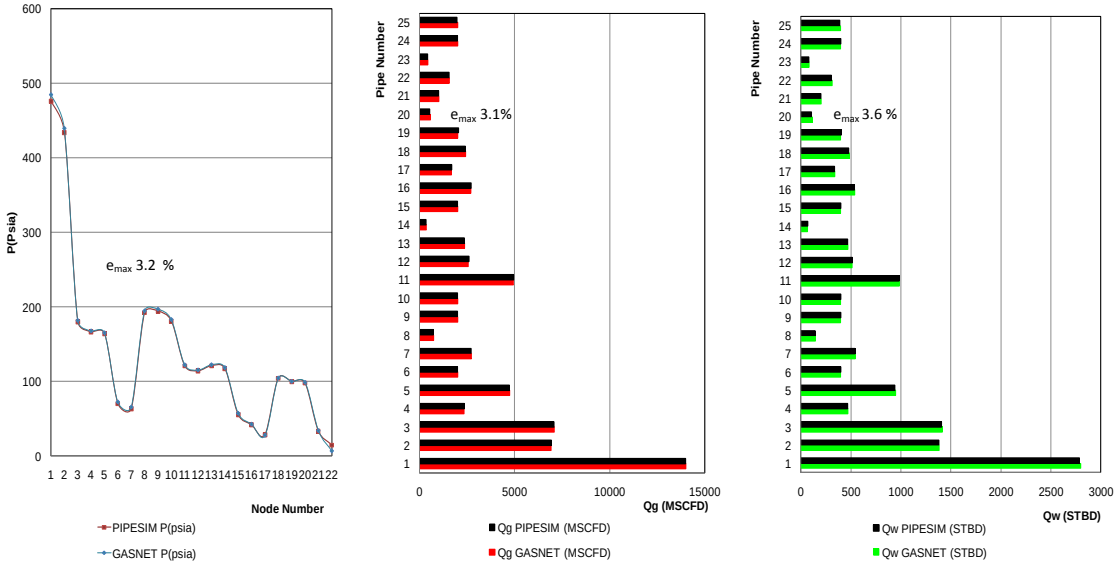

Figure 22 Results for two phases in a gas Network 2. Run with GASNET (Even Split) and PIPESIM (22 nodes 25 pipes 4 loops)

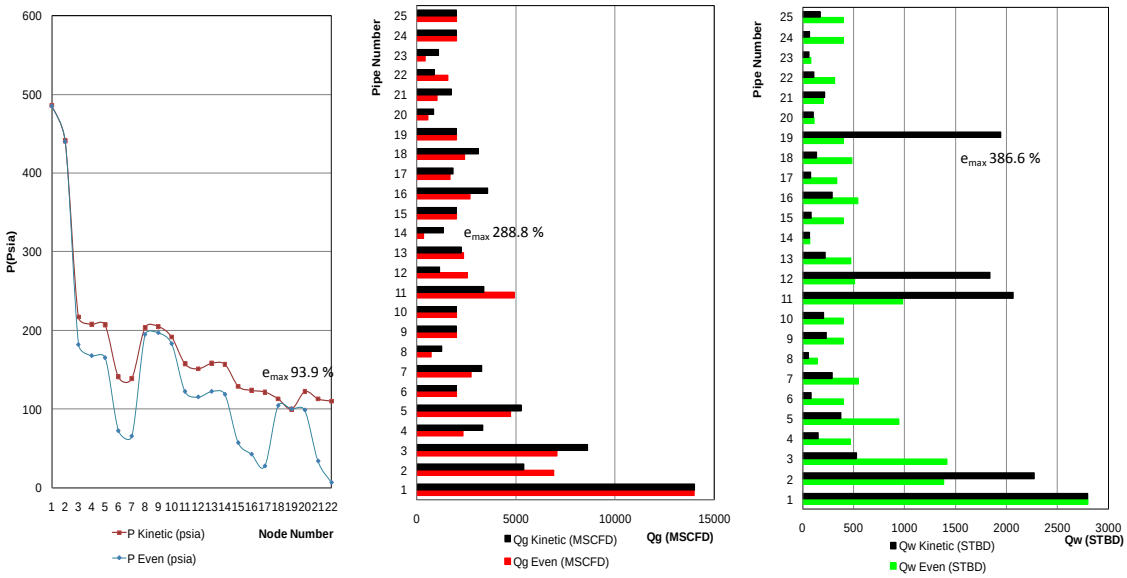

Figure 23 Results for two phases in gas Network 2. Run with GASNET (Even Split and Kinetic Energy Split) (22 nodes 25 pipes 4 loops)

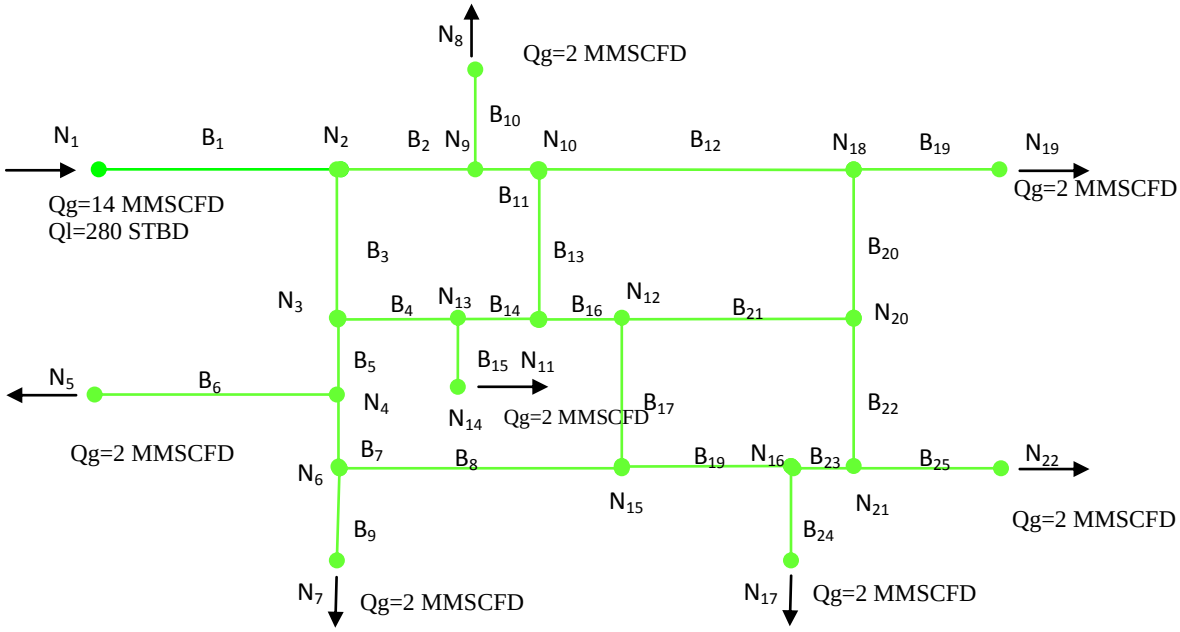

Figure 24 Liquid and gas distribution in a gas Network 2. Solved with two phases GASNET (22 nodes 25 pipes 4 loops)

One important effect analyzed here is the potential re-routing of water upon changes in gas demand conditions. In an attempt to create such a route selectivity test, one of the demands in this network is changed to track the water distribution changes. Results are presented in Figure 25. The prediction with the new demands shows differences range between 0.0 and 2.2% with an average of 0.78% for pressure values, and from 0.0 to 100.0% with an average of 44.4 % for the

gas distribution profile. Water distribution profiles show a differences range between 0.0 and 133.2%, with an average of 39.6%. For this case it is possible to see that the pipe number 14 was initially wet and when changing the demand the pipe section changed to transport only gas.

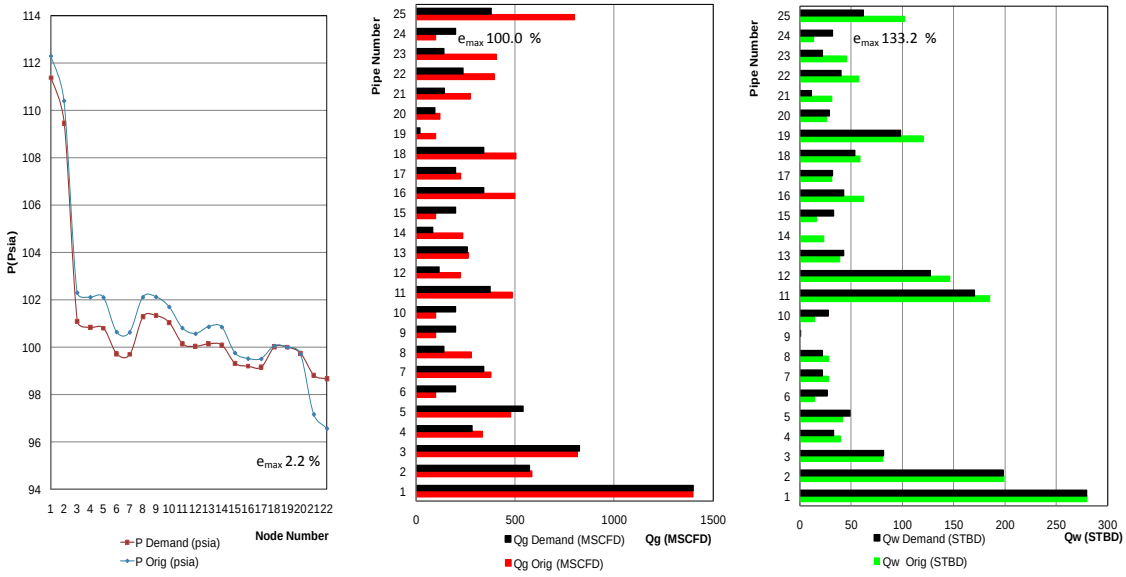

Figure 25 Results for two phases in a gas Network 2. Run with GASNET (Kinetic Energy Split) (22 nodes 25 pipes 4 loops) for low flowrates of water and water and changing the demands on several nodes

Figure 26 and Figure 27 demonstrate that while varying the gas demands in pipes 6, 9, 10, 15, 19, 24 and 25, the new conditions can force the system to change operating from a fully two-phase system with no dry paths (Figure 24) to the creation of one dry path (Figure 26) or two (Figure 27).

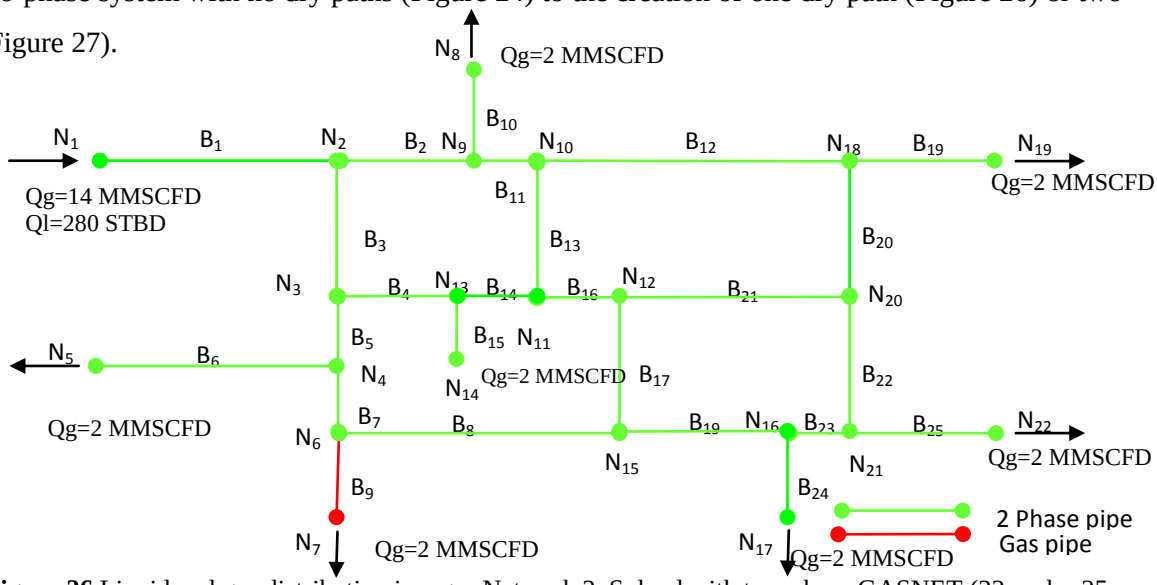

Figure 26 Liquid and gas distribution in a gas Network 2. Solved with two phase GASNET (22 nodes 25 pipes 4 loops). By reducing all the supplies and demand, it was found that there is one dry pipe that initially had liquid (Pipe B-9)

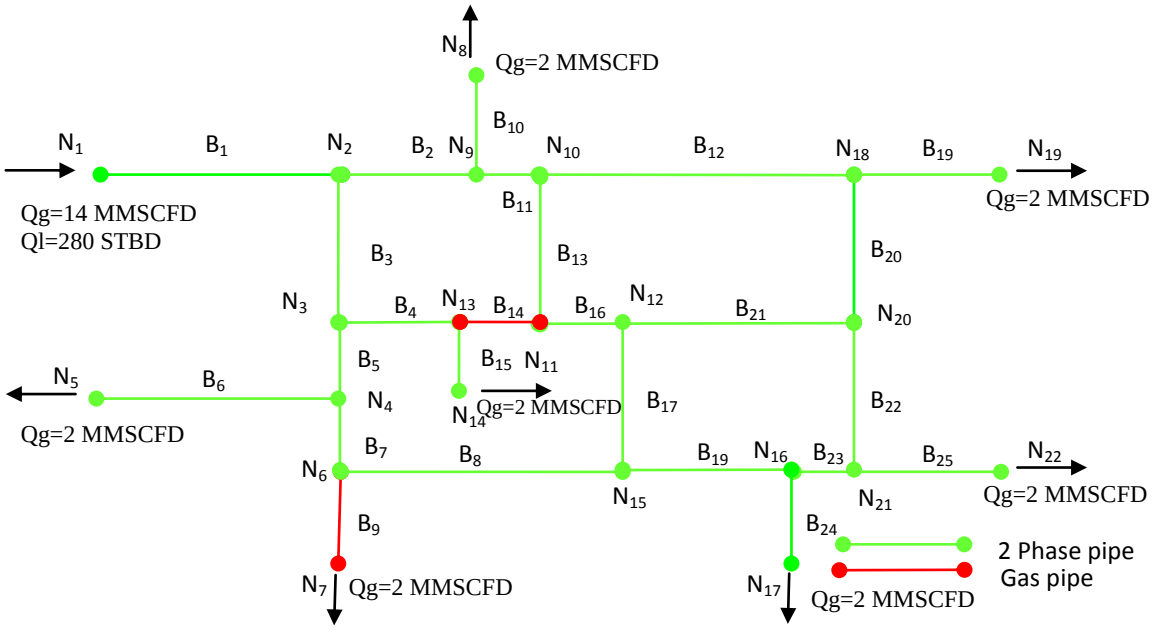

Figure 27 Liquid and gas distribution in gas Network 2. Solved with two phase GASNET (22 nodes 25 pipes 4 loops). By reducing all the supplies and demand by 10 %.

Figure 28 shows the results when running Network 2 under the Kinetic Energy Ratio Split factor and the Dual Stream Model. Even though the pressure distribution profile using the Kinetic Energy Model shows a range of differences between 0.0 and 11.1 % with an average of 4.8% and the gas distribution profile has a differences range between 0.0 and 59.2% with an average of 7.3%, when compared with the Dual Stream Model, the water distribution profile shows a higher difference range, between 0.0 and 100.0 % with an average of 36.2%. It is evident that the pressure profile and the gas distribution profile using the Kinetic Energy Model approaches much better to the results from the Dual Stream Model, than the results of the Even Split presented in Figure 23.

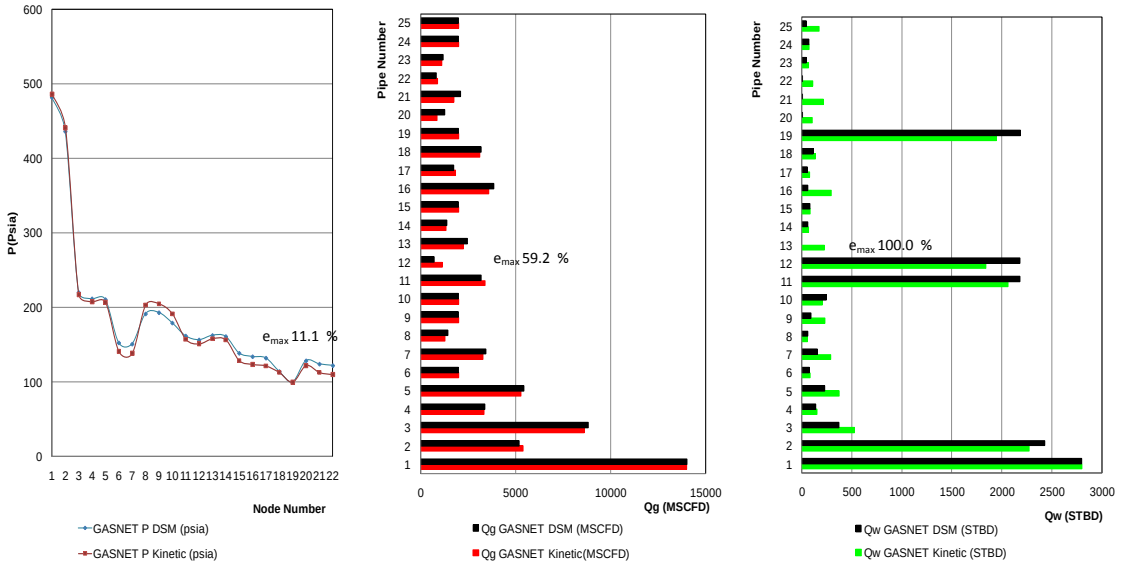

Figure 28 Results for two phases in a gas Network 2. Run with GASNET (Kinetic Energy Split and Dual Stream Model) (22 nodes 25 pipes 4 loops)

Several different cases can be tested to cause significant changes in the liquid-phase routing. For this particular network, it can be demonstrated that most of the water paths can be maintained under different conditions, with the creation of one of two dry paths using the Kinetic Energy Model, while for this system four dry paths developed when using the Dual Stream Model. It was also proven that even though the Kinetic Energy Model gives better results than the Even Split Model, there are still some important differences in the water distribution profile when compared to the Dual Stream Model. However, different network topologies can show very significant sensitivities to water preferential paths, as will be discussed in upcoming network scenarios.

Network 3

Network 3, depicted in Figure 29, represents a portion of an actual pipeline system in operation in Centre County, Pennsylvania. The operational conditions are presented in Table 6 and Table 7 and Figure 58 in APPENDIX C. This network was used to test and deploy previously developed single phase models that preceded this research (Krishnamurthy, 2008, and Alexis, 2009). The portion of the network under study consists of 38 pipes or branches and 38 nodes, one pipe loop, and 15 points of supply with 3 demands. This scenario employs the newly developed model under actual operating conditions and with known values of pipe lengths, diameters, roughness and elevation, as well as gas supply and demand. The only unknown that introduces uncertainty to this system is the volume of water present in the network, which is changed for the

purposes of understanding the effect of water loading on system performance. The network is shown in Figure 29 and the results for single phase and two phases Even Splits are presented in Figure 30 and Figure 31, respectively. Another important reason for analyzing this network is the possibility of coupling network behavior with actual inflow performance relationships of wells in operation. It is expected that any increase in the water loading in the network should increase pressure requirements on the system and eventually force some wells to be shut down, which is particularly critical and undesirable in stripper well systems.

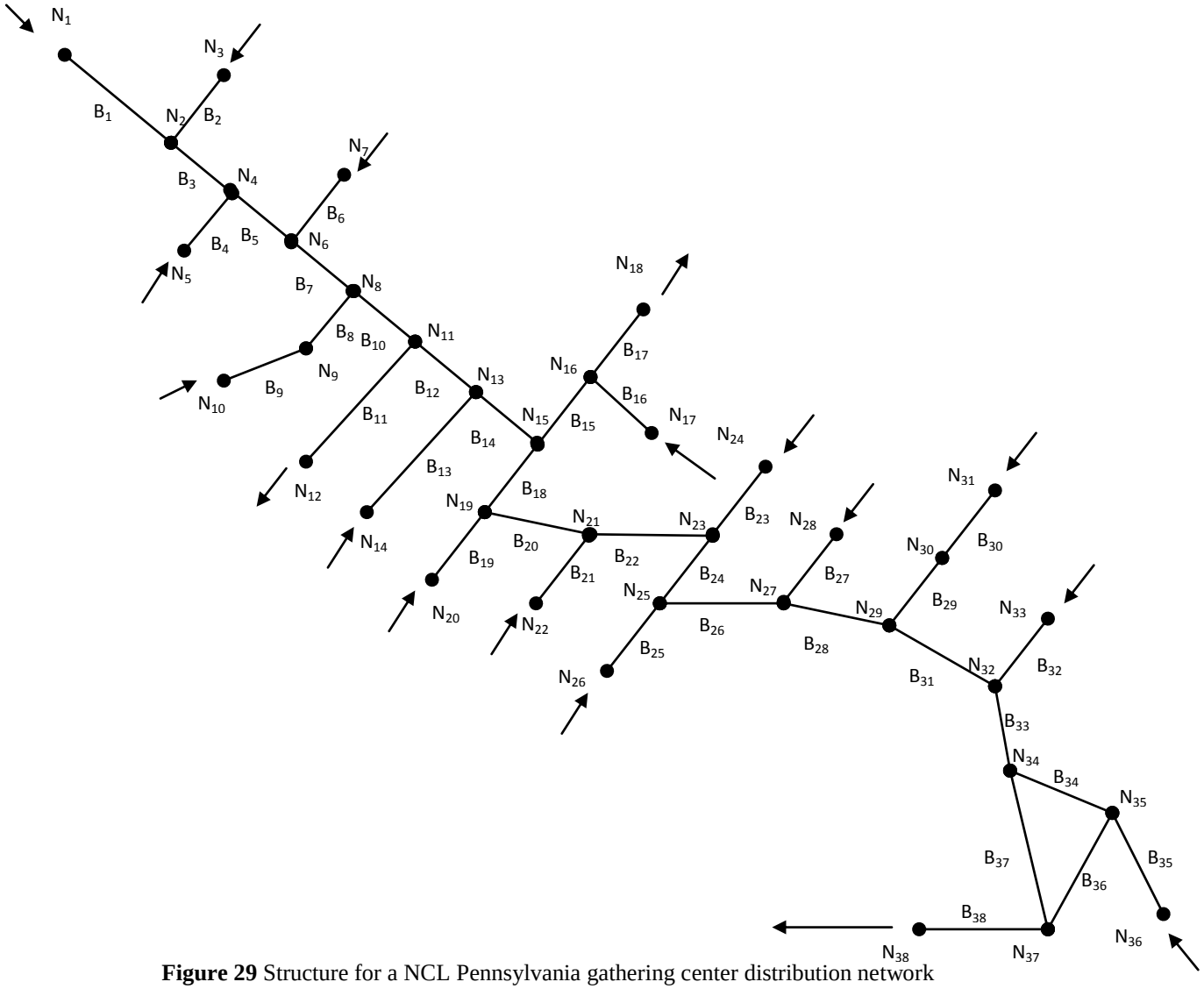

Figure 29 Structure for a NCL Pennsylvania gathering center distribution network (38 nodes 38 pipes 1 loops)

Table 6 Operating conditions for Network 3

Network	3			**T average of the system**			60 [F]
Number of Pipes	38			**Flow efficiency**			0.9501 [-]
Number of Nodes	38			**Pipe Roughness**			0.001 [in]
Number of Loops	1			**Gas Comp. Factor (Z)**			0.8801 [-]
Supply and Demand Information				**Gas Specific Gravity**			0.5517 [-]
Node	Table 7	**Supply q_g**	Table 7	**Gas Viscosity**			0. 01270[cp]
Node	37	**P Specif.**	40.65 [psia]	**T_{SC}**	60 [F]	**P_{SC}**	14.7 [psia]
				Liquid Density			62.4 [lb/ft^3]
				Liquid Viscosity			0.8566 [cp]
				Surface Tension			59.667 [dynes/cm]

Pipe	Diameter (in)	Length (ft)	Pipe	Diameter (in)	Length (ft)	Pipe	Diameter (in)	Length (ft)
1	1.58	467.86	14	2.38	259.03	27	1.58	203.53
2	1.58	227.86	15	1.58	116.19	28	2.38	1139.21
3	1.58	783	16	1.58	541.88	29	1.58	960.15
4	1.58	126.32	17	1.58	545.3	30	1.58	1501.59
5	1.58	365.67	18	2.38	600.78	31	2.38	305.43
6	1.58	1778.25	19	1.58	1020.12	32	1.58	192.24
7	2.38	96.75	20	2.38	138.86	33	2.38	274.81
8	1.58	239.95	21	1.58	274.49	34	2.00	302.86
9	1.58	1809.26	22	2.38	340.43	35	2.00	313.62
10	2.38	143.43	23	1.58	355.6	36	2.00	481.17
11	1.58	708.66	24	2.38	617.74	37	2.38	302.86
12	2.38	183.14	25	1.58	1585.25	38	2.00	288.25
13	1.58	766.80	26	2.38	616.45			

Table 7 Supply for Network 3

Node With well	Well Performance Constant	Shut In Pressure (psia)	Well Exponent	WGR (STB/scf)	Node WO Well	Qg MMscfd	WGR (STB/scf)
1	0.326	175.000	0.50	0.1	10	47.19	0
3	0.096	106.204	0.75	0.1	12	14.44	0
5	0.0735	164.807	0.5	0.1	24	26.94	0
7	0.045	170.710	0.75	0.1	26	12.34	0
14	0.086	178.959	0.5	0.4	28	28.04	0
17	0.0117	131.732	0.75	0.4	33	21.29	0
18	0.0086	167.7954	0.75	0.4	36	15.00	0
20	0.0248	95.000	0.75	10			
22	0.0126	151.960	0.75	0.4			
31	0.0201	138.542	0.75	0.4			

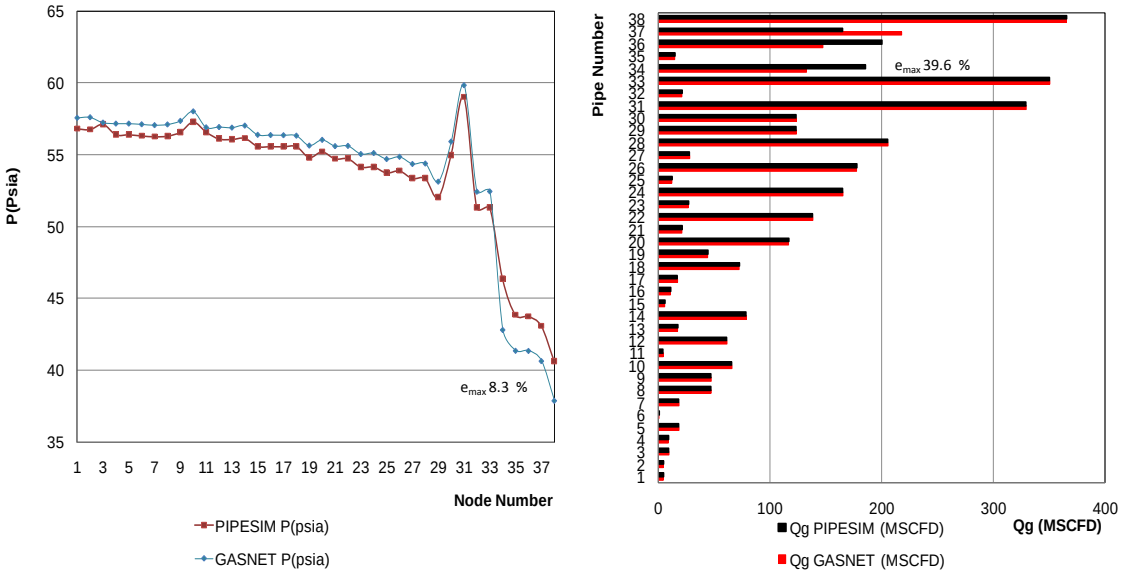

Figure 30 Results for a single phase of the NCL Pennsylvania gas distribution system. Run with GASNET (single phase) and PIPESIM (38 nodes 38 pipes 1 loops)

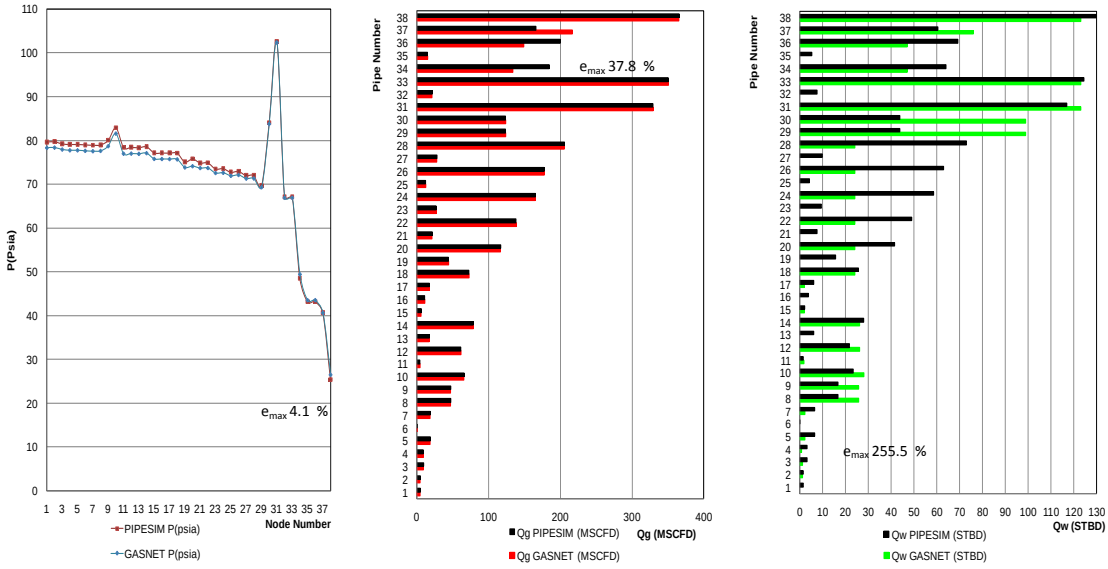

Figure 31 Results for two phases of the NCL Pennsylvania gas distribution system. Run with GASNET (Even Split) and PIPESIM (38 nodes 38 pipes 1 loops)

As discussed before, it is clear that excellent matches between GASNET and commercial simulators (PIPESIM) are achieved when using single-phase conditions (Figure 30) and two-phase conditions with Even Split assumptions (Figure 31). For the single phase case, the pressure distribution profile differences range was found to be between 0.0 to 8.3% with an average of 2.2%. For the Even Split the pressure differences range was found between 0.0 and 4.1% with an average of 1.4%. The gas distribution profile differences were: in the range of 0.0 to 39.7% with

an average of 2.6% for the single phase and between 0.0 and 37.8% with an average 2.5% for the two phases Even split. However there are some differences in the water distribution profile, difference range from 1.1 to 255.5 % with an average of 82.5 %. As shown in Figure 32, the majority of the junctions in this system are merging junctions instead of splitting junctions and therefore no significant differences between using Even Split models and the Kinetic Energy Models are to be expected. However, the flow distribution profile (Figure 32) shows three major difference points, which are nodes 34, 36 and 37 where the water predicted by the Kinetic Energy Model is considerably lower than the volume predicted by the Even Split distribution. The difference range in the pressure distribution profile is found between 0.0 and 2.4%, with an average of 0.7%. For the gas distribution profile the differences range was found between 0.0 and 50.2 % with an average 3.3 % and finally for the water distribution profile it was found between 0.0 and 83.3% with an average of 8.9 %. As was indicated before, the Kinetic Energy approach is considered a better approximation to the real world than the Even Split.

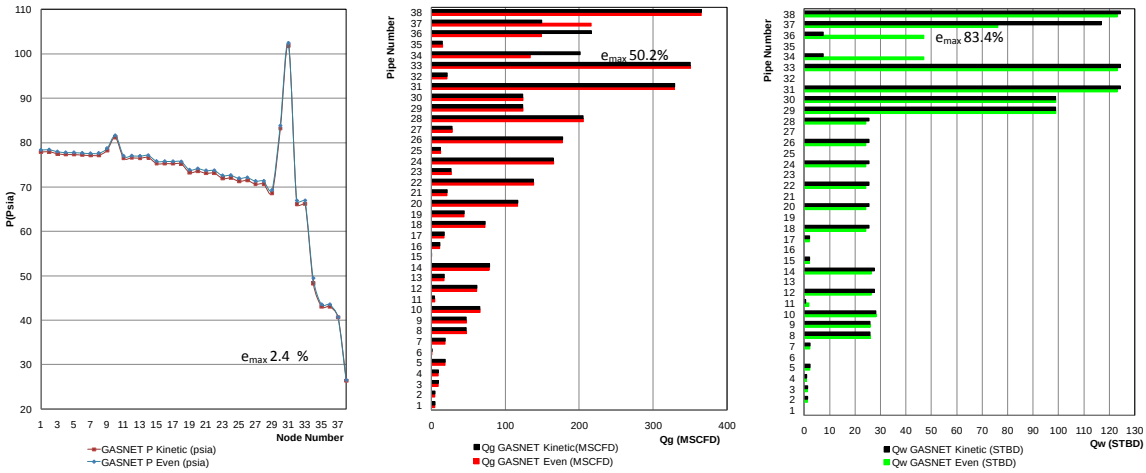

Figure 32 Results for two phases in the NCL Pennsylvania gas distribution system. Run with GASNET (Even Split and Kinetic Energy Split) (38 nodes 38 pipes 1 loops)

As indicated before, this gathering system was employed to test the Inflow Performance Relationship (IPR) option in the new model. Wells located on nodes 1, 3, 5, 7, 14, 17, 18, 20, 22 and 31 were modeled using field-generated IPRs. The only fixed demand for this case was left on node 38. The rest of the nodes are supply nodes without IPR wells. To better observe network behavior and the resulting well performances, a varying volume of incoming water was fed through the well located on node 20. The volume of water was introduced gradually and the results are displayed in Figure 33 and Figure 34, where a maximum difference of 14.7%, 99.7%

and 100% are achieved for the pressure profile, gas distribution and water distribution respectively.

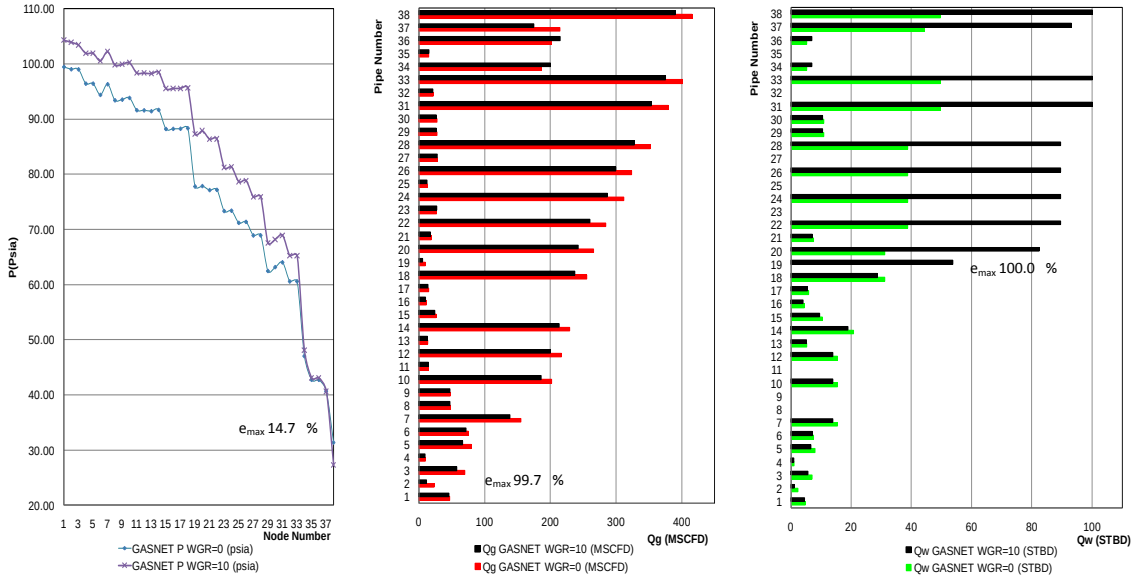

Figure 33 Results for two phases in the NCL Pennsylvania gas distribution system. Run with GASNET Kinetic Energy Split, while increasing the water content from the well on node 20 (38 nodes 38 pipes 1 loops)

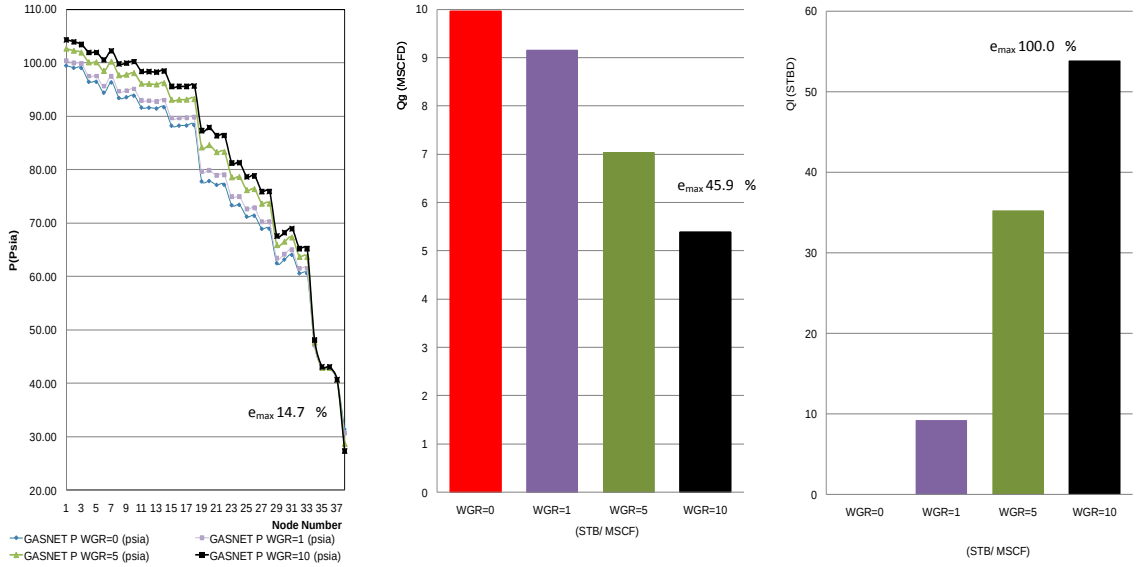

Figure 34 Results for two phases in the NCL Pennsylvania gas distribution system. Run with GASNET Kinetic Energy Split, while increasing the water content from the well in node 20 (38 nodes 38 pipes 1 loops)

Figure 33 includes two of the results of solving the NCL gas distribution network with several wells connected to the line for conditions when WGR=0.0 and WGR=10.0 STB/MSCF (WGR=producing water-gas ratio). To fully evaluate the performance of the entire network and to

draw meaningful conclusions, Figure 34 was prepared. From these two figures it is evident that when increasing the inflow water to the system through the well located in node 20 (at the outlet of branch 19), more energy is required by the system. Therefore, the pressure requirements in all nodes in the system increase. The unfortunate effect is that, while increasing the amount of water traveling in the system, the increased pressure losses in the gathering system represent an undue burden on the producing wells which are now able to produce even less. Since the increase in the volume of water increases the pressure requirements on the nodes, these new higher nodal pressures can reach values higher than the shut-in pressure of the well connected to that node. If that happens, some wells will be shut down and total gas production from the field is curtailed. Therefore, as the volume of water incoming in node 20 increases, the total gas production from the system decreases.

Network 4

Another network structure has been tested based on the published topology of Sung (Sung, 1998). The structure refers to the distribution gas system between different cities in Korea. The original structure (Figure 35 A) was adapted to our study and the equivalent network that avoids junctions with more than three pipes is presented in Figure 35 B. The operating conditions for this network are presented in Table 8 and in Figure 59 of APPENDIX C. As has been shown before, an excellent match results between GASNET and PIPESIM for the pressure profiles, and small differences in the water and gas distribution profiles are obtained in Figure 36 (for single-phase conditions) and Figure 37 (for two-phase conditions embracing Even Split). Once again Figure 38 highlights the significant difference in flow distribution and pressure profile obtained by proper handling of the liquid splits.

Figure 39 displays a visualization of the system and the resulting water preferential paths that are created within the network, which highlights the water tracking capabilities of the proposed model.

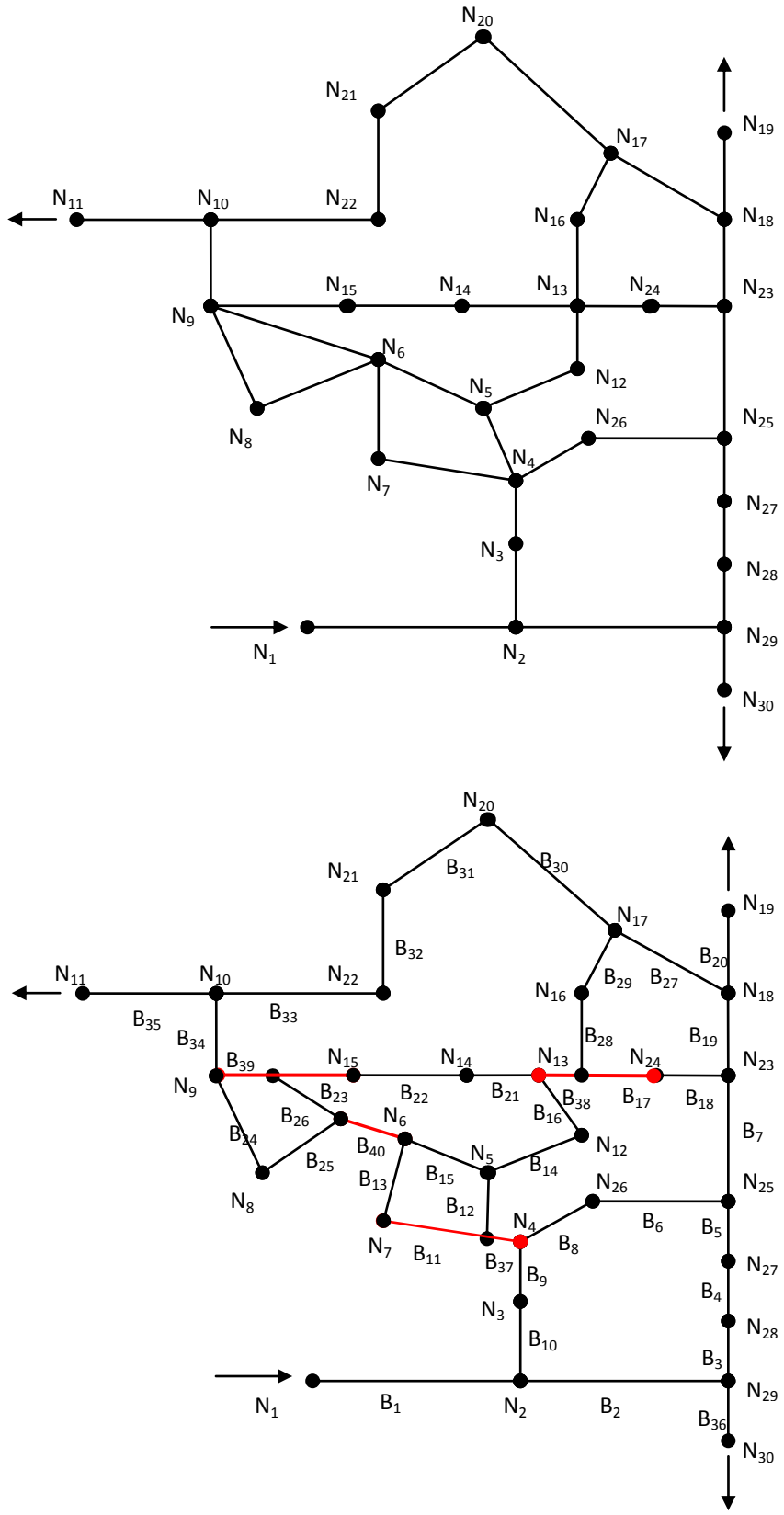

Figure 35 Model of the Korea gas distribution network (A) and the equivalent system (B) (To avoid more than three pipes on a node) Network solved for two phase (34 nodes 40 pipes 7 loops).
The pipes marked with red indicate where the modification was done to match a realistic case (i.e avoiding more than 3 pipes per junction)

Table 8 Operating conditions for Network 4

Network			4	**T average of the system**			82 [F]	
Number of Pipes			40	**Flow efficiency**			1.0000 [-]	
Number of Nodes			34	**Pipe Roughness**			0.0001[in]	
Number of Loops			7	**Gas Comp. Factor (Z)**			0.9303 [-]	
Supply and Demand Information				**Gas Specific Gravity**			0.5517 [-]	
Node	1	**Supply q_g**	3 [MMscfd]	**Gas Viscosity**			0. 0119[cp]	
Node	11	**Dem. q_g**	0.3 [MMscfd]	**T_{SC}**	60 [F]	**P_{SC}**	14.7 [psia]	
Node	19	**Dem. q_g**	1.0 [MMscfd]	**Liquid Density**			62.4 [lb/ft^3]	
Node	30	**Dem. q_g**	1.7 [MMscfd]	**Liquid Viscosity**			0.8555 [cp]	
Node	1	**P Specif.**	500 [psia]	**Surface Tension**			64.6871 [dynes/cm]	

Pipe	**Diameter (in)**	**Length (ft)**	**Pipe**	**Diameter (in)**	**Length (ft)**	**Pipe**	**Diameter (in)**	**Length (ft)**
1	5.0	5026.35	15	5.0	3982.09	29	2.0	1804.61
2	6.0	5249.59	16	2.0	3588.84	30	5.0	3937.06
3	5.0	6561.67	17	4.0	3280.39	31	5.0	3280.39
4	5.0	5249.59	18	4.0	3280.39	32	5.0	3608.22
5	7.0	5741.72	19	4.0	4868.35	33	5.0	3421.65
6	5.0	7217.66	20	2.0	3917.76	34	2.0	5244.51
7	5.0	6233.68	21	2.0	3280.39	35	2.0	4921.56
8	5.0	5249.59	22	2.0	4021.22	36	6.0	34713.01
9	5.0	5473.9	23	2.0	3604.83	37	2.0	10
10	5.0	7181.17	24	6.0	3608.22	38	2.0	2
11	6.0	3608.22	25	6.0	3608.22	39	2.0	2
12	5.0	3636.11	26	2.0	3280.39	40	3.0	10
13	6.0	3608.22	27	2.0	5417.66			
14	4.0	3469.18	28	2.0	4471.85			

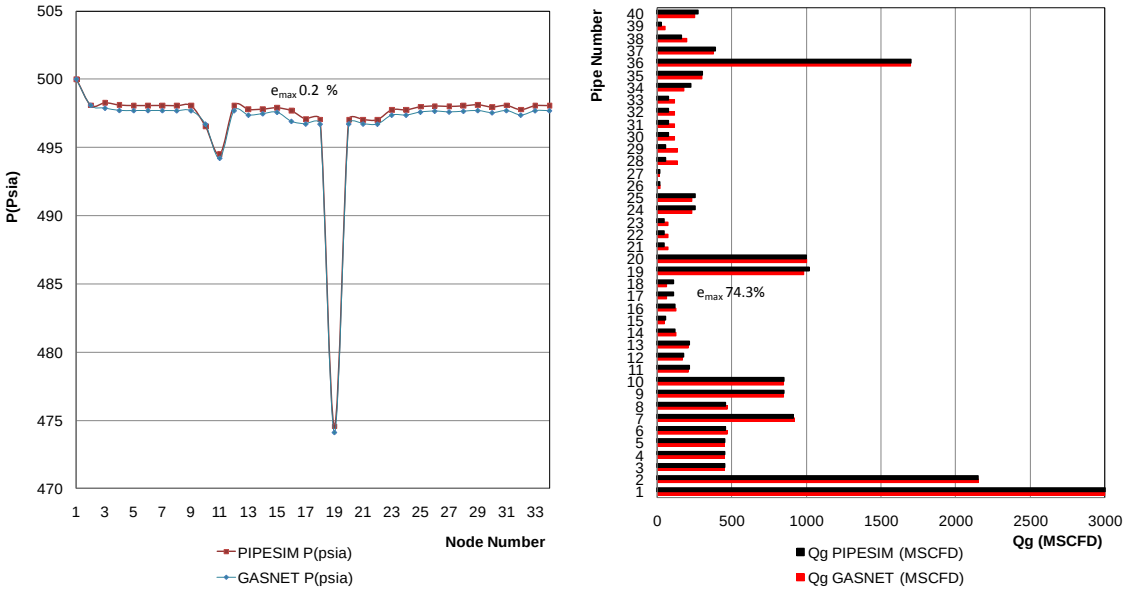

Figure 36 Results for single phase of the Korea gas distribution system. Run with GASNET (single phase) and PIPESIM (34 nodes 40 pipes 7 loops)

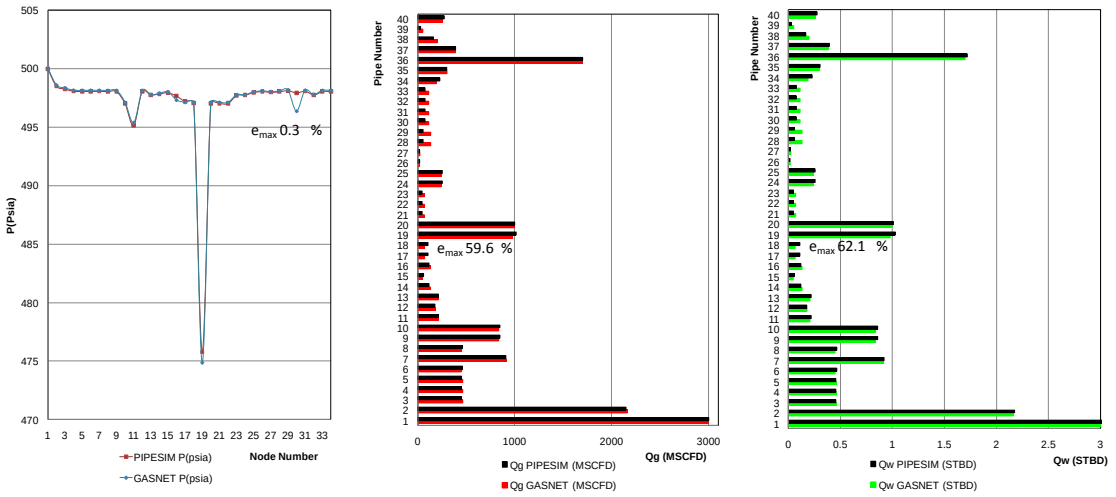

Figure 37 Results for two phases of the Korea gas distribution system. Run with GASNET (Even Split) and PIPESIM (34 nodes 40 pipes 7 loops)

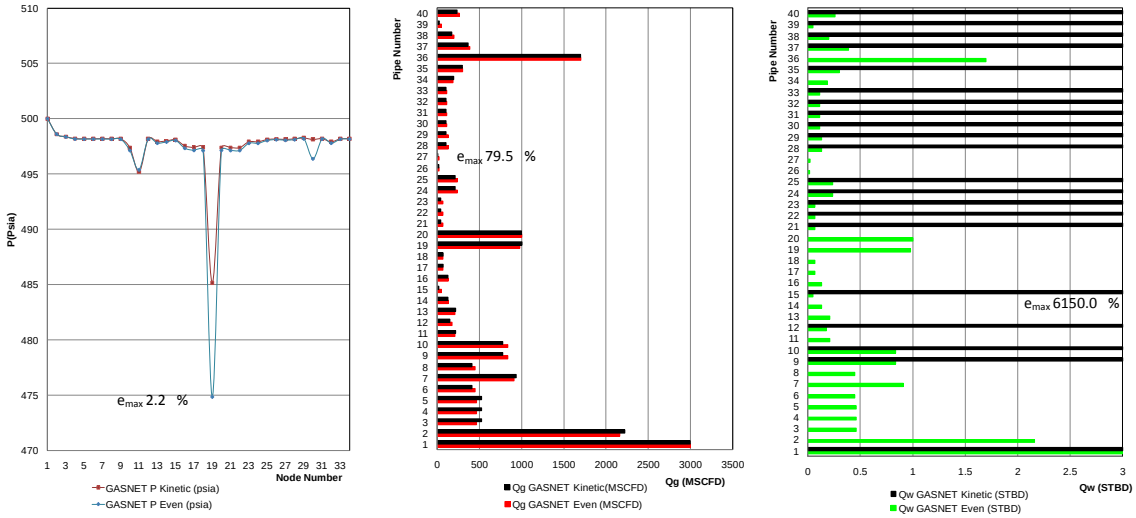

Figure 38 Results for two phases in the Korea gas distribution system. Run with GASNET (Even Split and Kinetic Energy Split) (34 nodes 40 pipes 7 loops)

In Figure 36 the differences range for the pressure profile in single phase is between 0.0 and 0.2% with an average of 0.07%. For the gas distribution profile the differences are found between 0.0 and 74.9% with an average of 17.4%. For the two phase Even Split the differences range for the pressure profile is found between 0.0 and 0.3% with an average of 0.03%. The gas distribution profile the differences range is found between 0.0 and 59.6% with an average of 16.1% and, for the water distribution profile the differences range was from 0.3 to 62.1% with

average of 16.5%. Finally, when comparing the Even Split Model with the Kinetic Energy Model, the differences range for the pressure profile is found between 0.0 and 2.1% with an average value of 0.1%. The gas distribution profile is found between 0.0 and 79.6% with an average of 13.5% and for the water distribution profile between 0.0 and 6150% with an average of 1237.6% which confirm once again the proper split handling is required for new simulators.

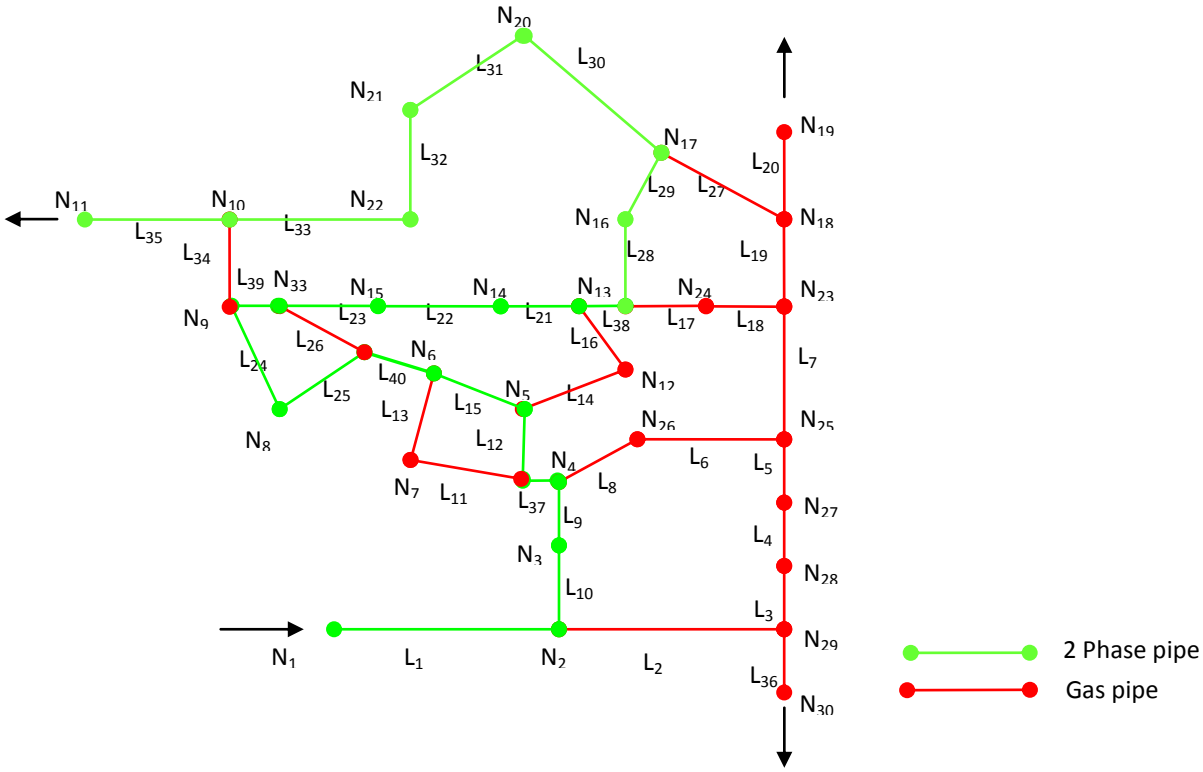

Figure 39 Liquid distribution profile for initial parameter of the Korea gas distribution system GASNET (Kinetic Energy Split) (34 nodes 40 pipes 7 loops)

After verifying that there was a match between GASNET and PIPESIM for the single phase condition and Even Split, and after proving that there was some difference in the pressure profiles and flow distribution profile when using the Kinetic Energy Model, the Dual Stream Model was activated and the results are presented in Figure 40.

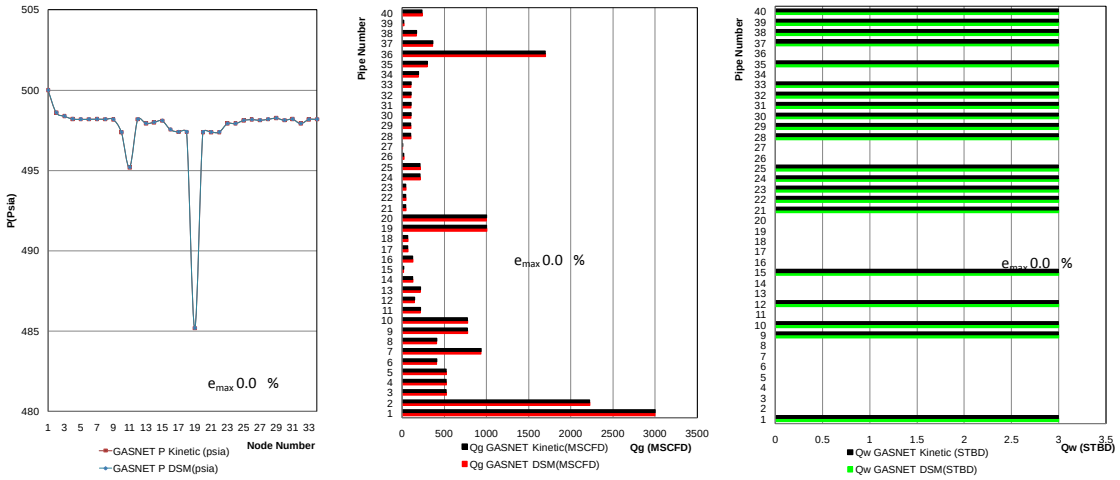

Figure 40 Results for two phases in the Korea gas distribution system. Run with GASNET (Kinetic Energy Split and dual stream model) (34 nodes 40 pipes 7 loops)

The results presented in Figure 40 show that for this specific network there is no difference between the Kinetic Energy Model and the Dual Stream Model on the water flow profile and a discrete difference in the gas distribution profile.

Network 5

One final network has been tested using the commercial simulator (PIPESIM) and the proposed model (GASNET). The network, displayed in Figure 41 is one of the most complex systems tested in this particular study. The system is made up of 31 pipes, 26 nodes and 6 loops, 2 supplies and 4 demands; the rest of the parameters are presented in Table 9 and in Figure 61 of APPENDIX C. This network will be used for sensitivity analysis of water routing within the system based on changes on gas demands at the delivery nodes. The conditions for this network are: all the pipes had a length of 10000 ft, internal diameter of 6 in., roughness 0.006 in, temperature 82 F. The system consists of 31 pipes, 26 nodes and 6 loops, 2 supplies and 4 demands.

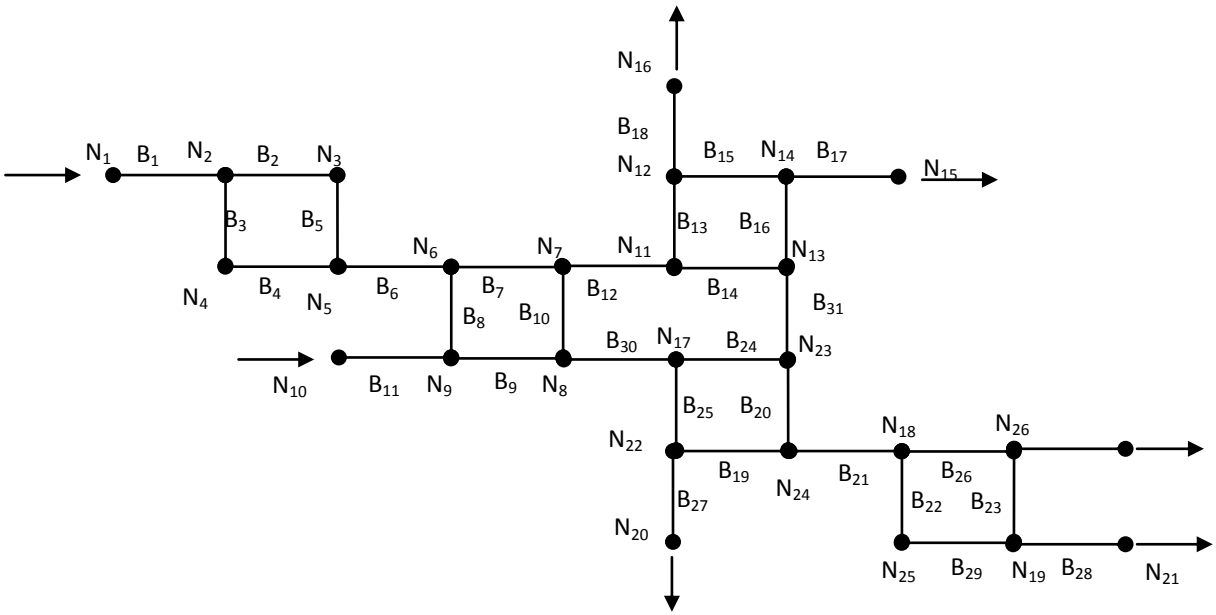

Figure 41 Model of complex gas distribution network solved for two phase (26 nodes 31 pipes 6 loops)

Table 9 Operating conditions for Network 5

Network		5		**T average of the system**			82 [F]
Number of Pipes		31		**Flow efficiency**			1.0000 [-]
Number of Nodes		26		**Pipe Roughness**			0.006[in]
Number of Loops		6		**Gas Comp. Factor (Z)**			0.9303 [-]
Supply and Demand Information				**Gas Specific Gravity**			0.5517 [-]
Node	1	**Supply q_g**	2.7 [MMscfd]	**Gas Viscosity**			0. 0119[cp]
Node	10	**Supply q_g**	0.3 [MMscfd]	**T_{SC}**	60 [F]	**P_{SC}**	14.7 [psia]
Node	1	**Supply q_L**	27 [STBD]	**Liquid Density**			62.4 [lb/ft^3]
Node	10	**Supply q_L**	3 [STBD]	**Liquid Viscosity**			0.8555 [cp]
Node	15	**Dem. q_g**	1.0 [MMscfd]	**Surface Tension**			64.6871 [dynes/cm]
Node	16	**Dem. q_g**	0.8 [MMscfd]				
Node	20	**Dem. q_g**	0.7 [MMscfd]				
Node	21	**Dem. q_g**	0.5 [MMscfd]				
Node	15	**P Specif.**	60 [psia]				

Pipe	**Diameter (in)**	**Length (ft)**	**Pipe**	**Diameter (in)**	**Length (ft)**	**Pipe**	**Diameter (in)**	**Length (ft)**
1	6.0	100000	11	6.0	100000	21	6.0	100000
2	6.0	100000	12	6.0	100000	22	6.0	100000
3	6.0	100000	13	6.0	100000	23	6.0	100000
4	6.0	100000	14	6.0	100000	24	6.0	100000
5	6.0	100000	15	6.0	100000	25	6.0	100000
6	6.0	100000	16	6.0	100000	26	6.0	100000
7	6.0	100000	17	6.0	100000	27	6.0	100000
8	6.0	100000	18	6.0	100000	28	6.0	100000
9	6.0	100000	19	6.0	100000	29	6.0	100000
10	6.0	100000	20	6.0	100000	30	6.0	100000

Not surprisingly, and as systematically shown before, there is an excellent correlation between results obtained with PIPESIM and GASNET for the single phase case and for the Even Split ratio, as shown in Figure 42 and Figure 43, respectively. The maximum differences range for pressure values for single phase are found between 0.0 to 2.1 % with an average of 1.1% , and between 0.0 and 5.0 % with an average of 0.6% in the gas distribution profile. For the two phases the differences range was found between 0.0 and 49.9 % with an average of 3.9% in the pressure profile, between 0.0 and 21.5% with an average of 2.6% for the gas distribution profile and the water distribution profile range is found between 0.3 and 22.0% with an average of 2.9%. For this particular network, when running the simulation with the Kinetic Energy ratio a good match is obtained in the gas distribution profile with minor differences in the pressure profile. However, there is a considerable difference in the water rate distribution profile presented in Figure 44. Figure 45 presents the visualization of the resulting water distribution in the network under the stated conditions. Red pipes represent dry regions in the network and green pipes the water-selected routes.

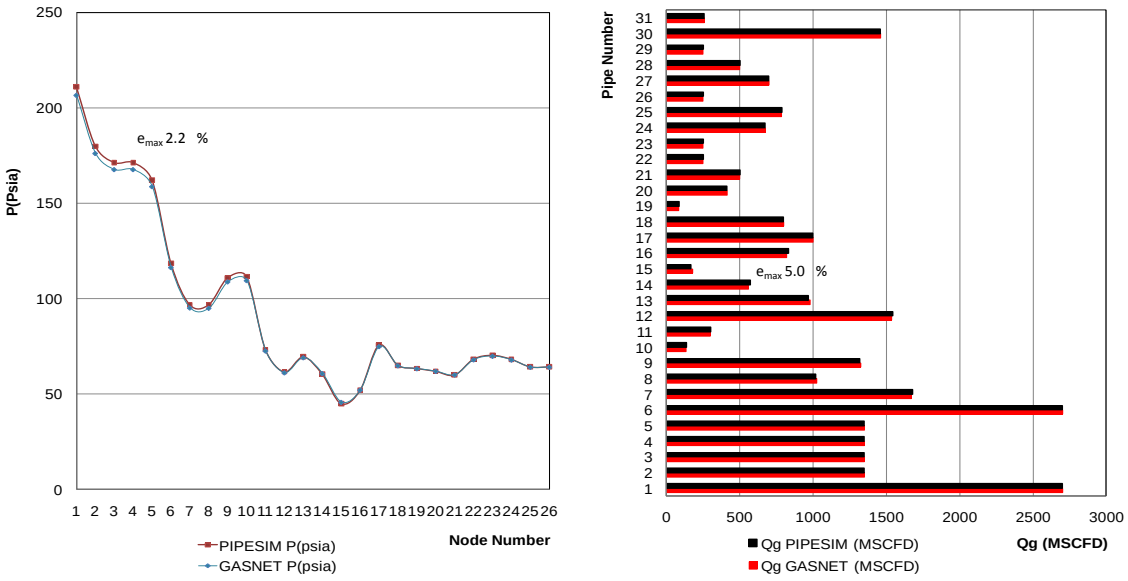

Figure 42 Results for single phase of the complex gas distribution network. Run with GASNET (single phase) and PIPESIM (26 nodes 31 pipes 6 loops)

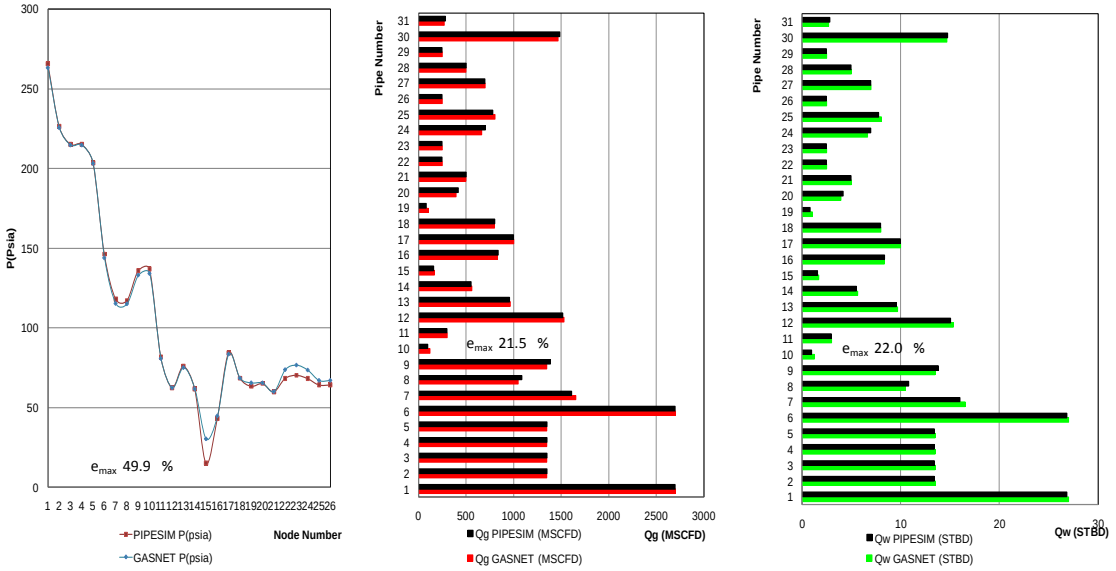

Figure 43 Results for two phases in a complex gas distribution network. Run with GASNET (Even Split) and PIPESIM (26 nodes 31 pipes 6 loops)

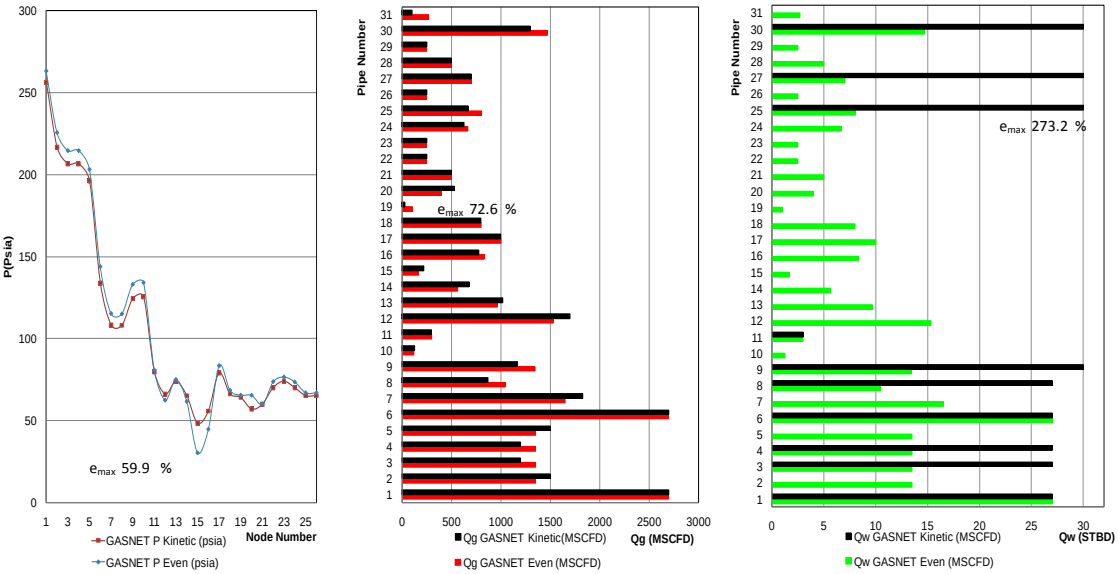

Figure 44 Results for two phases in a complex gas distribution network. Run with GASNET (Even Split and Kinetic Energy Split) (26 nodes 31 pipes 6 loops)

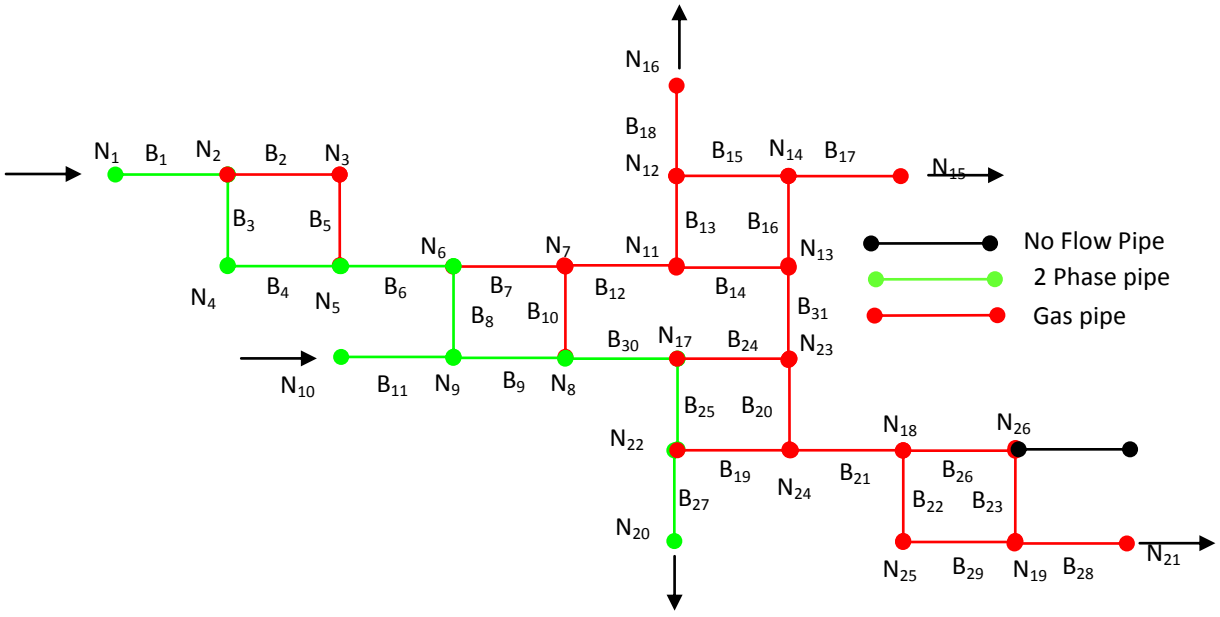

Figure 45 Model of liquid and gas preference route for a complex gas distribution network

It can be demonstrated that changing gas demand has an important effect on water routing. For example, when the gas demand at node 14 is eliminated and reallocated to node 26, a new water distribution profile can be established. This is shown in Figure 46, which should be compared to the original water distribution illustrated in Figure 45.

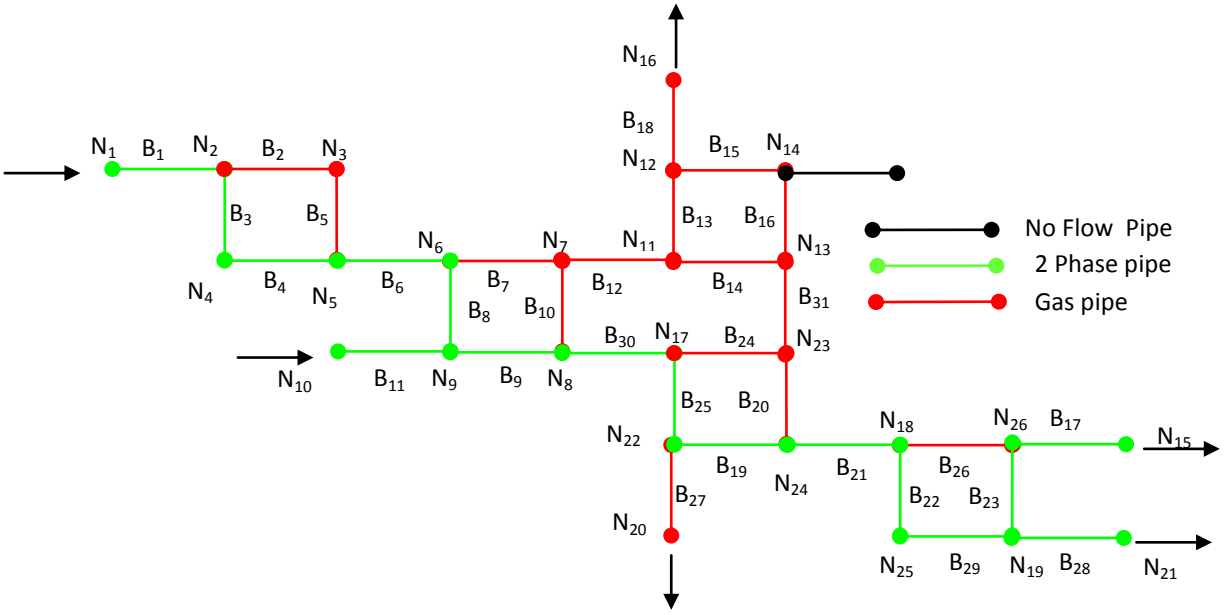

Figure 46 Model of liquid and gas preference route for a complex gas distribution network, changing the position of the demand

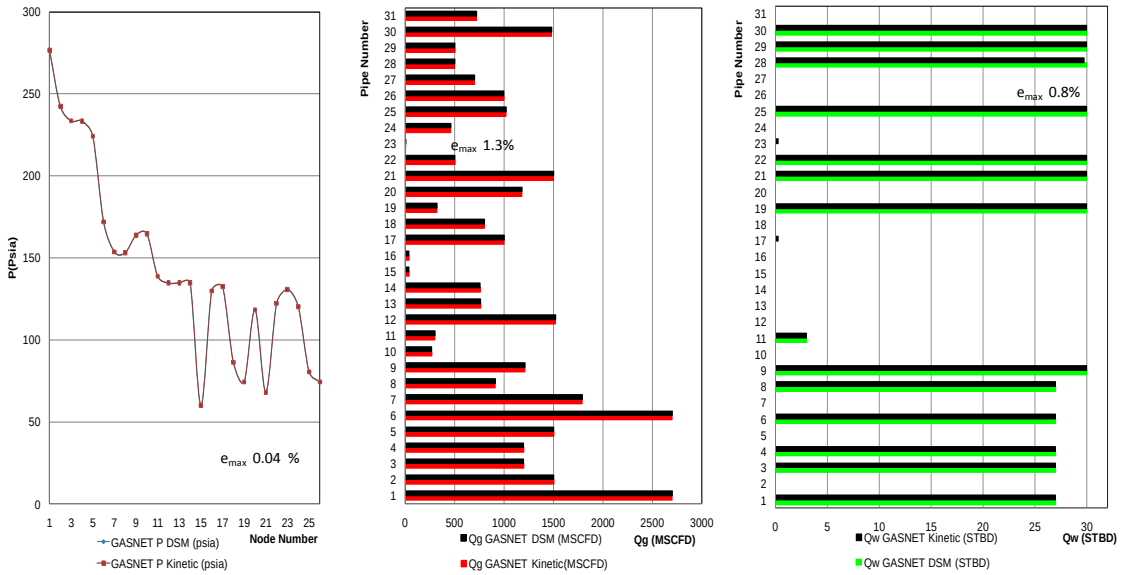

Figure 47 Results for two phases in a complex gas distribution network. Run with GASNET (Kinetic Energy Split and the Dual Stream Model) (26 nodes 31 pipes 6 loops)

Figure 47 shows the results for the application of the Dual Stream Model to the Network 5. As opposed to the results presented in Figure 40, this case shows some minor differences between the Kinetic Energy Model and the Dual Stream Model. From the above figure it is possible to conclude that the Kinetic Energy Model is a better approximation in the determination of the fluid distribution profile and the fluid flow path through the network, than the Even Split model.

Additional sensitivity analysis for water routing is possible. Figure 48 through Figure 51 display the results of these attempts, whose details are presented next. Another possibility, for instance, is to change the location of the pressure specification node from node 14 to node 26 (specified pressure=60 psia). Results are presented in Figure 48. It can be seen that the pressure profile, gas flow profile and the water flow profile changed accordingly, forcing water in pipes that originally were dry. Similar effects can be observed when pressure specification is changed to node 21, this time with a specification level of 100 psia instead of 60 psia. The results obtained are shown in Figure 49. In this case, even though the pressure profiles have changed, there was no significant change in gas or water distributions.

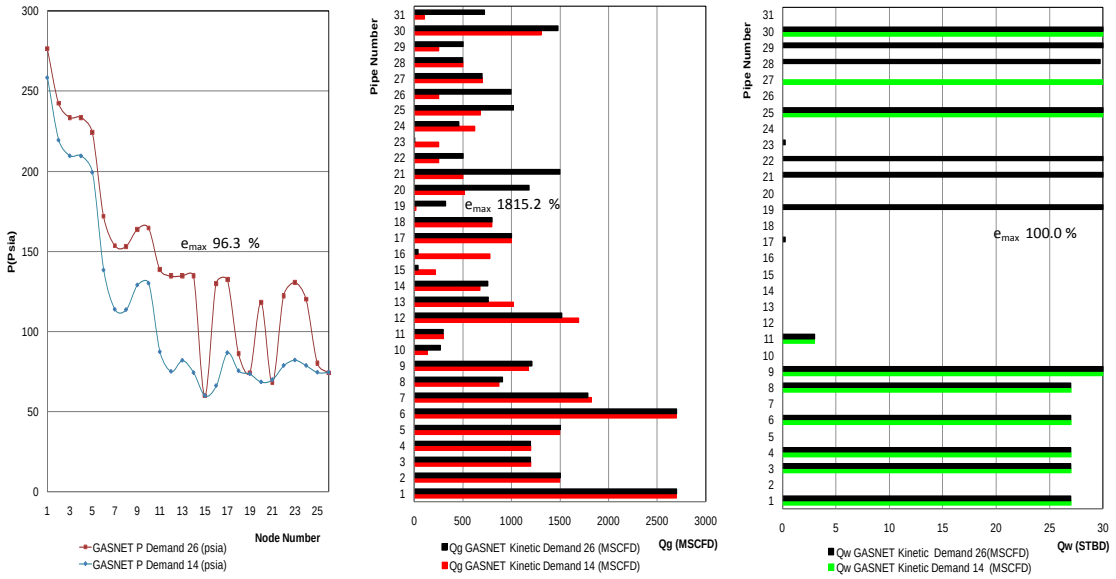

Figure 48 Results for two phases in a complex gas distribution network. Run with GASNET (Kinetic Energy Split) changing the P specified from node 14 to node 26 (26 nodes 31 pipes 6 loops)

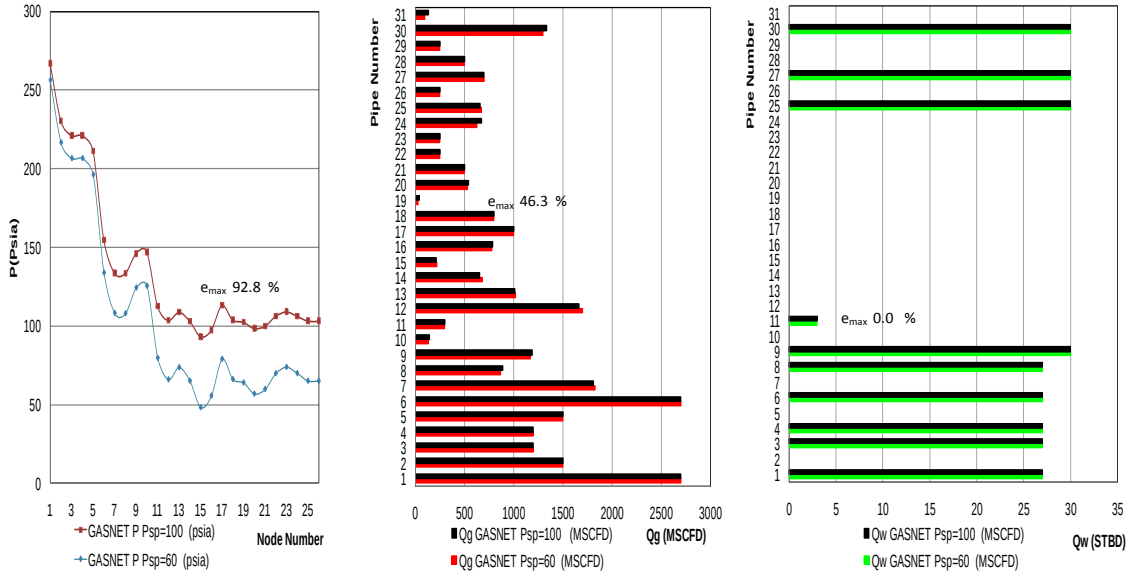

Figure 49 Results for two phases in a complex gas distribution network. Run with GASNET (Kinetic Energy Split) changing the P specified from 60 psia to 100 psia on node 21 (26 nodes 31 pipes 6 loops)

The volume of incoming water to the network also plays an important role in route selectivity. To explore this, incoming water-gas ratios (WGR) at supply nodes were changed tenfold from 0.01 to 0.1 STB/SCF. Such change allocates 300 STB/D of water at each supply node instead of 30 STB/D originally used. Results are presented in Figure 50. It is clear that since the gas demand remains constant the gas distribution remains the same. However, the pressure

distribution and water distribution are significantly different. It is not surprising that pressure losses were bound to increase since more water is found within the system; however, the new water distribution profile could not have been forecasted accordingly.

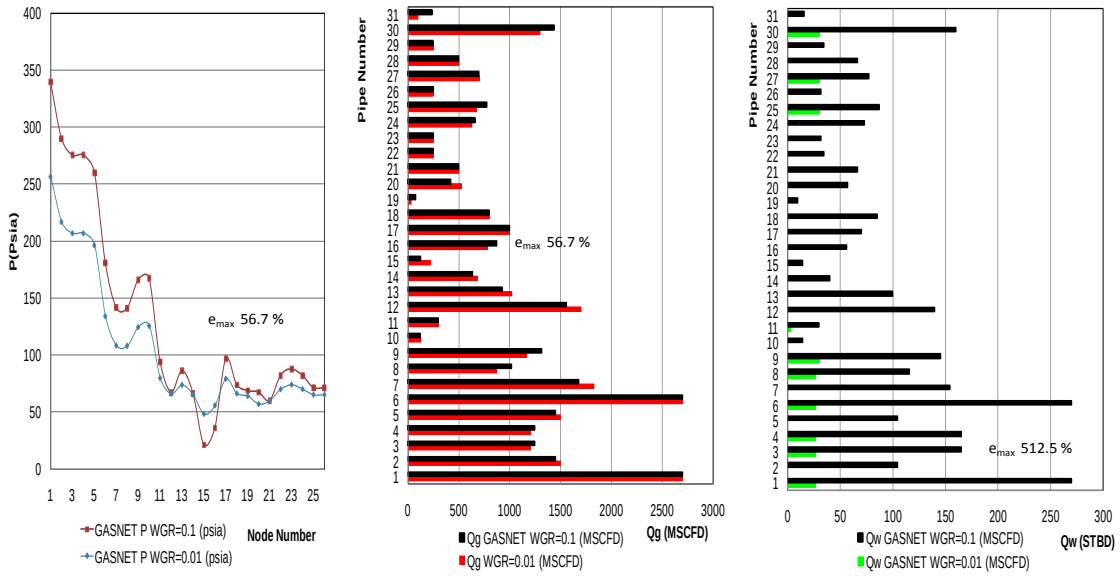

Figure 50 Results for two phases in a complex gas distribution network. Run with GASNET (Kinetic Energy Split) changing the water-gas ratio from 0.01 to 0.1 for the two inlets (26 Nodes 31 Pipes 6 Loops)

From the five scenarios tested it was possible to confirm that operational conditions have a significant impact on route selectivity of fluid flow. Current simulations that heavily rely on assumptions such as entire single phase, and Even Split sometimes lead to miscalculation of pressure drop in the system that might increase the operation and compression cost to the operators. Future generations of multiphase flow should consider the incorporation of uneven split treatment for better optimization of pipeline networks.

CHAPTER 6
CONCLUSIONS AND RECOMMENDATIONS

A comprehensive network model has been completed with the successful development and testing of a new flexible two-phase simulator (GASNET) capable of handling complex networks, and treating more rigorously the flow splits at tee-junctions. The developed code is able to handle and effectively model single-phase and two-phase flows in complex pipeline networks. Currently available commercial models heavily rely on single-phase-flow assumptions and Even Split of phases at tee-junctions during two-phase-flow. Not only is two-phase flow a common occurrence in gas pipeline networks, but when two-phase flow does occur, Even Split rarely takes place at pipe tee-junctions. The use of such common assumptions has been shown to introduce significant deviation in the prediction of actual water distribution in networks. As a consequence, anticipated pressure drops due to the second phase can also be affected significantly. The proposed model has been shown to allow the user to effectively trace the liquid's path inside the network and plan to undertake adequate corrective operational measures to maintain system capacity and minimize compression requirements. As such, the GASNET two-phase code allows improvement of the gas transmission process analysis, identifying the places were compressors and traps should be located and pigging operations should be expected. Even small improvements in pipeline network performance can translate into significant economic savings, since less compression and less maintenance would be required.

The proposed two-phase GASNET model has been tested and validated with PIPESIM for the cases of single phase and Even Split for five different networks. Single phase results show a differences range from 0.03 to 4.7% with an average 2.0 % for the pressure distribution profile and a range of differences between 0.0 to 31.0% with an average of 5.4% for the gas distribution profile. For the Even Split, the range of differences were found between 0.0 to 13.4% for the pressure distribution profile, from 0.0 to 27.9 %with an average of 5.2 % for the gas distribution profile and between 0.0 and 72% with an average of 20 % for the water distribution profile. Even though the total average difference for the water distribution profile seems high, the value of 72% was obtained in a single network. Deviations are significantly more pronounced when comparing predictions from the Even Split against the Kinetic Energy Model and the Dual Stream model. The Kinetic Energy Model shows an average differences range of 0.0 to 34.6% for the pressure distribution profile, an average range of differences between 0.0 and 118.0% for the gas distribution profile an average range of between 0.0 and 1414.3% for the liquid distribution

profile. The Dual Stream Model provides more realistic predictions of actual split conditions at Tee-junctions, and thus it represents a better approach to multiphase flow network modeling than the Even-Split and/or Kinetic Energy Ratio models.

In terms of the predictions of preferential liquid routes, the uniform or Even Split assumption commonly used in commercial simulators oversimplifies the problem considerably. Splits based on the Kinetic Energy Ratio are shown to generate more realistic predictions of gas and liquid distribution in the network. However, the Kinetic Energy Model can still misrepresent the correct phase distribution and associated pressure drops when compared to the predictions from the Double Stream Model. For these cases there can be some considerable differences that have an important impact on the route selectivity process that affects the liquid distribution in the system. Hence, in order to properly handle fluid migration in a gas pipeline network, the new generations of network models should consider the implementation of the Dual Stream Model.

The proposed new liquid-tracking tool relies on the Newton Raphson numerical method for the solution of the resulting highly non-linear set of governing equations. In general, the number of iterations needed for convergence will depend on the complexity of a network. For the simple cases between 5 to 7 iterations will be required and for the more complex systems between 7 and 15 iterations will be required. A maximum number of iterations was set to 500 to avoid excessively long runs. The current version of the GASNET model allows the user to either specify well information in terms of fixed demands and supplies or use the Inflow Performance Relationship (IPR) when evaluating the performance of wells feeding the network. These results can be used to suggest optimal well operating conditions. New generations of the two phase models are recommended to incorporate the temperature effect and compressor performance along the lines, to be able to fully link it to an economic decision process.

BIBLIOGRAPHY

Abdel Waly, A., El-Massry, Y., Darweesh, T., and Sallaly, M. E. (1996). "Network model for an integrated production system applied to the Zeit Bay fiel Egypt", Journal of Petroleum Science and Engineering , 15, p.p 57-68.

Adewumi, M., and Mucharam, L. (1991). "A study of the Effect of Condensate Formation on Performance Predictions in a gas Pipeline Network". SPE Production Operations Symposium, 7-9 April, Oklahoma City, Oklahoma , p.p 897-910.

Adewumi, M., and Shifeng, T. (1990). " A compositional two-phase flow model for analyzing and designing complex pipeline network systems ". CIM/SPE International Technical Meeting, 10-13 June 1990, Calgary, Alberta, Canada , p.p 1-24.

Alexis, D. A. (2009). "Assesment of deliverability of a natural gas gatherig and production system: Development of an integrated reservoir- surface model". MS Thesis The Pennsylvania State University, University Park PA.

Alp, D. (2009). "Characterizzing two-phase transport and flow dynamics in complex natural gas networks". PhD Thesis Dissertation The Pennsylvania State University, University Park PA.

Aragón, A., Suárez, M. C., Moya, S., and Izquierdo, G. (2007). "The use of Inflow Performance Relationships to Identify Reservoir Response During Production Tests in a Geothermal Well", Thirty-Second Workshop on Geothermal Reservoir Engineering , Stanford University, Stanford, California, p.p 22-24.

Asante, B. (2000). Two Phase Flow : Accounting for the Presence of Liquid in Gas Pipeline Simulation. http://www.psig.org/papers/2000/02W3.pdf Last accesed December 10, 2009.

Ayala, L. (2008-2009). "Natural Gas Engineering (PNG-530)" Class notes The Pennsylvania State University, University Park PA.

Aziz, K., Govier, G., and Fogarasi, M. (1972)." Pressure drop in Wells producing Oil and Gas", Journal of Canadian Petroleum Technology, Volume 14, Number 4 p.p 38-48

Baker, O. (1954). "Design of Pipelines for simultaneous Flow or Oil and Gas", Oil & Gas Journal, 53, p.p 185

Beggs, H. D. (2003). "Production Optimization Using Nodal Analysis", OGCI and Petroskills Publications, Tulsa, Oklahoma p.p 191-196

Brill James, H. B. (1972). "Two phase flow in inclined pipes", PhD diseerrtation The University of Tulsa, Tulsa, Oklahoma

Brill, J. P., and Mukherjee, H. (1999). "Multiphase Flow in Wells", Society of Petroleum Engineers Inc. Richardson, Texas p.p. 5-55.

Fazeli, A., Vatani, A., and Darab, M. (2006). "Computer programing Simulation of two Phase - Flow Pipelines using Mechanistic and Semiempirical Models" 6th International Pipeline conference , p.p 1-8.

Gardel, A. (1957). "Les pertes de changeles évoulements au travers de branchements en té." . Bulletin Technique de la Suisse Romande , 122-130 and 10(1957) p.p 143-148.

Gould, T., and Ramsey, E. (March 1975) "Design Of Offshore Gas Pipelines Accounting For Two-Phase Flow", Journal Of Petroleum Technology Volume 27, Number 3, p.p 366-374

Hagedorn, A., and Brown, K. (April 1965). "Experimental Study of pressure Gradients Ocurring During Continuos Two Phase Flow in small Diameter Vertical Conduit", Journal of Petroleum Technology , p.p 475-484.

Hart, Hamersma, J., and Fortuin, J. M. (1989). "Correlations Predicting Frictional Pressure Drop and Liquid Holdup During Horizontal Gas-Liquid Pipe Flow with a Small Liquid Holdup", International Journal of Multiphase , Volume 15, p.p 947-964.

Hart, J., Hamersma, P., and Fortuin, J. (1991). "Phase distribution during gas-liquid flow through horizontal dividing junctions", Nuclear Engineering Design , p.p 293-312.

Hart, J., Hamersma, P., and Fourtuin, J. (1991). "A Model Predicting Liquid Route Preference", Chemical Engineering Science , Volume 46, Issue 7:160922.

Hein, M. (1985). "Rigorous and approximate Methods for CO2 Pipieline analysis. Facilities, pipelines, and measurements " 41st Petroleum Mechanical Engineering Workshop and Conference , Fullerton, CA p.p 123-151.

Hope, P., and Nelson, R. (September 1977). "A New Approach To The Design Of Wet Gas Pipelines", Houston: ASME Conference.

Ikoku, C. U. (1984). "Natural gas production engineering" New York : John Wiley & Sons .

Kelkar, M. (2008). "Natural Gas Prodcuction Engineering" Oklahoma: Penn Well Corporation.

Kelner, E., Ayala, L. F., and Garcia-Hernandez, A. (2007, July). "Model Improves Measurement And Control; Helps Locate Liquids" Pipeline & Gas Journal , p.p 38-41.

Krishmamurthy, J. K. (2008). "Performance analysis of a Natural Gas gathering and production system and diagnosis of operational bottlenecks", MS Thesis The Pennsylvania State University, University Park, PA

Liao, J., Meia, R., and Klausner, J. F. (1995). "A study on the numerical stability of the two-fluid model near ill-posedness", International Journal of Multiphase Flow , p.p 335-349.

Martinez, F.F (1994). "Twp phase gas-condensate flow in pipeline open-networks system", MS Thesis The Pennsylvania State University, University Park, PA

Menon, E. S. (2005). "Gas pipeline hydraulics" In E. S. Menon, Gas pipeline hydraulics: Taylore & francis Editorial. Boca Raton, FL p.p 31-81.

Mukherjee, H., and Brill, J. (1985). "Pressure drop correlations for inclined two-phase flow" Energy Resource Technology , p.p 549-554.

Oranje, L. (1973). "Condensate behavior in gas pipelines is predictable.". Oil and Gas Journal , p.p 39-44.

Ottens, M. H. (2001). "Effect of small branch inclination on gas-liquid flow separation in T junctions", AIChE Journal , Volume 45 Issue 3 p.p 465-474.

Poettmann, F., and Carpenter, P. (1952). "The Multiphase Flow of Gas Oil and Water trough Vertical Flow Strings". Drilling and Production Practice

Raymond, T. (1995). "Fourteenth International Conference on Numerical Methods in Fluid Dynamics". France: Springer Berlin / Heidelberg. Volume 453/1995 p.p 299-306

Shoham, O. D. Barnea, , Y. Taitel and A.E. Dukler (2005). "Gas-liquid flow in inclined tubes: Flow pattern transitions for upward flow", Chemical Engineering Science, Volume 40, Issue 1, 1985, p.p 131-136

Shoham, O., Brill, J., and Taitel, Y. (1987). "Two-Phase Flow Splitting in a Tee junction Experiment and Modeling" Chemical Engineering Science , Volume 2 2667

Schlumberger PIPESIM (2007). Patent No. 6,018,497, 6,078,869 and 6,106,561 GB 2,326,747 B and GB 2,336,008 B. US and UK Patents.

Sung, W., and Daegee Huh, J. L. (August 1998). "Optimization of Pipeline Networks With Hybrid MCST-CD Networking Model". SPE Production & Facilities , p.p 213-219.

Ullah, M. (1987). "A Comparative Assesment Of the Perfomance Of Dry-Gas Methods For Predicting The Occurence Of Wet-Gas Flow Condtions" Journal Of Pipelines (Netherlands) Volume 6 Issue 1, p.p 41-48

US Department of Energy (US DOE), 2010,"About US Natural Gas Pipelines – Transporting Natural Gas", http://www.eia.doe.gov/pub/oil_gas/natural_gas/analysis_publications/ngpipeline/, last accessed: February 24, 2010.

Vogel, J. (1968). "Inflow Performance Relationships for Solution-Gas Drive Wells", Journal Of Petroleum Technology ,Volume 248 p.p 83-92.

West, W., Garvin, W., and Sheldom, J. (1954). "Solution of Equations of Unsteady State Two Phase Flow in Oil Reservor", AIME , 201,217-229.

Weymouth, Panhandle A and B equations for Compressible Gas Flow. (2003)., from http://www.lmnoeng.com/Flow/weymouth.htm last accesed June 16, 2009

APPENDIX A

INPUT FILE STRUCTURE

The following section offers a practical step by step summary on how to operate the GASNET model, with requires the construction of the following input file as described below.

a) The first line of a GASNET input file corresponds to the simulation title. Do not leave blanks spaces, you can use letters and numbers as shown.

```
TITLE:Double_Loop_Sample_1_Dec_15
```

b) Nodes and pipes must be quantified. All nodes and pipes must be numbered. It is a good practice to try to maintain certain order from left to right or from top to bottom. As an example, the network in Figure 40 is considered. As shown in Figure 51

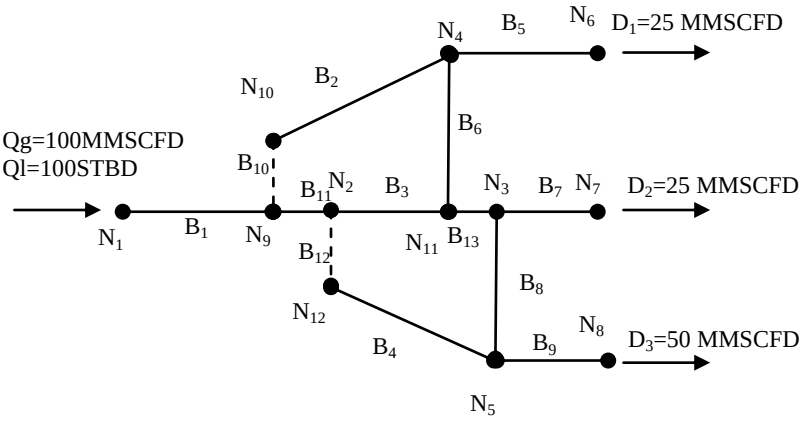

Figure 51 Equivalent system to avoid more than three pipes in a single node

In this network, the total number of nodes (NNODES) in the system is 12 nodes and the total number of pipes (NPIPES) is 13 and the number of pipe loops (NLOOPS) is 2. This information is now included in the next two lines of the input file, as shown below

```
TITLE: Double_Loop_Sample_1_Dec_15
NPIPES
13
NNODES
12
NLOOPS ( NLOOPS = NPIPES - NNODES + 1 )
2
```

c) The next section of the input file corresponds to the pipe information, in the following column wise :

i. Pipe number (Loc)
ii. Upstream node (JUP)
iii. Downstream node (JDN)
iv. Pipe Efficiency (fe)
v. Average Temperature in F (Tav)
vi. Internal Diameter (ID) (in)
vii. Pipe roughness (in)
viii. Total number of slopes of single pipe (#Slopes)
ix. Length of each slope (ft)
x. Actual endpoint elevation of each slope of the pipe

Thus, as a sample, the pipes information lines should appear as follows:

```
Loc/ JUP/JDN/Fe/  Tav/Id/Rough/Slop/Length/Elev/fromUPtoDOWN
1     1   9   1.0  70  4.0 0.06  1  316.8  0.0    0.0
2     19  21  0.95 60  2.3 0.01  2  138.8 212.1 280.0 270.0 240.0
```

In this example, and for the case of the first pipe (Loc=1), the information indicates that this pipe connects node 1 (JUP or Upstream Node) and node 9 (JDN or Downstream), is 100% efficient (“fe”), flowing at an average temperature of 70 F(Tav), with an internal diameter of 4 in(ID). In addition, the total roughness is 0.06 in(e), the pipe is described by 1 single slope (#slopes), and its total length is 316.8 ft(L ft), without elevation. For the second pipe (Loc=2), the information indicates that it connects the nodes 19 to 21, it has a 0.95 efficiency, the average temperature is 60 F, the internal diameter is 2.3 in, roughness is 0.01 in, the pipe has 2 slopes the first slope has a length of 138.8 ft. and the second section has a length of 212.1 ft, the elevation of the first slope is from 280.0 ft to 270.0, and the elevation of the second section is indicated from 270.0 to 240.0. For the example used in this appendix (Figure 40), the input file now should look as follows:

```
TITLE: Double_Loop_Sample_1_Dec_15
NPIPES
13
NNODES
12
NLOOPS ( NLOOPS = NPIPES - NNODES + 1 )
2
LOCATION(I)/JUP(I)/JDN(I)/fe/Tav(F)/ID(in)/e(in)   /#slopes
/L'sft(i=1,..,#slopes) /ActualElevations-ft(#slopes+1)
fromUPtoDOWN
1  1   9  1.0 82 4.0   0.0006 1  10     0.0   0.0
2  10  4  1.0 82 8.0   0.0006 1  198000 0.0   0.0
3  2  11  1.0 82 10.0  0.0006 1  171600 0.0   0.0
4  12  5  1.0 82 10.0  0.0006 1  198000 0.0   0.0
5  4   6  1.0 82 4.0   0.0006 1  10     0.0   0.0
6  4   11 1.0 82 6.0   0.0006 1  99000  0.0   0.0
7  3   7  1.0 82 2.0   0.0006 1  10     0.0   0.0
8  3   5  1.0 82 8.0   0.0006 1  99000  0.0   0.0
9  5   8  1.0 82 2.0   0.0006 1  10     0.0   0.0
10 9  10  1.0 82 2.0   0.0006 1    1    0.0   0.0
11 9   2  1.0 82 2.0   0.0006 1    1    0.0   0.0
12 2  12  1.0 82 2.0   0.0006 1    1    0.0   0.0
13 1   3  1.0 82 2.0   0.0006 1    1    0.0   0.0
```

d) The next step in the input file is to indicate the node and the value of pressure the user wants to specify. In our case: Node 6 with P=400 psia.

e) The next information required to put in the input file is the node information. The required order is as follows: Node number, 90 degrees pipe, select the type of node (balance node, fixed node, IPR), Gas supply or demand flowrate and Water Gas Ratio (if is a supply node). To help understand the 90 degrees pipe concept Figure 53 is presented as a clear example. In this case the 90 degrees pipe is B3 that connects nodes 2 and 4. If node type is set to 0 it indicates balance node, balance node can be only set at demands nodes and every system must have one balance node. If node type is set to 1, the node is considered as fixed node (no changes expected on that node). If the node type is set to 2, the Inflow Performance Relationship (IPR) is used. For IPR nodes, meaning that a well is present on that node, the information needed and the order which should be presented as follows: well performance constant, shut in pressure and the flow exponent for the well.

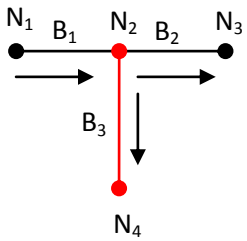

Figure 52 90 degrees pipe definition

The node information should look as follows:

```
NODE/90d-PIPE/0-1-2(Balance/Fixed/IPR)/Qg(MSCFD)  / WGR(STB/MSCFD
1     0     2     0.0326d0    175d0   0.5d0  4.4
2     3     1    0.0
3     0     1    -300
4     0     0     0
```

The information presented above can be interpreted as follows: For node 1 there is no 90 degrees pipe (indicated by 0), since it is type 2 node (IPR node) there is a well on that node, the well performance constant is 0.0326 mscfd/psi2n the shut in pressure for that well is 175 psia the well exponent factor is 0.5 and the Water Gas ratio (WGR) for the inflow of the well is 4.4 STB/SCF. Then for node 2 which is a tee junction the 90 degrees pipe is B3. It is a fixed node (1) and there is no supply or demand on that node. Following node 3, does not have a 90 degrees pipe connected, it is a fixed node, it has a demand of 300 MSCFD (Supply rates are positive and demand rates are negative) and finally, node 4 there is no 90 degrees pipe and it is a balance node, therefore no demand should be specified on that node. At this point, and for the sample problem described at the beginning of this Appendix, the input file looks as follows:

```
TITLE: Double_Loop_Sample_1_Dec_15
NPIPES
13
NNODES
12
NLOOPS ( NLOOPS = NPIPES - NNODES + 1 )
2
LOCATION(I)/JUP(I)/JDN(I)/fe/Tav(F)/ID(in)/e(in)  /#slopes
/L'sft(i=1,..,#slopes) /ActualElevations-ft(#slopes+1)
fromUPtoDOWN
1  1   9  1.0 82 4.0   0.0006 1  10     0.0  0.0
2  10  4  1.0 82 8.0   0.0006 1   198000 0.0 0.0
3  2  11  1.0 82 10.0  0.0006 1  171600 0.0  0.0
4  12  5  1.0 82 10.0  0.0006 1  198000 0.0  0.0
5  4   6  1.0 82 4.0   0.0006 1    10     0.0 0.0
6  4   11 1.0 82 6.0   0.0006 1    99000 0.0 0.0
7  3   7  1.0 82 2.0   0.0006 1    10     0.0 0.0
8  3   5  1.0 82 8.0   0.0006 1    99000 0.0 0.0
9  5   8  1.0 82 2.0   0.0006 1    10     0.0 0.0
10 9  10  1.0 82 2.0   0.0006 1    1      0.0 0.0
11 9   2  1.0 82 2.0   0.0006 1    1      0.0 0.0
12 2  12  1.0 82 2.0   0.0006 1    1      0.0 0.0
13 11  3  1.0 82 2.0   0.0006 1    1      0.0 0.0
NODE-WITH-PRESSURE-SPECIFICATION: NodeNumber/Pressure(psia)
6    400d0
NODE INFORMATION: NODE / 90d-PIPE /0-1-2(Balance/Fixed/IPR)/
Qg(MSCFD) / WGR(STB/MSCFD)
1     0     1 100000d0       0.1d0
2     12    1 0d0            0d0
3     8     1 0d0            0d0
4     6     1 0d0            0d0
5     8     1 0d0            0d0
6     0     0 0d0            0d0
7     0     1 -25000d0       0d0
8     0     1 -25000d0       0d0
9     10    1 0d0            0d0
10    0     1 0d0            0d0
11    6     1 0d0            0d0
12    0     1 0d0            0d0
```

f) Following the input file must contain the gas information: Gas Specific gravity, compressibility factor, gas viscosity (cp) the Pressure (psi) and Temperature (F) at standard conditions. The gas information should look as follows:

```
Gas Gravity/ Zav(Zav=0 if Standing) / Gas Visc(cp) /  Psc (psia)
/ Tsc (F) [Base Conditions]
0.62       0.89     0.0127d0  14.7     60.0
```

If the compressibility factor is not known, the program can determine it using the Standing Katz correlation, the user needs to specify it as zero (Zav=0).

g) Then the liquid information should be provided. Liquid density (lb/ft3) liquid viscosity (cp) and the surface tension(dynes/cm), as shown bellow. This information is used by the Beggs and Brill two-phase flow correlation

```
LiqDens(lb/ft3) / LiquidVisc(cp)/ Surf Tension (dynes/cm)

  62.4d0   0.85d0           59.66d0
```

h) Next, the user needs to select the desired approach to solve the single phase case. The following options are available: (1) for Generalized Equation, (2) for Weymouth, (3) for Panhandle A and (4) Panhandle B. Also, in this section of the input file, the user can select if two phase calculations are needed or not (1 if it is needed and 2 if not). If two phase results are required, then the user must select the split type to be used. The options are (1) for uniform or Even Split, (2) Kinetic Energy ratio split and (3) for the Dual Stream Model, as shown:

```
GAS_Flow_Equation(1=Gen;2=Wey;3=Panh-A;4=Panh-B)/ YES(=1)-
  NO(=0)2PCalcBeggsandBrill/SPLIT_HANDLING:(1)=UNIFORM;(2)=KEbase
  d; (3)=DoubleStream

2   1   2
```

In the part of the input file shown above the user has selected to run single phase solved with Weymouth(2), the two phase results are requested(1) and the split must be solved with the Kinetic Energy Ratio option (2)

i) Since this model uses a Newton Raphson procedure as part of the numerical model solver, a Jacobian matrix needs to be built. For that the user has two options, a numerical or analytical

method. It is strongly recommended to use the numerical method as a default option, as shown:

```
Type of Jacobian Entry Calculation (1=Numerical ; 2=Analytical)
1
```

j) Since the Newton Raphson procedure is an iterative protocol it is highly dependent on the initial guess, this can accelerate the iteration process and can prevent the system from divergence. The final section of the input file allows the user to create an input file (that can be used on future runs and forecasting), or if the pressures are known or the user has an idea of a closer value, the

information can be input in a separate file. The file is just a txt file that contains only the pressure guess for each node. It is **very important** that the total number of pressures entries in this file matches the total number of nodes, if the number of pressures does not match the number of nodes, the program will lead to an error. A final view of the input file for the sample run in this Appendix is shown in Figure 53

```
TITLE: Double_Loop_Sample_1_Dec_15_APPENDIX_FILE
NPIPES
13
NNODES
12
NLOOPS ( NLOOPS = NPIPES - NNODES + 1 )
2
LOCATION(I)/JUP(I)/JDN(I)/fe/Tav(F)/ID(in)/e(in)  /#slopes /L'sft(i=1,..,#slopes) /ActualElevations-ft(#slopes+1) fromUPtoDOWN
1       1      9       1.0 82  4.0     0.0006 1         10      | 0.0   0.0
2       10     4       1.0 82  8.0     0.0006 1        198000    0.0   0.0
3       2      11      1.0 82  10.0    0.0006 1        171600    0.0   0.0
4       12     5       1.0 82  10.0    0.0006 1        198000    0.0   0.0
5       4      6       1.0 82  4.0     0.0006 1         10       0.0   0.0
6       4      11      1.0 82  6.0     0.0006 1         99000    0.0   0.0
7       3      7       1.0 82  2.0     0.0006 1         10       0.0   0.0
8       3      5       1.0 82  8.0     0.0006 1         99000    0.0   0.0
9       5      8       1.0 82  2.0     0.0006 1         10       0.0   0.0
10      9      10      1.0 82  2.0     0.0006 1         1        0.0   0.0
11      9      2       1.0 82  2.0     0.0006 1         1        0.0   0.0
12      2      12      1.0 82  2.0     0.0006 1         1        0.0   0.0
13      11     3       1.0 82  2.0     0.0006 1         1        0.0   0.0
NODE-WITH-PRESSURE-SPECIFICATION: NodeNumber/Pressure(psia)
6    400d0
NODE INFORMATION: NODE / 90d-PIPE /0-1-2(Balance/Fixed/IPR)/ Qg(MSCFD) / WGR(STB/MSCFD)
1       0      1       100000d0        0.1d0
2       12     1       0d0             0d0
3       8      1       0d0             0d0
4       6      1       0d0             0d0
5       8      1       0d0             0d0
6       0      0       0d0             0d0
7       0      1       -25000d0        0d0
8       0      1       -25000d0        0d0
9       10     1       0d0             0d0
10      0      1       0d0             0d0
11      6      1       0d0             0d0
12      0      1       0d0             0d0
Gas Information: Gas Gravity/ Zav(Zav=0 if Standing) / Gas Visc(cp) /  Psc (psia) / Tsc (F) [Base Conditions]
                        0.62                    0.89                    0.0127d0                14.7        60.0
Liquid Information: LiqDens(lb/ft3) / Liquidvisc(cp)/ Surf Tension (dynes/cm)
        62.4d0          0.8566d0                59.66671626d0
1PGAS_Flow_Equation(1=Gen;2=Wey;3=Panh-A;4=Panh-B)/ YES(=1)-NO(=0)2PCalcBeggs&Brill     / SPLIT_HANDLING: (1)=UNIFORM;(2)=KEbased; (3)=DoubleStream
2       1       2
Type of Jacobian Entry Calculation (1=Numerical ; 2=Analytical)
1
PressInitial.txt        file    (0=Not  needed  ;       1=Create        it      ;       2=Use   it      when    available       for     P-initialization)
1
```

Figure 53 Final view of input file for the problem shown in the APPENDIX

Since this code was developed in FORTRAN it is very important that the input file does not have any blank line, if the user leaves blank lines within the inputs, the program will not run, and displays an error message. It is important that both "txt" files (the input file and the nodal pressure specification file) are located in the same folder where GASNET two-phase executable is located. Once the input file is ready you can start to run the program by double clicking on the executable file. The program will start to run on a command screen window, and the following message will appear (Figure 55).

```
Model has processed the following values as specified (constant):
*) P          at node                    6   =     400.0000000000000       psia

NETWORK CONNECTIVITY DIAGNOSTICS:
Network is fully communicating!
OVERALL Interconnectivy test a SUCCESS
Node Trail followed to establish overall interconnectivity...
 6   4  10  11   9   2   3   1  12   7   5   8
SPANNING TREE ** Pipes Belonging to the Tree:
 1   2   3   5   6   7   8   9  10  12  13
Number of LOOPS detected =            2  (= Number of out-of-tree pipes)
READY TO START COMPUTATIONS ... Please press [ENTER]
```

Figure 54 Initial message when the program starts to run

As shown in Figure 54 the result is the pressure in each node, pipe conductivity (MSCFD/psi) Gas flowrate (MSCFD) and liquid flowrate (STB/D). These results can be exported to a txt fileor an excel file for plotting purposes.

```
NR It: 18 -- dPmax=     0.0000022 psia -- Resmax=          0.00020 JacRow=   7
  Diverg. T-junction at NODE:    2: SplitG =  0.60887 SplitL =  0.15398
  Diverg. T-junction at NODE:    5: SplitG =  0.33297 SplitL =  1.00000
  Diverg. T-junction at NODE:    9: SplitG =  0.38444 SplitL =  0.17351
  Diverg. T-junction at NODE:   11: SplitG =  0.47998 SplitL =  0.25165
NR It: 19 -- dPmax=     0.0000009 psia -- Resmax=          0.00007 JacRow=   8
  Diverg. T-junction at NODE:    2: SplitG =  0.60887 SplitL =  0.15398
  Diverg. T-junction at NODE:    5: SplitG =  0.33297 SplitL =  1.00000
  Diverg. T-junction at NODE:    9: SplitG =  0.38444 SplitL =  0.17351
  Diverg. T-junction at NODE:   11: SplitG =  0.47998 SplitL =  0.25165
NR It: 20 -- dPmax=     0.0000001 psia -- Resmax=          0.00001 JacRow=   7
  Diverg. T-junction at NODE:    2: SplitG =  0.60887 SplitL =  0.15398
  Diverg. T-junction at NODE:    5: SplitG =  0.33297 SplitL =  1.00000
  Diverg. T-junction at NODE:    9: SplitG =  0.38444 SplitL =  0.17351
  Diverg. T-junction at NODE:   11: SplitG =  0.47998 SplitL =  0.25165
 *Successful* N-R convergence achieved in          20  iterations

TITLE:
P,C,Q PREDICTIONS BASED ON 1P Beggs & Brill EQUATION

Nodal Pressures (psia)   * Conductiv(MSCFD/psi) * Pipe Gas Flows,  Qg (MSCFD)
P(   1)=    1294.93 psia * Cg(  1)=     578.566 * Qg(  1)=   100000.000 MSCFD
                           FPattern(   1)=    3  Qw(   1)=    10000.000 STB/D
P(   2)=    1257.69 psia * Cg(  2)=      31.746 * Qg(  2)=    38443.866 MSCFD
                           FPattern(   2)=    5  Qw(   2)=     1735.148 STB/D
P(   3)=    1033.65 psia * Cg(  3)=      33.749 * Qg(  3)=    24076.419 MSCFD
                           FPattern(   3)=    6  Qw(   3)=     6992.200 STB/D
P(   4)=     408.99 psia * Cg(  4)=      58.664 * Qg(  4)=    37479.714 MSCFD
                           FPattern(   4)=    5  Qw(   4)=     1272.652 STB/D
P(   5)=    1077.88 psia * Cg(  5)=     586.390 * Qg(  5)=    50000.000 MSCFD
                           FPattern(   5)=    3  Qw(   5)=     3494.733 STB/D
P(   6)=     400.00 psia * Cg(  6)=      12.144 * Qg(  6)=   -11556.134 MSCFD
                           FPattern(   6)=    4  Qw(   6)=    -1759.585 STB/D
P(   7)=     968.13 psia * Cg(  7)=      69.032 * Qg(  7)=    25000.000 MSCFD
                           FPattern(   7)=    3  Qw(   7)=     6505.267 STB/D
P(   8)=    1067.39 psia * Cg(  8)=      40.834 * Qg(  8)=   -12479.714 MSCFD
                           FPattern(   8)=    5  Qw(   8)=    -1272.652 STB/D
P(   9)=    1283.34 psia * Cg(  9)=     166.637 * Qg(  9)=    25000.000 MSCFD
                           FPattern(   9)=    2  Qw(   9)=        0.000 STB/D
P(  10)=    1278.18 psia * Cg( 10)=     334.299 * Qg( 10)=    38443.866 MSCFD
                           FPattern(  10)=    3  Qw(  10)=     1735.148 STB/D
P(  11)=    1035.79 psia * Cg( 11)=     241.104 * Qg( 11)=    61556.134 MSCFD
                           FPattern(  11)=    3  Qw(  11)=     8264.852 STB/D
P(  12)=    1253.00 psia * Cg( 12)=     345.615 * Qg( 12)=    37479.714 MSCFD
                           FPattern(  12)=    3  Qw(  12)=     1272.652 STB/D
P(****)= ********** psia * Cg( 13)=     188.191 * Qg( 13)=    12520.286 MSCFD
                           FPattern(  13)=    3  Qw(  13)=     5232.615 STB/D

PRODUCTION FROM VARIABLE-FLOW NODES [Balance Node and Nodes Type 2]
NODE=   6 - ** BALANCE NODE **                     - Qbalc= -50000.000 MSCFD

 Beggs&Brill FPattern Nomenclature:
 FP=1  LIQUID        - FP=2  GAS         - FP=3  DISTRIBUTED
 FP=4  INTERMITTENT  - FP=5  SEGREGATED  - FP=6  TRANSITION
Fortran Pause - Enter command<CR> or <CR> to continue.
```

Figure 55 Display after convergence is achieved

As shown in Figure 56, the result is the pressure in each node, pipe conductivity (MSCFD/psi) Gas flowrate (MSCFD) and liquid flowrate (STB/D). These results can be exported to a txt file or an excel file for plotting purposes.

APPENDIX B

BEGGS AND BRILL ALGORITHM

The Beggs and Brill subroutine requires the following input data:

1) Pipe diameter (D) [ft]
2) Pipe inlet pressure [psia]
3) Fluid densities (ρ_L, ρ_g) [lb/ft^3]
4) Superficial gas and liquid velocities (U_{sl}, U_{sg}) [ft/s]
5) Mixture velocities (U_m) [ft/s]

The routine will start as follows:

a) Determination of the Froude number

$$N_{fr} = \frac{U_m^2}{g\ D} \tag{B-1}$$

b) Calculation of the liquid fraction with the following expression:

$$\lambda l = \frac{U_{sl}}{U_m} \tag{B-2}$$

c) Calculation of the Liquid velocity number

$$N_{lv} = 1.938 \left(\frac{U_{sl}\rho_L}{g\ \sigma}\right)^{1/4} \tag{B-3}$$

d) Calculate the limits of the Beggs and Brill Application

$$L1 = 316\ \lambda_l^{\ 0.302}$$

$$L2 = 0.0009252 * \lambda_l^{\ -2.4682}$$

$$L3 = 0.1 * \lambda_l^{\ -1.4516}$$

$$L4 = 0.5 * \lambda_l^{\ (-6.738)}$$

(B-4)

e) Classify the flow type according to Nfr and λ_l according to the following classification:

λ_l <0.01 and Nfr<L1 or 0.01<= λ_l and Nfr<L2	==> Segregated flow
0.01<= λ_l <0.4 and L3<Nfr<=L4 or 0.4< λ_l and L3< λ_l <=L4	==> Intermittent flow
λ_l <0.4 and L1<=Nfr or 0.4<= λ_l and L4<Nfr	==> Distributed flow

$0.01 < \lambda_l$ and L2<Nfr<L3 ==> Transition flow

f) Determination of the correction term due to inclination and liquid holdup for horizontal case according to the flow pattern

$$H_{l(0)} = \frac{a\lambda_l^b}{N_{fr}^c} \tag{B-5}$$

Flow Regime	A	B	C
Segregated	0.98	0.4846	0.0868
Intermittent	0.845	0.5351	0.0173
Distributed	1.065	0.5824	0.0609

Constant for the inclination factor

$$C = (1-\lambda_l)\ln(d C\lambda_l^e N_{lv}^f N_{fr}^g) \tag{B-6}$$

Flow Regime	d	e	f	g
Segregated Uphill	0.011	-3.768	3.539	-1,614
Intermittent Uphill	2.96	0.305	-0.4473	0.0978
Distributed Uphill	--	--	--	--
All Flows downhill	4.7	-0.3692	0.1244	-0.056

For transition flow the holdup is calculated with the following expression

$$H_{l(tran)} = A * H_{l(Segr)} + B H_{l(Interm)} \tag{B-7}$$

g) Calculation of the inclination factor:

$$\Psi = 1 + C\left(Sin(1.8\theta) - \frac{1}{3}Sin^3(1.8\theta)\right) \tag{B-8}$$

h) Calculation of the holdup on the inclination plane:

$$H_{(Angle)} = \Psi * H_{(0)} \tag{B-9}$$

i) Calculate the properties of the two phase and nonslip:

$$\rho_{tp} = Rho_l\left(H_{(Angle)}\right) + Rho_g(1 - H_{(Angle)}) \tag{B-10}$$

$$\rho_{ns} = Rho_l(\lambda_l) + Rho_g(1-\lambda_l) \tag{B-11}$$

$$\mu_{tp} = \mu_l\left(H_{(Angle)}\right) + \mu_g(1 - H_{(Angle)}) \tag{B-12}$$

$$\mu_{ns} = \mu_l(\lambda_l) + \mu_g(1 - \lambda_l)$$

(B-13)

j) Calculation of the pressure drop due to hydrostatic head

$$\left(\frac{dP}{dz}\right)_{el} = \frac{\rho_{tp}\, g\, Sin\,(Angle\,)}{gc}$$

(B-14)

k) Determination of the nonslip Reynolds Number

$$Re_{ns} = \frac{\rho_{ns}\, U_m\, D\ (1488.16)}{\mu_{ns}}$$

(B-15)

l) Determination of Non slip friction factor with Jain equation:

$$Fns = \left(1.14 - 2 * Log\left(\frac{e}{D} + \frac{21.25}{Re_{ns}^{0.9}}\right)\right)^{-2}$$

(B-16)

m) Calculation of y:

$$y = \left(\frac{\lambda}{H^2_{(Angle\ )}}\right)$$

(B-17)

n) Determination of the Beggs and Brill Coefficient

$$s = Ln(2.2y - 1.2)\ if\ 1 < y < 1.2$$

(B-18)

$$s = \frac{Log\,(y)}{-0.0524 + 3.182\,Log\,(y) - 0.872\,(Log\,(y))^2 + 0.01853\,(Log\,(y))^4}$$

(B-19)

o) Determination of non slip friction factor with Jain equation:

$$Ftp = Fns(e)^s$$

(B-20)

p) Calculation of the pressure gradient

$$\left(\frac{dP}{dz}\right)_{fric} = \frac{F_{tp}\,(Um)^2 \rho_{ns}}{2g_c\, D}$$

(B-21)

q) Determination of the acceleration term

$$Ek = \frac{\rho_{ns}(U_m)U_{sg}}{g_c\, P} \tag{B-22}$$

r) Determination of the pressure drop

$$\frac{dP}{dl} = \frac{\left(\frac{dP}{dz}\right)_{el} + \left(\frac{dP}{dz}\right)_{fric}}{1 - Ek} \tag{B-23}$$

s) Conversion from PSF to PSIA [lb/ft^2] to [lb/in^2]

t) Determination the total pipe pressure drop

$$\Delta P = \frac{dP}{dl} Length \tag{B-24}$$

APPENDIX C

SAMPLE INPUT DATA FILES

The next figures are a caption of the input files for all the networks tested with GASNET 2 phases

```
TITLE:1st_System_Gasnet_2_PHases_2_Triaigle_Loops_Figure_8
NPIPES
13
NNODES
12
NLOOPS ( NLOOPS = NPIPES - NNODES + 1 )
2
LOCATION(I)/JUP(I)/JDN(I)/fe  /Tav(F) /ID(in)   /e(in)  /#slopes/L's-ft(i=1,..,#slopes)/ ActualElevations-ft(#slopes+1)fromUPtoDOWN
1       7       2   1.0         82      10.0    0.0006  1       198000          0.0     0.0
2       2       8   1.0         82      8.0     0.0006  1       99000           0.0     0.0
3       4       3   1.0         82      6.0     0.0006  1       99000           0.0     0.0
4       9       4   1.0         82      8.0     0.0006  1       198000          0.0     0.0
5       6       3   1.0         82      10.0    0.0006  1       171600          0.0     0.0
6       5       1   1.0         82      4.0     0.0006  1       10              0.0     0.0
7       1       9   1.0         82      2.0     0.0006  1       1               0.0     0.0
8       1       6   1.0         82      2.0     0.0006  1       1               0.0     0.0
9       6       7   1.0         82      2.0     0.0006  1       1               0.0     0.0
10      4       10  1.0         82      4.0     0.0006  1       10              0.0     0.0
11      3       8   1.0         82      2.0     0.0006  1       1               0.0     0.0
12      8       11  1.0         82      2.0     0.0006  1       10              0.0     0.0
13      2       12  1.0         82      2.0     0.0006  1       10              0.0     0.0
NODE-WITH-PRESSURE-SPECIFICATION: NodeNumber/Pressure(psia)
10    400d0
NODE INFORMATION: NODE / 90d-PIPE /0-1-2(Balance/Fixed/IPR)/ Qg(MSCFD) / WGR(STB/MSCFD)
1       7       1   0d0             0d0
2       2       1   0d0             0d0
3       3       1   0d0             0d0
4       3       1   0d0             0d0
5       0       1   100000d0        0.1d0
6       9       1   0d0             0d0
7       0       1   0d0             0d0
8       2       1   0d0             0d0
9       0       1   0d0             0d0
10      0       0   0d0             0d0
11      0       1   -25000d0        0d0
12      0       1   -25000d0        0d0
Gas Information: Gas Gravity/ Zav(Zav=0 if Standing) / Gas Visc(cp) /  Psc (psia) / Tsc (F) [Base Conditions]
        0.62    0.89    0.0127d0    14.7        60.0
Liquid Information: LiqDens(lb/ft3) / LiquidVisc(cp)/ Surf Tension (dynes/cm)
        62.4d0  0.8566d0        59.66671626d0
1PGAS_Flow_Equation(1=Gen;2=Wey;3=Panh-A;4=Panh-B)/ YES(=1)-NO(=0)2PCalcBeggs&Brill     / SPLIT_HANDLING: (1)=UNIFORM;(2)=KEbased; (3)=DoubleStream
2       1       2
Type of Jacobian Entry Calculation (1=Numerical ; 2=Analytical)
1
PressInitial.txt        file    (0=Not  needed  ;       1=Create        it      ;       2=Use   it      when    available       for     P-initialization)
1
```

Figure 56 Input file for Network 1

```
TITLE:2nd_System_Gasnet_2_PHases_4_Squares_4_Loops_Figure_12
NPIPES
25
NNODES
22
NLOOPS ( NLOOPS = NPIPES - NNODES + 1 )
4
LOCATION(I)/JUP(I)/JDN(I)/fe  /Tav(F) /ID(in)   /e(in)  /#slopes/L's-ft(i=1,..,#slopes)/ ActualElevations-ft(#slopes+1)fromUPtoDOWN
1       1       2       1.0     70      4.0     0.0006  1       500d0  0.0     0.0
2       2       9       1.0     70      4.0     0.0006  1       7900d0  0.0     0.0
3       2       3       1.0     70      4.0     0.0006  1       7900d0  0.0     0.0
4       3       13      1.0     70      4.0     0.0006  1       7800d0  0.0     0.0
5       3       4       1.0     70      4.0     0.0006  1       500d0  0.0     0.0
6       4       5       1.0     70      4.0     0.0006  1       500d0  0.0     0.0
7       4       6       1.0     70      4.0     0.0006  1       7200d0  0.0     0.0
8       6       15      1.0     70      4.0     0.0006  1       8100d0  0.0     0.0
9       6       7       1.0     70      4.0     0.0006  1       500d0  0.0     0.0
10      9       8       1.0     70      4.0     0.0006  1       500d0  0.0     0.0
11      9       10      1.0     70      4.0     0.0006  1       500d0  0.0     0.0
12      10      18      1.0     70      4.0     0.0006  1       7900d0  0.0     0.0
13      10      11      1.0     70      4.0     0.0006  1       7900d0  0.0     0.0
14      11      13      1.0     70      4.0     0.0006  1       500d0  0.0     0.0
15      13      14      1.0     70      4.0     0.0006  1       500d0  0.0     0.0
16      11      12      1.0     70      4.0     0.0006  1       500d0  0.0     0.0
17      12      15      1.0     70      4.0     0.0006  1       7900d0  0.0     0.0
18      15      16      1.0     70      4.0     0.0006  1       500d0  0.0     0.0
19      18      19      1.0     70      4.0     0.0006  1       500d0  0.0     0.0
20      18      20      1.0     70      4.0     0.0006  1       7900d0  0.0     0.0
21      12      20      1.0     70      4.0     0.0006  1       7800d0  0.0     0.0
22      20      21      1.0     70      4.0     0.0006  1       7900d0  0.0     0.0
23      16      21      1.0     70      4.0     0.0006  1       7800d0  0.0     0.0
24      16      17      1.0     70      4.0     0.0006  1       500d0  0.0     0.0
25      21      22      1.0     70      4.0     0.0006  1       500d0  0.0     0.0
NODE-WITH-PRESSURE-SPECIFICATION: NodeNumber/Pressure(psia)
19    100d0
NODE INFORMATION: NODE / 90d-PIPE /0-1-2(Balance/Fixed/IPR)/ Qg(MSCFD) / WGR(STB/MSCFD)
1       0       1       14000d0         0.2d0
2       3       1           0d0         0d0
3       4       1           0d0         0d0
4       6       1           0d0         0d0
5       0       1       -2000d0         0d0
6       8       1           0d0         0d0
7       0       1       -2000d0         0d0
8       0       1       -2000d0         0d0
9       10      1           0d0         0d0
10      13      1           0d0         0d0
11      13      1           0d0         0d0
12      17      1           0d0         0d0
13      15      1           0d0         0d0
14      0       1       -2000d0         0d0
15      17      1           0d0         0d0
16      24      1           0d0         0d0
17      0       1       -2000d0         0d0
18      20      1           0d0         0d0
19      0       1       -2000d0         0d0
20      21      1           0d0         0d0
21      22      1           0d0         0d0
22      0       0           0d0         0d0
Gas Information: Gas Gravity/ Zav(Zav=0 if Standing) / Gas Visc(cp) /  Psc (psia) / Tsc (F) [Base Conditions]
        0.70    0.90    0.018d0         14.7    60.0
Liquid Information: LiqDens(lb/ft3) / LiquidVisc(cp)/ Surf Tension (dynes/cm)
        62.40d0         1.0d0           8.41d0
1PGAS_Flow_Equation(1=Gen;2=Wey;3=Panh-A;4=Panh-B)/ YES(=1)2PCalcBeggs&Brill-NO(=0)/ SPLIT_HANDLING: (1)=UNIFORM;(2)=KEbased; (3)=DoubleStream
2       1       1
Type of Jacobian Entry Calculation (1=Numerical ; 2=Analytical)
1
PressInitial.txt        file    (0=Not  needed  ;       1=Create        it      ;       2=Use   it      when    available       for     P-initialization)
0
```

Figure 57 Input file for Network 2

```
TITLE:3rd_System_Gasnet_2_PHases_NCL_Centre_County_Pennsylvania_10 Wells_IPR_Figure_20
NPIPES
38
NNODES
38
NLOOPS ( NLOOPS = 1 + NPIPES - NNODES )
1
PIPE/JUP/JDN Ef  Tav(F) ID      ROUGH #SLOPES - L's (ft) - Elevation Data (ft)
1       1       2       1       60      1.58    0.001   3       467.86  249.75  402.36  1700.00 1700.00 1700.00 1660.00
2       3       2       1       60      1.58    0.001   12      227.86  393.22  764.89  593.00  645.59  266.27  252.30  438.87  1289.53 518.83  426.17  88.59
3       2       4       1       60      1.58    0.001   5       783.00  425.91  255.26  190.95  306.10  1660.00 1860.00 1880.00 1900.00 1940.00 1980.00
4       5       4       1       60      1.58    0.001   1       126.32  1980.00 1980.00
5       4       6       1       60      1.58    0.001   4       365.67  548.95  643.37  106.42  1980.00 2000.00 1980.00 1950.00 1950.00
6       7       6       1       60      1.58    0.001   1       1778.25 2000.00 1950.00
7       6       8       1       60      2.38    0.001   3       96.75   573.72  1018.07 1950.00 1950.00 1940.00 1950.00
8       9       8       0.9501  60      1.58    0.001   2       239.95  410.45  1950.00 1950.00 1950.00
9       10      9       0.9501  60      1.58    0.001   1       1809.26 1980.00 1950.00
10      8       11      0.9501  60      2.38    0.001   8       143.43  184.15  548.76  233.61  541.92  103.98  94.71   142.50  1950.00 1960.00 1960.00 1980.
11      12      11      0.9501  60      1.58    0.001   1       708.66  2000.00 1980.00
12      11      13      0.9501  60      2.38    0.001   1       183.14  1980.00 1980.00
13      14      13      0.9501  60      1.58    0.001   2       766.80  349.25  1920.00 1960.00 1980.00
14      13      15      0.9501  60      2.38    0.001   6       259.03  157.85  634.96  402.07  149.69  760.77  1980.00 1960.00 1960.00 2000.00 2000.00 2050.
15      16      15      0.9501  60      1.58    0.001   1       116.19  2160.00 2150.00
16      17      16      0.9501  60      1.58    0.001   2       541.88  170.70  2180.00 2180.00 2160.00
17      18      16      0.9501  60      1.58    0.001   2       545.30  733.23  2200.00 2150.00 2180.00
18      15      19      0.9501  60      2.38    0.001   5       600.78  1254.57 1636.07 1798.64 228.84  2150.00 2050.00 2240.00 2280.00 2300.00 2280.00
19      20      19      0.9501  60      1.58    0.001   1       1020.12 2250.00 2280.00
20      19      21      0.9501  60      2.38    0.001   2       138.86  212.12  2280.00 2270.00 2240.00
21      22      21      0.9501  60      1.58    0.001   1       274.49  2240.00 2240.00
22      21      23      0.9501  60      2.38    0.001   2       340.43  1094.51 2240.00 2240.00 2240.00
23      24      23      0.9501  60      1.58    0.001   1       355.60  2220.00 2240.00
24      23      25      0.9501  60      2.38    0.001   1       617.74  2240.00 2240.00
25      26      25      0.9501  60      1.58    0.001   1       1585.25 2150.00 2240.00
26      25      27      0.9501  60      2.38    0.001   1       616.45  2240.00 2200.00
27      28      27      0.9501  60      1.58    0.001   1       203.53  2200.00 2200.00
28      27      29      0.9501  60      2.38    0.001   2       1139.21 260.02  2200.00 2200.00 2200.00
29      30      29      0.9501  60      1.58    0.001   1       960.15  2100.00 2200.00
30      31      30      0.9501  60      1.58    0.001   1       1501.59 2100.00 2100.00
31      29      32      0.9501  60      2.38    0.001   1       305.43  2200.00 2200.00
32      33      32      0.9501  60      1.58    0.001   1       192.24  2200.00 2200.00
33      32      34      0.686   60      2.38    0.001   4       274.81  273.17  363.68  856.98  2200.00 2180.00 2150.00 2100.00 2100.00
34      34      35      0.9501  60      2       0.001   2       302.86  954.49  2080.00 2100.00 2050.00
35      36      35      0.9501  60      2       0.001   4       313.62  717.79  1211.30 366.97  2100.00 2100.00 2100.00 2100.00 2050.00
36      35      37      0.9501  60      2       0.001   1       481.17  2050.00 2050.00
37      34      37      0.9501  60      2.38    0.001   3       302.86  954.49  481.17  2080.00 2100.00 2050.00 2050.00
38      37      38      0.9501  60      2       0.001   1       288.25  2050.00 2050.00
NODE-WITH-PRESSURE-SPECIFICATION: NodeNumber/Pressure(psia)
37 40.650d0
NODE INFORMATION: NODE / 90d-PIPE /0-1-2(Balance/Fixed/IPR)/ Qg(MSCFD) / WGR(STB/MSCFD)
1       0       2       0.326d0     175d0       0.5d0         0.1
2       1       1       0       0
3       0       2       0.096d0     106.2046d0  0.75d0        0.1
4       3       1       0       0
5       0       2       0.0735d0    164.8074    0.5d0         0.1
6       6       1       0       0
7       0       2       0.0450d0    170.7107    0.75d0        0.1
8       7       1       0       0
9       0       1       0       0
10      0       1       47.19   0
11      11      1       0       0
12      0       1       14.44   0
13      12      1       0       0
14      0       2       0.086d0     178.9597    0.5d0         0.4
15      15      1       0       0
16      16      1       0       0
17      0       2       0.0117d0    131.732     0.75d0        0.4
18      0       2       0.0086d0    167.7954    0.75d0        0.4
19      18      1       0       0
20      0       2       0.0248d0    95          0.75d0        10
21      21      1       0       0
22      0       2       0.0126d0    151.96      0.75d0        0.4
23      22      1       0       0
24      0       1       26.94   0
25      24      1       0       0
26      0       1       12.34   0
27      26      1       0       0
28      0       1       28.04 0
29      28      1       0       0
30      0       1       0       0
31      0       2       0.0201d0    138.5425    0.75d0        0.4
32      31      1       0 0
33      0       1       21.29   0
34      34      1       0       0
35      34      1       0       0
36      0       1       15      0
37      37      1       0.0     0
38      0       0       0       0
Gas Information: Gas Gravity/ Zav(Zav=0 if Standing) / Gas visc(cp) /  Psc (psia) / Tsc (F) [Base Conditions]
        0.551724138     0.8801      0.0127d0    14.7    60.0
Liquid Information: LiqDens(lb/ft3) / Liquidvisc(cp)/ Surf Tension (dynes/cm)
        62.4d0          0.8566d0        59.66671626d0
1PGAS_Flow_Equation(1=Gen;2=Wey;3=Panh-A;4=Panh-B)/ YES(=1)-NO(=0)2PCalcBeggs&Brill     / SPLIT_HANDLING: (1)=UNIFORM;(2)=KEbased; (3)=DoubleStream
2       1       2
Type of Jacobian Entry Calculation (1=Numerical ; 2=Analytical)
1
```

Figure 58 Input file for Network 3

```
TTITLE:4th_System_Gasnet_2_PHases_KOREA_MODEL_Figure_26
NPIPES
40
NNODES
34
NLOOPS ( NLOOPS = NPIPES - NNODES + 1 )
7
LOCATION(I)/JUP(I)/JDN(I)/fe  /Tav(F) /ID(in)   /e(in)  /#slopes/L's-ft(i=1,..,#slopes)/ ActualElevations-ft(#slopes+1)fromUPtoDOWN
1       1       2       1.0     82.0    5.0     0.0001  1       5026.35         0       0
2       2       29      1.0     82.0    6.0     0.0001  1       5249.59         0       0
3       29      28      1.0     82.0    5.0     0.0001  1       6561.67         0       0
4       28      27      1.0     82.0    5.0     0.0001  1       5249.59         0       0
5       27      25      1.0     82.0    7.0     0.0001  1       5741.72         0       0
6       25      26      1.0     82.0    5.0     0.0001  1       7217.66         0       0
7       25      23      1.0     82.0    5.0     0.0001  1       6233.68         0       0
8       26      4       1.0     82.0    5.0     0.0001  1       5249.59         0       0
9       4       3       1.0     82.0    5.0     0.0001  1       5473.90         0       0
10      3       2       1.0     82.0    5.0     0.0001  1       7181.17         0       0
11      31      7       1.0     82.0    6.0     0.0001  1       3608.22         0       0
12      31      5       1.0     82.0    5.0     0.0001  1       3636.11         0       0
13      7       6       1.0     82.0    6.0     0.0001  1       3608.22         0       0
14      5       12      1.0     82.0    4.0     0.0001  1       3469.18         0       0
15      5       6       1.0     82.0    5.0     0.0001  1       3982.09         0       0
16      12      13      1.0     82.0    2.0     0.0001  1       3588.84         0       0
17      32      24      1.0     82.0    4.0     0.0001  1       3280.39         0       0
18      24      23      1.0     82.0    4.0     0.0001  1       3280.39         0       0
19      23      18      1.0     82.0    4.0     0.0001  1       4868.35         0       0
20      18      19      1.0     82.0    2.0     0.0001  1       3917.76         0       0
21      13      14      1.0     82.0    2.0     0.0001  1       3280.39         0       0
22      14      15      1.0     82.0    2.0     0.0001  1       4021.22         0       0
23      15      33      1.0     82.0    2.0     0.0001  1       3604.83         0       0
24      9       8       1.0     82.0    6.0     0.0001  1       3608.22         0       0
25      8       34      1.0     82.0    6.0     0.0001  1       3608.22         0       0
26      34      33      1.0     82.0    2.0     0.0001  1       3280.39         0       0
27      18      17      1.0     82.0    2.0     0.0001  1       5417.66         0       0
28      32      16      1.0     82.0    2.0     0.0001  1       4471.85         0       0
29      16      17      1.0     82.0    2.0     0.0001  1       1804.61         0       0
30      17      20      1.0     82.0    5.0     0.0001  1       3937.06         0       0
31      20      21      1.0     82.0    5.0     0.0001  1       3280.39         0       0
32      21      22      1.0     82.0    5.0     0.0001  1       3608.22         0       0
33      22      10      1.0     82.0    5.0     0.0001  1       3421.65         0       0
34      9       10      1.0     82.0    2.0     0.0001  1       5244.51         0       0
35      10      11      1.0     82.0    2.0     0.0001  1       4921.56         0       0
36      29      30      1.0     82.0    6.0     0.0001  1       3471.01 0       0
37      4       31      1.0     82.0    2.0     0.0001  1       10.00           0       0
38      13      32      1.0     82.0    2.0     0.0001  1       2.00            0       0
39      33      9       1.0     82.0    2.0     0.0001  1       2.00            0       0
40      6       34      1.0     82.0    3.0     0.0001  1       10.00           0       0
NODE-WITH-PRESSURE-SPECIFICATION: NodeNumber/Pressure(psia)
1   500d0
NODE INFORMATION: NODE / 90d-PIPE /0-1-2(Balance/Fixed/IPR)/ Qg(MSCFD) / WGR(STB/MSCFD)
1       0       1       3000    0.001
2       10      1       0.0     0.0
3       0       1       0.0     0.0
4       37      1       0.0     0.0
5       15      1       0.0     0.0
6       15      1       0.0     0.0
7       0       1       0.0     0.0
8       0       1       0.0     0.0
9       39      1       0.0     0.0
10      34      1       0.0     0.0
11      0       0       0.0     0.0
12      0       1       0.0     0.0
13      16      1       0.0     0.0
14      0       1       0.0     0.0
15      0       1       0.0     0.0
16      0       1       0.0     0.0
17      29      1       0.0     0.0
18      27      1       0.0     0.0
19      0       1       -1000.0 0.0
20      0       1       0.0     0.0
21      0       1       0.0     0.0
22      0       1       0.0     0.0
23      18      1       0.0     0.0
24      0       1       0.0     0.0
25      6       1       0.0     0.0
26      0       1       0.0     0.0
27      0       1       0.0     0.0
28      0       1       0.0     0.0
29      3       1       0.0     0.0
30      0       1       -1700.0 0.0
31      12      1       0.0     0.0
32      28      1       0.0     0.0
33      39      1       0.0     0.0
34      25      1       0.0     0.0
Gas Information: Gas Gravity/ Zav(Zav=0 if Standing) / Gas Visc(cp) /  Psc (psia) / Tsc (F) [Base Conditions]
                                0.551724138             0.9303          0.0119d0        14.7    60.0
Liquid Information: LiqDens(lb/ft3) / LiquidVisc(cp)/ Surf Tension (dynes/cm)
                                62.4d0          0.8555d0                64.68716636
1PGAS_Flow_Equation(1=Gen;2=Wey;3=Panh-A;4=Panh-B)/ YES(=1)-NO(=0)2PCalcBeggs&Brill     / SPLIT_HANDLING: (1)=UNIFORM;(2)=KEbased; (3)=DoubleStream
2       1       3
Type of Jacobian Entry Calculation (1=Numerical ; 2=Analytical)
1
PressInitial.txt        file    (0=Not  needed  ;       1=Create        it      ;       2=Use   it      when    available       for     P-initialization)
0
```

Figure 59 Input file for Network 4

```
TITLE:5th_System_Gasnet_2_PHases_Complex_System_6_Loops_Figure_44_46
NPIPES
31
NNODES
26
NLOOPS ( NLOOPS = NPIPES - NNODES + 1 )
6
LOCATION(I)/JUP(I)/JDN(I)/fe  /Tav(F) /ID(in)   /e(in)  /#slopes/L's-ft(i=1,..,#slopes)/ ActualElevations-ft(#slopes+1)fromUPtoDOWN
1       1       2   1.0  82     6.0     0.006   1       100000  0.0     0.0
2       2       3   1.0  82     6.0     0.006   1       100000  0.0     0.0
3       2       4   1.0  82     6.0     0.006   1       100000  0.0     0.0
4       4       5   1.0  82     6.0     0.006   1       100000  0.0     0.0
5       3       5   1.0  82     6.0     0.006   1       100000  0.0     0.0
6       5       6   1.0  82     6.0     0.006   1       100000  0.0     0.0
7       6       7   1.0  82     6.0     0.006   1       100000  0.0     0.0
8       9       6   1.0  82     6.0     0.006   1       100000  0.0     0.0
9       9       8   1.0  82     6.0     0.006   1       100000  0.0     0.0
10      8       7   1.0  82     6.0     0.006   1       100000  0.0     0.0
11      10      9   1.0  82     6.0     0.006   1       100000  0.0     0.0
12      7       11  1.0  82     6.0     0.006   1       100000  0.0     0.0
13      11      12  1.0  82     6.0     0.006   1       100000  0.0     0.0
14      11      13  1.0  82     6.0     0.006   1       100000  0.0     0.0
15      14      12  1.0  82     6.0     0.006   1       100000  0.0     0.0
16      13      14  1.0  82     6.0     0.006   1       100000  0.0     0.0
17      26      15  1.0  82     6.0     0.006   1       100000  0.0     0.0
18      12      16  1.0  82     6.0     0.006   1       100000  0.0     0.0
19      22      24  1.0  82     6.0     0.006   1       100000  0.0     0.0
20      23      24  1.0  82     6.0     0.006   1       100000  0.0     0.0
21      24      18  1.0  82     6.0     0.006   1       100000  0.0     0.0
22      18      25  1.0  82     6.0     0.006   1       100000  0.0     0.0
23      26      19  1.0  82     6.0     0.006   1       100000  0.0     0.0
24      17      23  1.0  82     6.0     0.006   1       100000  0.0     0.0
25      17      22  1.0  82     6.0     0.006   1       100000  0.0     0.0
26      18      26  1.0  82     6.0     0.006   1       100000  0.0     0.0
27      22      20  1.0  82     6.0     0.006   1       100000  0.0     0.0
28      19      21  1.0  82     6.0     0.006   1       100000  0.0     0.0
29      25      19  1.0  82     6.0     0.006   1       100000  0.0     0.0
30      8       17  1.0  82     6.0     0.006   1       100000  0.0     0.0
31      13      23  1.0  82     6.0     0.006   1       100000  0.0     0.0
NODE-WITH-PRESSURE-SPECIFICATION: NodeNumber/Pressure(psia)
15    60d0
NODE INFORMATION: NODE / 90d-PIPE /0-1-2(Balance/Fixed/IPR)/ QG(MSCFD) / WGR(STB/MSCFD)
1       0       1       2700d0          0.01d0
2       3       1          0d0          0d0
3       0       1          0d0          0d0
4       0       1          0d0          0d0
5       5       1          0d0          0d0
6       8       1          0d0          0d0
7       10      1          0d0          0d0
8       10      1          0d0          0d0
9       8       1          0d0          0d0
10      0       1        300d0          0.01d0
11      13      1          0d0          0d0
12      15      1          0d0          0d0
13      14      1          0d0          0d0
14      0       1          0d0          0d0
15      0       1      -1000d0          0d0
16      0       1       -800d0          0d0
17      25      1          0d0          0d0
18      22      1          0d0          0d0
19      23      1          0d0          0d0
20      0       1       -700d0          0d0
21      0       0          0d0          0d0
22      19      1          0d0          0d0
23      20      1          0d0          0d0
24      19      1          0d0          0d0
25      0       1          0d0          0d0
26      23      1          0d0          0d0
Gas Information: Gas Gravity/ Zav(Zav=0 if Standing) / Gas Visc(cp) /  Psc (psia) / Tsc (F) [Base Conditions]
        0.551724138     0.9303  0.0119d0        14.7    60.0
Liquid Information: LiqDens(lb/ft3) / Liquidvisc(cp)/ Surf Tension (dynes/cm)
        62.4d0          0.8555d0        64.68716636
1PGAS_Flow_Equation(1=Gen;2=Wey;3=Panh-A;4=Panh-B)/ YES(=1)-NO(=0)2PCalcBeggs&Brill     / SPLIT_HANDLING: (1)=UNIFORM;(2)=KEbased; (3)=DoubleStream
2       1       2
Type of Jacobian Entry Calculation (1=Numerical ; 2=Analytical)
1
PressInitial.txt        file    (0=Not  needed  ;       1=Create        it      ;       2=Use   it      when    available       for     P-initialization)
0
```

Figure 60 Input file for Network 5